Received: 23 December 2022 | Revised: 14 March 2023 | Accepted: 1 April 2023

DOI: 10.1002/inf2.12424

REVIEW ARTICLE

WILEY

Advanced polymer materials-based electronic skins for tactile and non-contact sensing applications

Feifei Yin[1] | **Hongsen Niu**[1] | **Eun-Seong Kim**[1] | **Young Kee Shin**[2] | **Yang Li**[3] | **Nam-Young Kim**[1]

[1]Department of Electronics Engineering, Kwangwoon University, Seoul, South Korea

[2]Department of Molecular Medicine and Biopharmaceutical Sciences, Seoul National University, Seoul, South Korea

[3]School of Information Science and Engineering, University of Jinan, Jinan, China

Correspondence

Yang Li, School of Information Science and Engineering, University of Jinan, Jinan, 250022, China.
Email: sunny_lee2011@hotmail.com

Eun-Seong Kim and Nam-Young Kim, Department of Electronics Engineering, Kwangwoon University, Seoul, 01897, South Korea.
Email: 3037eskim@gmail.com and nykim@kw.ac.kr

Funding information

National Research Foundation of Korea, Grant/Award Numbers: 2018R1A6A1A03025242, 2018R1D1A1A09083353

Abstract

Recently, polymer materials have been at the forefront of other materials in building high-performance flexible electronic skin (e-skin) devices due to conspicuous advantages including excellent mechanical flexibility, good compatibility, and high plasticity. However, most research works just paid considerable attention and effort to the design, construction, and possible application of e-skins that reproduce the tactile perception of the human skin sensory system. Compared with tactile sensing devices, e-skins that aim to imitate the non-contact sensing features in the sensory system of human skin tend to avoid undesired issues such as bacteria spreading and mechanical wear. To further promote the development of e-skins to the human skin sensory system where tactile perception and non-contact sensing complement each other, significant progress and advances have been achieved in the field of polymer materials enabled e-skins for both tactile perception and non-contact sensing applications. In this review, the latest progress in polymer material-based e-skins with regard to tactile, non-contact sensing capabilities and their practical applications are introduced. The fabrication strategies of polymer materials and their role in building high-performance e-skins for tactile and non-contact sensing are highlighted. Furthermore, we also review the research works that integrated the polymer-based tactile and non-contact e-skins into robots and prostheses, smart gloves, and VR/AR devices and addressed some representative problems to demonstrate their suitability in practical applications in human–machine interactions. Finally, the current challenges in the construction of high-performance tactile and non-contact e-skins are highlighted and promising properties in this direction, by taking advantage of the polymer materials, are outlined.

KEYWORDS

electronic skins, human–machine interaction, non-contact sensing, polymer materials, tactile sensing

Feifei Yin and Hongsen Niu contributed equally to this work.

1 | INTRODUCTION

As a significantly important function of the human skin, tactile perception can help humans answer external stimuli and act with the surroundings via direct physical contact. By mimicking haptic properties in the sensory system of the human skin, electronic skin (e-skin) enables the conversion of contact stimuli (e.g., pressure, strain) that can cause microcosmically physical deformation on the object into electrical signals, providing the possibility for human health monitoring,[1–5] the interaction between the machine and human beings, or between machines.[6–10] The e-skins based on different transduction mechanisms, such as capacitive,[11–14] piezoresistive,[15–18] piezoelectric,[19–22] and triboelectric[23–26] have been explored to achieve tactile sensing capabilities. Generally, such e-skins tend to rely on physical contact with the external objects; however, repetitive physical contact may easily result in the abrading of materials and shortening the lifetime of these devices.[27,28] In addition, considering that infection through direct contact is the main transmission route for many diseases, non-contact e-skin relying on the detection of humidity, light, magnetic, and even proximity signals that do not result in physical deformation of objects would contribute to avoiding bacterial spreading and mechanical wear, which has attracted considerable attention in recent years.[29,30] In fact, tactile perception and non-contact sensing are complemented each other in building the human skin sensory system. Great advances have been made in the construction of e-skins that are comparable to the sensory system of the human skin, in terms of the design of e-skins with both tactile and non-contact sensing capabilities.

Extensive materials involving carbon-based,[31–34] metal,[35–38] polymer,[39–42] textile,[43–46] and ionic materials[47–50] offer opportunities for building e-skins with tactile and noncontact sensing capabilities. Polymer materials, possessing the salient merits of lightweight, mechanical flexibility, good compatibility, and high plasticity, are widely employed as substrate material and functional layers of e-skins to enable high-performance in both tactile sensing and noncontact sensing aspects. The most commonly used polymer materials include polydimethylsiloxane (PDMS),[51] polyimide (PI),[52] poly (3,4-ethylene dioxythiophene): poly(styrene sulfonate) (PEDOT:PSS),[42] and poly(vinylidene fluoride) (PVDF),[53] and so on. Currently, these polymer materials have been used to construct e-skins individually or in advanced composites with others, and a few works have been published to review and summarize the corresponding progress in this area.[54–59] For instance, Fan et al. reviewed the importance of developing PEDOT:PSS and stressed its critical role in next-generation e-skins that are wearable, deformable, printable, ultrathin, and transparent.[42] Chen et al. systematically outlined the preparation of the conductive polymer composites and the representative utilization of diverse sensors such as pressure, strain, and temperature sensors.[57] Gong et al. summarized the design and preparation approaches for high-performance e-skins that exploited functional polymer nanocomposite mesh scaffolds.[59] However, few studies have reviewed the progress of e-skins that employ polymer materials for both tactile and noncontact sensing. Additionally, with the improvement of polymer materials fabrication and the advent of the intelligent information age, a large number of e-skin systems for tactile perception and non-contact sensing have been developed by taking advantage of polymer materials.[60–64] Therefore, a review article timely summarizing the recently high density of research and providing necessary guidance for future research on the e-skins design involving polymer materials is highly desired.

In this review, we focus on e-skins with tactile and non-contact sensing capabilities that are enabled by polymer materials and their practical applications in human–machine interactions such as robots and prostheses, smart gloves, and virtual reality/augmented reality (VR/AR) (Figure 1). First, we briefly introduce the mechanical properties and fabrication strategies of polymer materials. Then, by discussing certain representative paradigms, the unique roles of polymer materials in building high-performance e-skins are highlighted, and the approaches used for constructing e-skins with tactile and non-contact sensing capabilities using the extensive polymer materials are summarized. Additionally, the practical applications of e-skins constructed by various polymer materials in human–machine interactions like robots and prostheses, smart gloves, and VR/AR are reviewed. Finally, the currently faced challenges in the development of tactile and non-contact e-skins are concluded, and we outline the perspective direction of high-performance e-skins exploiting the polymer materials. We hope that this review can guide future research on building high-performance e-skins using the polymer materials and achieving human–machine interaction systems.

2 | POLYMER MATERIALS AND THEIR FABRICATIONS

As one of the most important material categories, polymer materials present conspicuous merits encompassing lightweight, mechanical flexibility, good compatibility, and good processability, showing their phenomenal superiority in enabling high-performance

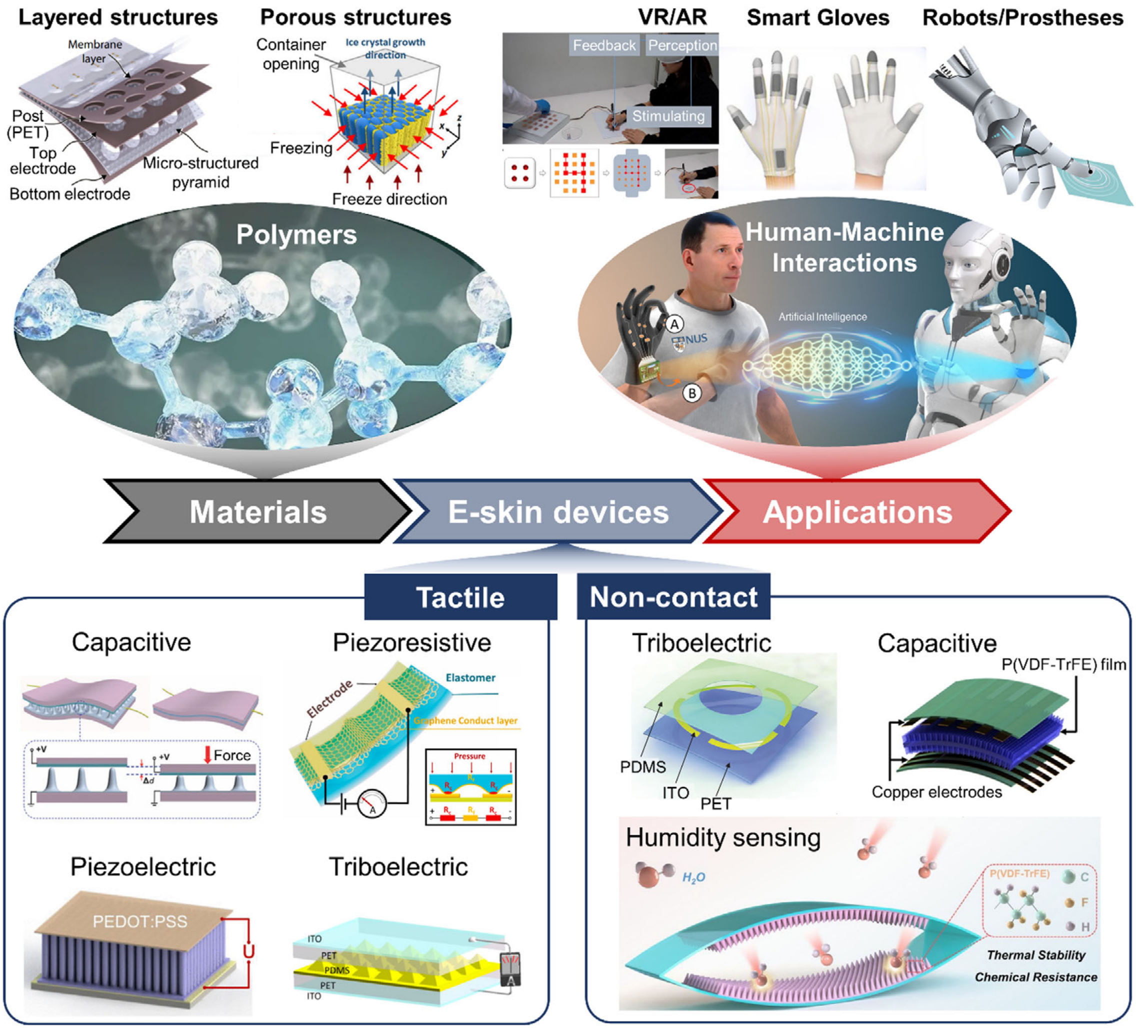

FIGURE 1 The e-skins with tactile and non-contact sensing capabilities enabled by polymer materials and their applications in human-machine interactions. Materials: Layered structures (Reproduced under the terms of the CC BY-NC-ND License.[65] Copyright 2020, The authors.); Porous structures (Reproduced with permission.[66] Copyright 2022, Elsevier Ltd.). The e-skin devices: Tactile-Capacitive (Reproduced with permission.[67] Copyright 2018, Wiley-VCH.); Tactile-Piezoresistive (Reproduced with permission.[4] Copyright 2019, Elsevier Ltd.); Tactile-Piezoelectric (Reproduced with permission.[68] Copyright 2014, IEEE.); Tactile-Triboelectric (Reproduced with permission.[69] Copyright 2012, American Chemical Society.); Non-contact: Triboelectric (Reproduced with permission.[70] Copyright 2017, Wiley-VCH.); Capacitive (Reproduced with permission.[12] Copyright 2019, American Chemical Society.); Humidity sensing (Reproduced with permission.[71] Copyright 2021, Elsevier Ltd.). Human–Machine Interaction (Reproduced with permission.[72] Copyright 2021, American Chemical Society.): VR/AR (Reproduced under the terms of the CC BY-NC License.[73] Copyright 2021, The authors.); Smart Gloves (Reproduced under the terms of the CC-BY License.[74] Copyright 2021, The authors.); Robot/Prostheses (Reproduced under the terms of the CC BY-NC License.[75] Copyright 2022, The authors.)

e-skins (as summarized in Table 1). PDMS, PI, PVDF, and other insulating polymer materials have been widely explored to work as flexible substrate layers for those e-skins because of their excellent transparency, good elasticity, and plasticity.[76,77,80,86–90] In 2013, by interlocking two high-aspect-ratio PDMS nanofiber films deposited with Pt-coating, Suh et al. presented a flexible strain sensor with high sensitivity for mimicking the complex characteristics of the human skin.[76] Zhang et al. fabricated a microstructured PDMS substrate for supporting Au electrode materials and proposed a flexible tactile sensor by combining it with a polystyrene (PS) microsphere dielectric layer, demonstrating that the sensor with a patterned PDMS substrate could contribute to higher sensitivity and low detection limit compared with that nonpatterned ones.[77] Apart from their use as flexible substrates, insulating polymer materials have also played a considerably essential role in the functional layers of e-skins.[12,13,65,78,91–94] A porous pyramid-microstructured PDMS film was fabricated by Park et al. and was adopted

TABLE 1 Summarized parameters on the performance of the polymer materials-based sensing devices.

	Functions	Materials	Device type	Stimulus	Sensitivity	Refs.
Insulating polymers	Supporting/ substrate layer	PDMS nanofiber	Tactile	Pressure Shear Torsion	Pressure: 11.45 Shear: 0.75 Torsion: 8.53	[76]
		Structured PDMS	Tactile	Pressure	0.815 kPa^{-1}	[77]
		PDMS pyramid	Tactile	Pressure	~3.73 kPa^{-1}	[78]
	Functional layer					
		P(VDF-TrFE) nanopillars	Both tactile and non-contact	Pressure	~0.35 kPa^{-1}	[12]
		P(VDF-TrFE) nanocone	Non-contact	Humidity	—	[71]
Conductive polymers	Working electrode	PEDOT:PSS	Tactile	Pressure	0.08 kPa^{-1}	[79]
	Functional layer	Micro-pyramidal PPy	Tactile	Pressure	1537.59 kPa^{-1}	[80]
	Functional layer (CPCs)	MXene/PVA	Tactile	Stain	≈0.4	[81]
		MXene/Ecoflex	Non-contact	Charged objects	Within 20 cm	[82]
		Microstructured TPV/Ni	Tactile	Pressure	10^6 kPa^{-1}	[83]
Other polymer composites	Functional layer	CCTO@PU sponge	Tactile	Pressure	0.73 kPa^{-1}	[84]
		PVDF/ZnO NFM	Tactile	Pressure	52.09 mV kPa^{-1}	[85]

to build an ultrahigh-sensitive capacitance pressure sensor by serving as the dielectric layer.[93] And, Ko et al. proposed the interlocked microridge structured polymer architectures of the PVDF layer in combination with the PDMS layer for developing ultrathin, highly sensitive, and wearable triboelectric sensors.[91] Polymer materials serving as substrates or functional layers have been designed with various micro- and nanostructures to construct high-performance e-skins. Currently, typical processing technologies for preparing micro- and nanostructures such as three-dimensional (3D) printing,[95] magnetic-assisted,[96] electrospinning,[61] and template methods[97] have been explored. Particularly, due to the superiorities of high accuracy and reliability in micro- and nanoprocessing, the template method has been widely used to introduce micro- and nanostructures including pyramids,[78] pillars,[12] cones,[13] and domes[94] in polymer materials for enhancing the sensing performance of the e-skins. For instance, Pan et al. replicated a PDMS film with pyramid microstructures from the microstructured silicon mold and developed a capacitance pressure sensor, which simultaneously realized high sensitivity as well as low hysteresis.[78] Park et al. developed a PDMS substrate with micro-pyramid arrays using the same silicon mold and then deposited electrode materials on that substrate, enabling a stretchable pressure sensor.[15] Corresponding details for the preparation of those micro-pyramid PDMS are illustrated in Figure 2A. First, a silicon mold with homogeneous microstructures was fabricated by etching processes involving conventional photolithography and wet etching. Then, a mixture of PDMS elastomer and cross-linker was cast onto the microstructured silicon mold and cured for a period of time. After that, by peeling it off the silicon mold, a micro-pyramid PDMS film was obtained. It is obvious that the template method exploiting lithography and silicon etching process shows considerable advantages in the precise controlling of the size, spacing, and morphology of the micro- and nanostructures, which is desired for large-area fabrication of micro- and nanostructures. However, it is quite challenging to design polymer materials with diverse microstructures and achieve the construction of high-performance e-skins by using such a photolithography template method. First, lithography machines and the mask used for lithography technology are expensive. Second, the lithography process and subsequent silicon wet etching process are time-consuming and complicated. Therefore, the bionic structure,[98] anodic aluminum oxide (AAO),[12] pre-stretched,[79] laser marking,[99] and other simple and low-cost template methods have been extensively explored for the design of e-skins with microstructured polymer materials. It is worth pointing out that the bionic structure template method, which has been widely used in the

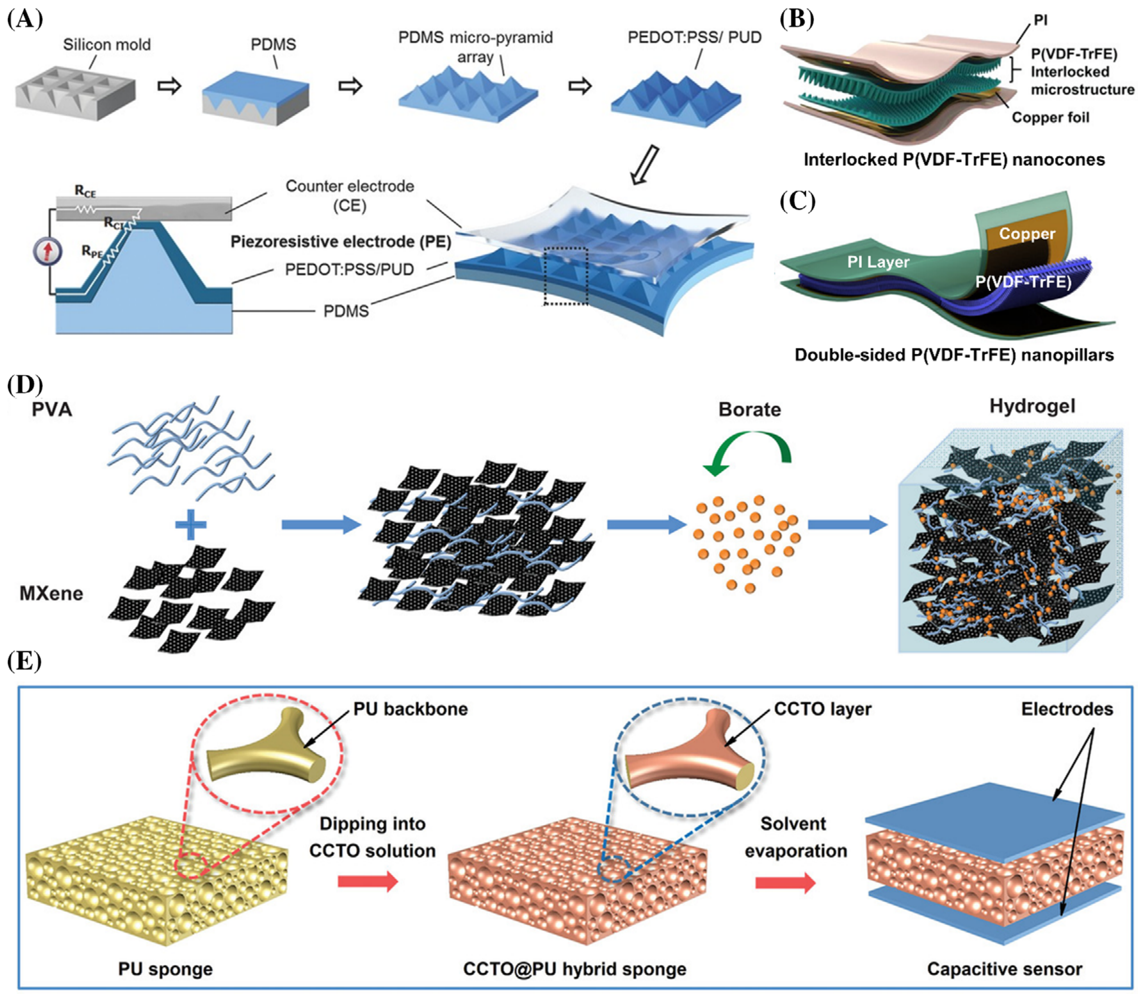

FIGURE 2 (A) Si mold fabricated by photolithography and etching processes for preparation of the micro-pyramid PDMS substrate supporting electrode materials. Reproduced with permission.[15] Copyright 2014, Wiley-VCH. (B) Interlocked asymmetric P(VDF-TrFE) nanocone arrays (Reproduced with permission.[13] Copyright 2019, Wiley-VCH) and double-sided P(VDF-TrFE) nanopillars (Reproduced with permission.[12] Copyright 2019, American Chemical Society) working as dielectric layers of capacitive tactile sensors. (D) Schematic of the preparation of the highly stretchable and self-healing MXene/PVA hydrogel electrode. Reproduced with permission.[81] Copyright 2019, Wiley-VCH. (E) Fabrication for a capacitive pressure sensor based on a high permittivity dielectric layer of the hybrid sponge (CCTO@PU). Reproduced with permission.[84] Copyright 2020, Wiley-VCH.

manufacture of wearable e-skins over the past years, paves a facile and environmentally friendly path for fabricating polymer materials with microstructures. Lotus leaves,[67] banana leaves,[100] rose petals,[98] and vein structures of mimosa leaf[101] that can be considered to be natural structure molds, have unique microstructures and have inspired researchers and scientists to design a variety of microstructural materials and develop high-performance e-skins. In addition, with the help of AAO template, Li et al. successfully proposed two typical capacitive sensors by adopting the interlocked asymmetric poly(vinylidenefluoride-co-trifluoroethylene) P(VDF-TrFE) nanocone arrays (Figure 2B)[13] and double-sided P(VDF-TrFE) nanopillars as dielectric layers (Figure 2C).[12]

Conductive polymer materials have become the most promising candidates for flexible electrode materials compared with the previous rigid materials, playing a dominant role in the emerging wearable e-skin devices. For example, Lu et al. deposited an active polypyrrole (PPy) conductive layer with surface wrinkling nanopatterns on PDMS stamps that were replicated from rose petals and reported a highly sensitive pressure sensor.[80] Another promising conductive polymer material, PEDOT:PSS has attracted extensive attention due to its outstanding air and thermal stability, and tunable conductivity. By adopting a stretchable PEDOT:PSS as the electrode layer, Sun et al. reported a high-performance tactile sensor based on the working mechanism of a triboelectric nanogenerator (TENG).[79] Here, a blade-coating procedure was used to prepare the stretchable PEDOT:PSS electrode layer on a pre-stretched PDMS film. In specific, the PDMS mixture was first poured into a model and cured. Then, the obtained PDMS film was pre-stretched by 100% onto a glass plate. Next, PEDOT:PSS solution was coated onto the pre-stretched PDMS film by using the blade technique and dried for a period. Lastly, the stretchable PEDOT:PSS electrode was formed when the PDMS was released. In addition to being deposited on pre-stretched elastomeric substrates, PEDOT:PSS has been developed as a stretchable conductor by using it as a conductive filler and inserting it into an elastomeric matrix such as polyurethane (PU) or PDMS to form a stretchable conductor.[102,103] Further, to develop robust and stretchable PEDOT:PSS conducting polymer films that meet the deformability requirements of e-skins, Jeong et al. presented a simple strategy of incorporating an excessive amount of a nonvolatile surfactant plasticizer.[104] In this way, the plasticizing effect of the plasticizer could contribute to the improvement in mechanical properties and stretchability of PEDOT:PSS conducting polymer without degradation in conductivity. Kee et al. proposed a stretchable PEDOT:PSS transparent electrode by mixing it with the ionic liquid compound, in which the ionic liquid enhanced the polymer conductivity and prolonged polymer elongations because it can not only serve as a dopant but also work as a plasticizer.[105] Benefiting from their intrinsic characteristic that is susceptible to non-covalent interactions, polymer materials tend to interact easily and effectively with other functional materials and yield newly synthesized polymer composites.[97,106–110] Polymer composites incorporating polymer materials with other distinct functional materials can present combined advantages and compensate for the disadvantages of the individual material. For instance, conductive polymer composites (CPCs) combining the flexibility of polymer materials and good conductivity of conductive fillers have exhibited promising perspectives in the construction of e-skins. Generally, CPCs are obtained by dispersing different conductive fillers including carbon nanotubes (CNTs), carbon black (CB), graphene, MXene, and metal nanoparticles into the insulating elastomeric matrix, which realized the required insulator/conductor transition of the composites.[81,83,111–113]

Until now, there are three typical routes reported for the development of CPCs. As for the solution mixing technique, a uniform dispersion with conductive fillers and polymer materials should be first formed in the solvent, and the good conductivity of conductive fillers in the elastomeric matrix is realized when the solvent is removed. Through such solution mixing and thermal annealing, Zhu et al. embedded the single-walled carbon nanotubes (SWCNTs) into the thermoplastic polyurethane (TPU) matrix and prepared conductive composites of TPU/SWCNTs to achieve non-contact human respiratory monitoring.[106] By mixing $Ti_3C_2T_x$ MXene solution with polyvinyl alcohol (PVA) aqueous solution and subjecting the mixture to a gelatinization process with the help of transparent sodium tetraborate solution (Figure 2D), Xuan et al. developed a self-healing and highly stretchable MXene/PVA hydrogel electrode.[81] As a demonstration, a very high bond (VHB) tape was sandwiched as a dielectric layer between two pieces of MXene/PVA hydrogel electrodes and used to construct a capacitive strain sensor, showing its sensing capability in the subtle and large-strain ranges was proved by mounting the sensor directly on human skin. Due to the necessary dispersion process of polymer and filler materials, the solution mixing method may be time-consuming. Different from that, the strategy of in situ polymerization enables the formation of polymer chains and a good dispersion of the filler on a molecular scale, resulting in good filler dispersion in the polymer matrix. However, there is a limitation that only certain polymer materials can be used to fabricate CPCs structures via in situ polymerization. In comparison, as a method for directly dispersing filler materials into a polymer matrix, melt compounding is simple and has attracted increasing attention in the fabrication of CPCs. For example, by combining hot compression processes to melt-blend nickel (Ni) powders into the thermoplastic vulcanizate (TPV), Fu et al. fabricated a microstructured TPV/Ni composite film and developed an ultra-sensitive pressure sensor under a wide detection range.[83]

Apart from CPCs, the composites of polymer materials and other distinct functional materials are also commonly employed for constructing e-skins endowed with fascinating properties. For example, considering that the calcium copper titanate (CCTO) possesses a strong dielectric property, and stability within a wide temperature range,[84] Park et al. dip-coated the PU sponge with a surface-modified CCTO solution and explored a hybrid sponge (CCTO@PU) with enhanced dielectric permittivity. Next, a highly-sensitive capacitive pressure sensor was assembled by sandwiching such a CCTO@PU hybrid sponge between two electrodes (Figure 2E), providing a facile and scalable way to design capacitive pressure sensors. Dickey et al. proposed a flexible tactile sensor array, of which the dielectric layers were composed of CNT/PDMS film offering a high dielectric permittivity and parylene film acting as the scaffold architecture, enabling robots to successfully manipulate light and heavy objects via a closed-loop pressure feedback.[114] Many published studies have proved that $BaTiO_3$ (BTO) has outstanding piezoelectric properties. Therefore, Yang et al. innovatively fabricated a composite matrix with outstanding piezoelectricity and flexibility properties, by incorporating a mixture matrix of PDMS and PVDF into the BTO, and realized a nanogenerator with high electrical output performance.[115] In light of the synergistic piezoelectric properties of polyacrylonitrile (PAN) and BTO, Chou et al. reported a self-powered flexible tactile sensor that was composed of a composite film of BTO, PAN, and Ecoflex, and illustrated the dynamic monitoring capability for human plantar pressure, posture, and other physiological information.[116] As early as 2006, Wang et al. successfully verified the capability of ZnO for converting mechanical energy to electrical energy, indicating excellent piezoelectric properties.[19] Following this, Liu et al. integrated ZnO nanorods (NRs) with PAN nanofiber to form a ZnO/PAN composite nano-fabric and observed significant improvement in the power output and pressure sensitivity of such a composite nano-fabric.[117] Recently, a hybrid piezoelectric layer that was prepared by doping ZnO nanoparticles into PVDF nanofibrous membrane was proposed by Ding et al. to serve as a pressure-sensing layer and achieve tactile spatial mapping with excellent sensing capacities.[85] By combining two different polymer materials of cellulose and PVA that have been proven with excellent biodegradability, Yu et al. developed a flexible, transparent, and biodegradable layer and used it as positive triboelectric material to fabricate a high-performance TENG device.[118]

3 | POLYMER MATERIALS ENABLED TACTILE E-SKINS BASED ON DIFFERENT MECHANISMS

3.1 | Tactile e-skins based on capacitive sensors

Typically, relying on the capacitance change when loading pressures, the capacitive tactile sensor that adopts a common "sandwich" configuration or planer structure presents excellent capability in detecting external pressure information.[14,119–121] The capacitance ($C = \varepsilon A/d$) of the sensor depends on the effective dielectric constant (ε) of the dielectric layer as well as the overlapping area (A) and the distance (d) between two electrodes. The e-skins that are based on such a capacitive tactile sensor have been widely used to reproduce the tactile perception behavior of human skin due to the conspicuous merits of the simple device structure, low power consumption, high sensitivity, and good repeatability.[12,13,122–124] Considering excellent mechanical flexibility, and good processability, polymer materials have become one of the most important and promising materials categories for working as the insulating dielectric layer in the capacitive tactile sensor. However, the bulky polymer dielectric layer is relatively hard to be compressed because the high compressive modulus brings high internal stress when applying pressures, resulting in a limited sensitivity.[122] In addition, most polymer materials are susceptible to severe viscoelasticity, which increases the hysteresis and response time of the sensing devices.[65,125,126] To address the above issues, incorporating various microstructures such as micro-pyramids,[59,127] micro-pillars,[128,129] micro-domes,[130,131] and micro-wrinkles[132] into the polymer dielectric layer has been proven to be effective in boosting the sensing properties of the tactile sensor. In 2010, Bao et al. first microstructured an elastomer PDMS dielectric layer and demonstrated that such a design can aid in building a capacitive e-skin device with enhanced sensitivity and fast response speed.[11] By investigating the pressure sensitivities of three capacitive sensors, with pyramidal, linear, and unstructured PDMS films as the dielectric layers, they concluded that the sensor exploiting unstructured PDMS dielectric film exhibited the lowest pressure sensitivity. The pressure sensitivities of the linear-structured and pyramid-structured PDMS dielectric films were 5 and 30 folds higher than that without microstructures, respectively. The authors concluded the dramatically enhanced sensing properties of the structured PDMS dielectric films to two main factors: (1) the existence of voids in the structured PDMS tends to lower the elastic modulus of the dielectric layer, offering a relatively larger deformation space when equivalent pressures are applied and thereby obtaining higher sensitivity; (2) when compression occurred due to applied pressure, the voids were replaced by the PDMS matrix with a higher dielectric constant, which accordingly gives rise to an increased effective dielectric constant and capacitance variation of the sensor. Linear- and pyramid-structured PDMS dielectric films also presented low hysteresis and rapid response speed, which can be explained that microstructures introduced into the PDMS dielectric layer finally reduces the viscoelasticity and adhesion between the polymer dielectric and electrode layers during the pressure loading/releasing processes.

Furthermore, with the help of a theoretical calculation model, Wei et al. simulated and highlighted that the spacing of the pyramid spacing of the microstructured PDMS dielectric layer is an important parameter affecting the sensing performance of the capacitive tactile e-skin device.[133] The authors then fabricated several capacitive pressure sensors utilizing graphene electrodes and the microstructured PDMS dielectric layers with varied pyramid spacings. The sensing performance of these capacitive pressure sensors was analyzed by recording the variations in capacitance under different pressures, and it

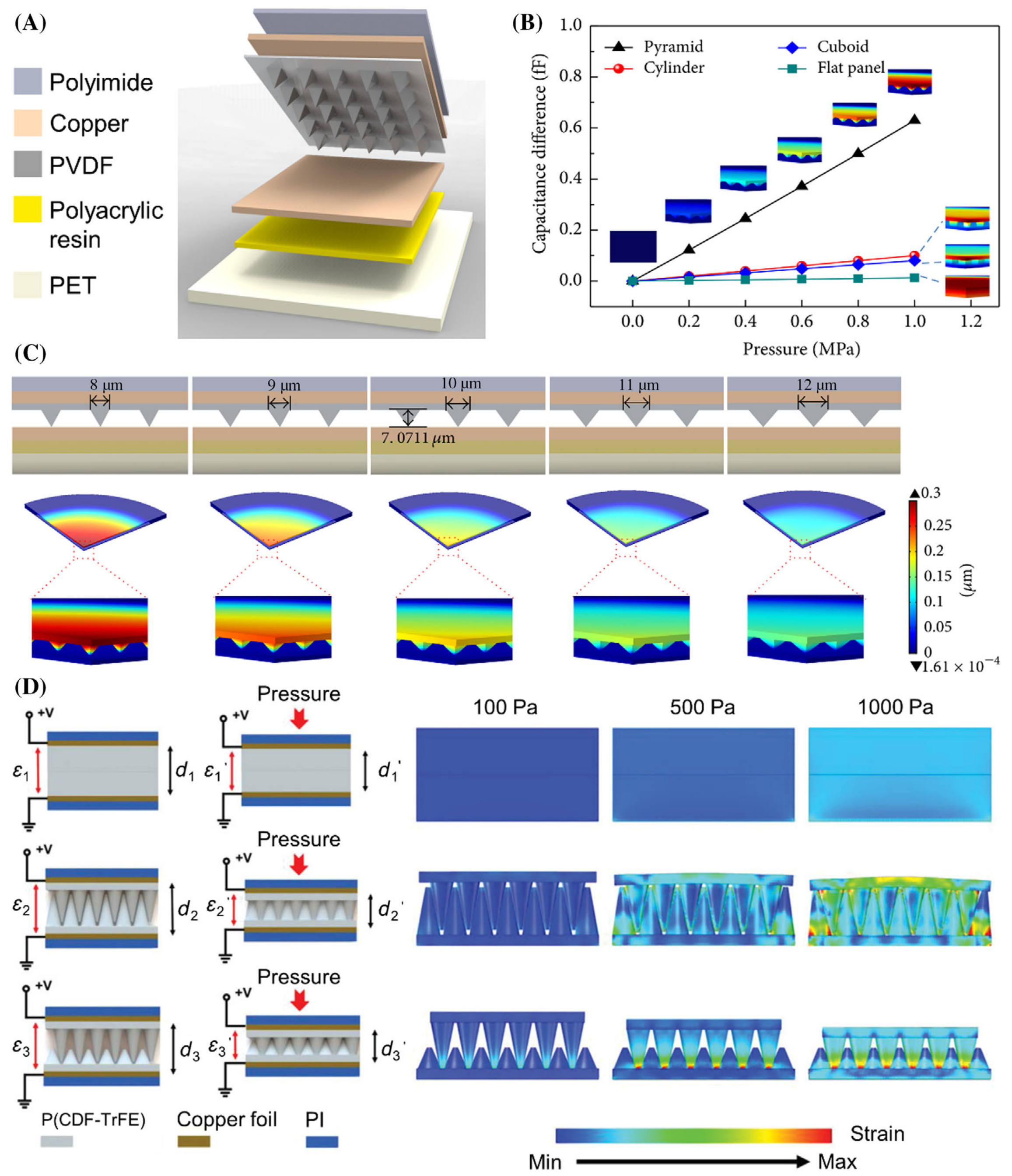

FIGURE 3 (A) Schematic of the microstructured capacitive pressure sensor for high-performance e-skin. (B) Comparison of capacitance responses toward pressure of capacitive pressure sensors with different microstructures. (C) Responses of the capacitive sensors of the pyramidal structure with different ratios of L/H at 1 MPa. Reproduced under the terms of the Creative Commons Attribution License.[134] Copyright 2016, The authors. (D) Deformation and strain distribution of three capacitive tactile e-skin devices with nonpatterned, symmetric nanocones, and asymmetric nanocones dielectric layers. Reproduced with permission.[13] Copyright 2019, Wiley-VCH.

was concluded that the sensitivity of the devices increased with PDMS pyramid spacing, which is consistent with the simulation results. As the spacing between the pyramid increases, a higher density of voids and a large air fraction in the dielectric layer are obtained, resulting in high compressibility and deformability of the PDMS dielectric layer as well as a higher sensitivity of the capacitance sensor. Excessive spacing between pyramids triggers the interfacial adhesion between the dielectric layer and the electrode layers, which relates the hysteresis issue to the response speed of the capacitance sensor. Therefore, it is essential to adjust and prepare the microstructured polymer dielectric layer with appropriate pyramid spacing for constructing the capacitive tactile sensor with high sensitivity and fast response time. Through a finite element analysis (FEA), Yang's group predicted a capacitive sensor with pyramid microstructures exhibited a 49 folds higher pressure sensitivity than that of non-microstructured ones,[134] as presented in Figure 3A,B. The authors further simulated and observed that the smaller ratio of the hemline length/the height (L/H) of the pyramidal structure can contribute to a highly sensitive capacitive sensor (Figure 3C). Thus, to achieve a higher sensitivity, the height of the pyramid microstructure could be selected to be as high as possible to obtain a sharper pyramid microstructure. The sharp part of the pyramid is easily compressed when applying pressures, however, the compressibility of the polymer dielectric layer with such a sharper pyramid microstructure is saturated easily, which results in improved sensitivity in low pressures but poor linearity over high pressures. Last, it was also demonstrated by the authors that a compromise of high sensitivity and good linearity could be realized when the value of L/H of the pyramidal structure was $\sqrt{2}$, providing reliable theory support for guiding the tactile e-skin research works. Apart from exploiting the dielectric layer with single-side microstructures, Li et al. proposed a capacitive tactile e-skin device that resorts to the PVDF dielectric layer with double-sided nanopillars and demonstrated the superiority of double-sided nanopillars in improving the pressure sensing properties via FEA simulation.[12] After that, by mimicking the interlocked micro ridges between the epidermis and dermis, the authors also incorporated two interlocked PVDF dielectric layers designed with asymmetric nanocones and developed a highly sensitive tactile sensor.[13] FEA simulations were also performed to illustrate the strain and stress distributions of three types of dielectric layers of which the configurations were the interlocked PVDF films with non-patterning, symmetric nanocones, and asymmetric nanocones (Figure 3D), respectively. When compared with the other two cases, the interlocked PVDF films with asymmetric nanocones exhibited a highly strengthened stress distribution as the sharper part of the upper nanocones could easily make contact with the base of the lower nanocones and be easily compressed under the external pressure. As a result, the capacitive tactile sensor enabled by the two interlocked PVDF dielectric layers with asymmetric nanocones realized a significantly enhanced sensitivity, and the feasibility of this tactile sensor for application in pressure mapping, sign language gesture detection, and physiological signal monitoring was demonstrated.

Numerous researchers also introduced various microstructures into the electrode layers by depositing conductive electrode materials on the microstructured polymer supporting layers to effectively enhance the sensing performance of the capacitive tactile sensor. For example, by sputtering Pt on a PDMS substrate that incorporated both small and large pyramid structures, Pan's group proposed a hierarchically microstructured Pt electrode layer and assembled a highly sensitive tactile sensor, which also exhibited a low hysteresis.[78] Here, the authors claimed that inserting smaller pyramid patterns into the larger pyramid arrays increases the spacing between two adjacent larger pyramids and is beneficial for improving sensitivity. Moreover, the inserted smaller pyramid patterns solved the hysteresis problem caused by the excessive spacing between pyramids in capacitive sensors. With the help of a lotus leaf natural template, Guo et al. fabricated a flexible PDMS substrate with micro-tower patterns after two replications, and ultrathin silver nanowires (Ag NWs) were uniformly coated onto the surface of the PDMS micro-towers as the bottom electrode layer (Figure 4A).[67] As illustrated in Figure 4B, a flexible capacitive tactile sensor was obtained by assembling the bottom electrode layer of Ag NWs micro-towers, a PI dielectric layer, and an Ag NWs top electrode layer, which presented higher compressibility and sensitivity than a capacitive sensor with a planar Ag NWs electrode layer. Similar to the human skin, most of these capacitive e-skins are designed with multilayer structures. However, the existing functional layers in such e-skins tend to be stacked via non-bonded interfaces, therefore, they may face greater challenges due to the weak adhesion and mechanical mismatch between the interlayers. To avoid impairing the sensing performance due to the above issues, Guo et al. introduced a quasi-homogeneous composition into the interlayers that ensured a good mechanical match between the interlayers and added the interlinked micro-coned interfaces to the multilayer structures (Figure 4C).[135] Thus, a highly stable pressure sensor was obtained, and it presented excellent signal stability though more than 10 000 cycles of repeated rubbing and shear tests were conducted or even fixed on the tire tread of a car and driven 2.6 km.

In addition to incorporating interfacial microstructures into dielectric and electrode layers, a sponge or foam-like polymer dielectric layer was also applied to adjust the sensing behaviors of the capacitive tactile e-skin devices due to its high porosity, good mechanical flexibility, and low compression modulus.[84,93,110,136] It is essential for realizing the high compressibility and sensitivity of such capacitive tactile e-skin devices to control the porosity and voids in polymeric foams. Currently, many efficient strategies have been developed for this purpose. In particular, because of the simple operability, the sacrificial hard template method that adopts sugar cubes, salt crystals, PS microbeads, and metal foams as sacrificial templates has been commonly used to achieve

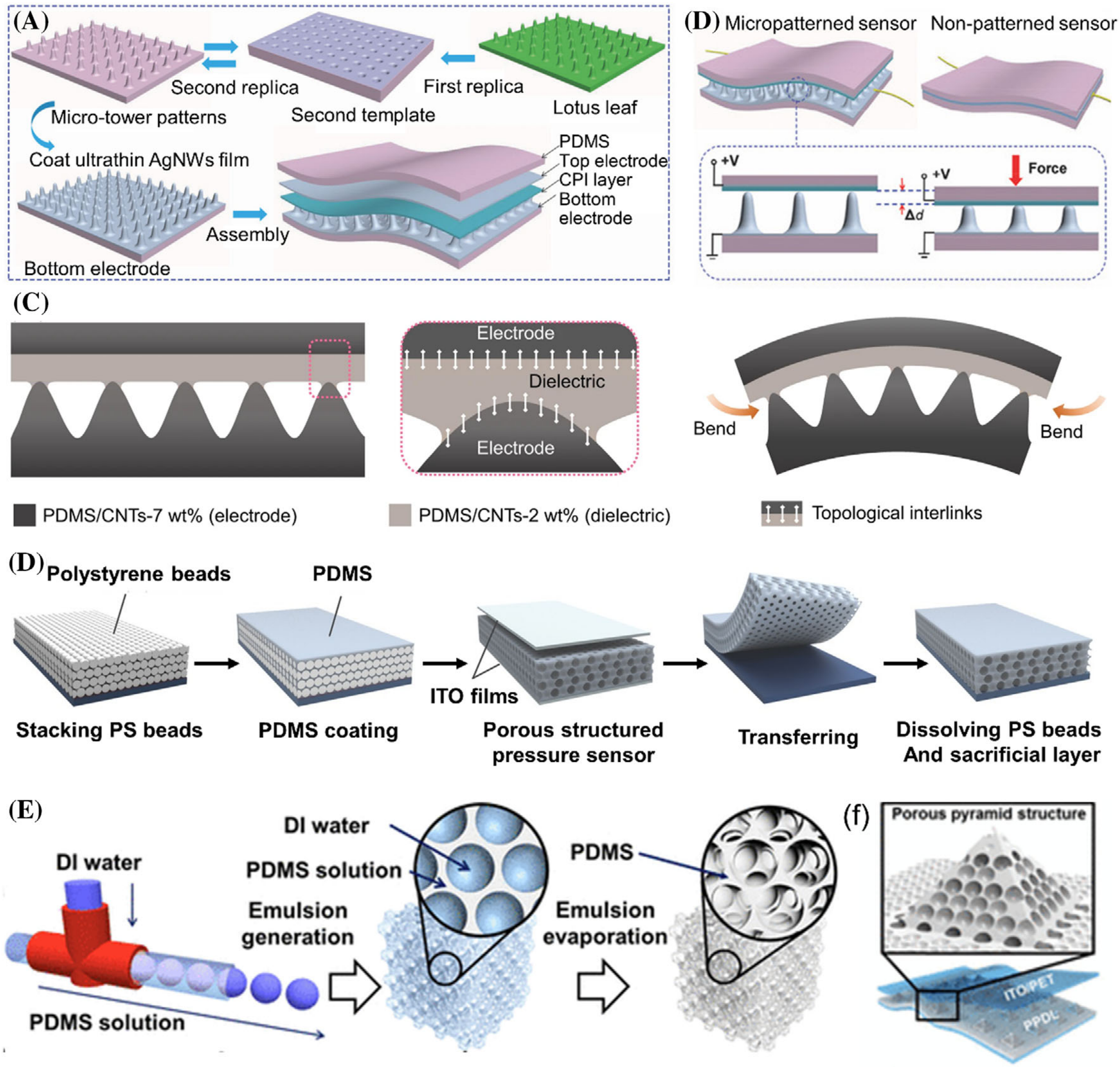

FIGURE 4 (A) Preparation of the capacitive tactile e-skin device with microstructured electrode layer. (B) Schematic of working principles of capacitive tactile e-skin devices based on microstructured and planar electrode layers. Reproduced with permission.[67] Copyright 2018, Wiley-VCH. (C) Quasi-homogeneous composition and the interlinked micro-coned interfaces in the multilayer structures for working stability under loading. Reproduced under the terms of the Creative Commons CC BY License.[135] Copyright 2022, The Authors. (D) Preparation steps of a porous PDMS dielectric layer for a capacitive tactile sensor. Reproduced with permission.[136] Copyright 2016, Wiley-VCH. (E) Fabrication of the DMESA method for a 3D microstructured PDMS dielectric layer. Reproduced with permission.[137] Copyright 2018, American Chemical Society. (F) Diagram of a capacitive tactile sensor using a porous PDMS dielectric layer with pyramid microstructured. Reproduced with permission.[93] Copyright 2019, American Chemical Society.

high porosity polymer foams. Through such a sacrificial hard template method, Lee et al. prepared a sponge-like PDMS dielectric layer and sandwiched the dielectric layer between two electrode layers of ITO/PET to present a capacitive tactile e-skin with high sensitivity.[136] As shown in Figure 4D, the authors first stacked PS microbeads on the silicon substrate and coated the PDMS mixture on the above substrate. After a curing process, the PS microbeads were removed completely by etching in acetone and dimethylformamide solutions, and a PDMS porous dielectric layer was finally prepared. Further, by using porous Ni foams as templates, Teo et al. developed a porous and ultralight boron nitride/PDMS (BNF@PDMS) composite foam with a density of 15 mg cm^{-3}.[110] Benefiting from the combination of boron nitride (BN) and PDMS, BNF@PDMS composite foam was demonstrated with numerous merits including excellent mechanical elasticity, ultrahigh compressibility, and desirable fatigue property. Further, the composite foam served as a dielectric layer to construct a high-performance capacitive tactile e-skin device, showing high sensitivity (0.854 kPa^{-1}) and a low-pressure detection limit (0.58 Pa). Additionally, Park et al. recommended another droplet-based and microfluidic-assisted emulsion self-assembly (DMESA) method to prepare a 3D microstructured PDMS dielectric layer and proposed a high-performance capacitive sensor for tactile e-skin applications.[137] Figure 4E depicts the preparation details of the microstructured PDMS layer via such a DMESA method. An aqueous solution of deionized water and an oil solution containing PDMS and surfactant were prepared respectively and then flowed through a perpendicularly arranged T-tube to meet at the junction. As a result, deionized water droplets were injected into the PDMS mixture and stabilized by the surfactant, forming a closely packed stacked lattice. The deionized water droplets were evaporated by a heating process, and a 3D uniformly microporous PDMS layer was left behind. Finally, the authors pointed out that the micropore size of the PDMS layer could be easily regulated by adjusting the flow speeds of the aqueous and oil solutions, thus tailoring capacitive tactile e-skins with high sensitivity.

To further enhance the sensing properties of the capacitive tactile e-skins, Park et al. proposed a porous PDMS dielectric layer with pyramid microstructures by simultaneously incorporating the microstructures fabrication method and the porosity introduction technique (Figure 4F), and reported a capacitive tactile sensor.[93] Such a sensor exhibited high sensitivity (up to 44.5 kPa^{-1}) within the pressure range of 0–100 Pa, and was capable of long-term monitoring of human wrist pulse signals. Dip-coating the sponge or foam-like polymer dielectric layers with high permittivity materials is another commonly used approach for enhancing the dielectric permittivity and sensitivity of capacitive sensors. For this purpose, a distinctly enhanced dielectric permittivity can be realized by embedding various conductive fillers into the sponge or foam-like polymer matrix and generating a network of micro-capacitors in the dielectric layer. For example, by dip-coating the graphene nanoplatelets (GNPs) and CNTs on PU sponge matrix, Xing et al. obtained a porous dielectric layer with high relative permittivity and excellent elastic property, achieving a rapid-response, and highly sensitive capacitive tactile sensor.[138] Liu et al. proposed a capacitive tactile sensor by using a porous dielectric layer of Ag NW/PVA nanocomposite.[139] Here, a PVA matrix was designed with numerous micropores for achieving high compressibility, and then Ag NWs were uniformly introduced to the porous PVA matrix to facilitate the formation of numerous micro-capacitors and increase permittivity. As a result, the capacitive tactile sensor based on the Ag NW/PVA nanocomposite realized high sensitivity of 1.8862 kPa^{-1}, a wide detection range of 0–250 kPa, and a fast response speed of 25 ms. Besides, it also has been proven that high dielectric constant ceramics like $BaTiO_3$ and $Ba_xSr_{1-x}TiO_3$ can be used as dielectric fillers to effectively improve the dielectric properties of conventional polymer materials. However, it should be pointed out that such ceramics might give rise to a strong piezoelectric effect and their dielectric properties are susceptible to fluctuations in ambient temperature. According to other excellent studies, CCTO, with a super dielectric property, presents good thermal stability over a wide temperature range and does not exhibit an obvious piezoelectric effect, thereby arousing extensive research interest. Zhang et al. presented a sponge-like composite that consisted of CCTO and PDMS matrix through a porogen-assisted process and achieved a flexible capacitive sensor showing a pressure response in a narrow range of 0–0.64 kPa.[140] To optimize the effect of CCTO on the dielectric permittivity of the sponge-like composite, Park et al. wrapped the CCTO on a low-modulus PU sponge to develop a microporous CCTO@PU hybrid sponge for designing a stretchable and highly sensitive capacitive tactile sensor.[84] For comparison, Table 2 summarizes the parameters of the typical capacitive sensors with polymer materials as the active dielectric layer and substrate layer supporting electrode materials.

3.2 | Tactile e-skins based on piezoresistive sensors

Due to the variation in device resistance as external pressure is applied, piezoresistive sensors have become one of the most important components in the construction of high-performance tactile e-skin, which presents distinguished advantages including the straightforward readout circuit, and excellent performance.[148,149] The resistance ($R = \rho L/S$) is related to the electrical resistivity (ρ), length (L), and the cross-sectional area (S) of the functional layer of the piezoresistive sensor. In terms of the configuration of the electrodes: sensors with planar electrodes and top-bottom electrodes are two dominant piezoresistive devices.[150] Table 2 lists the parameters of the sensing performance and fabrication methods of the piezoresistive sensors based on both planar electrodes and top-bottom electrodes.

3.2.1 | Tactile e-skins based on piezoresistive sensors with planar electrodes

By stacking a functional layer on a pair of in-plane electrodes, a piezoresistive sensor with planar electrodes is assembled, which serves as an important component of

TABLE 2 Typical polymer materials-based tactile e-skins with high performances (including capacitive and piezoresistive tactile e-skins).

	Fabrication method	Sensitivity	Working range	LOD	Res./rec. time (ms)	Refs.
Capacitive						
Microstructured electrode layer	Bionic template	≈1.2 kPa^{-1}	0–15 kPa	<0.8 Pa	36/58	[67]
	Si template	∼3.73 kPa^{-1}	0–100 kPa	0.1 Pa	21/—	[78]
	Bionic template	0.15 kPa^{-1}	0–450 kPa	0.35 Pa	6/6	[135]
Microstructured active layer	Si template	0.55 kPa^{-1}	0–7 kPa	3 Pa	ms range	[11]
	AAO template	6.583 kPa^{-1}	3 Pa	3 Pa	48/36	[13]
	Photoresist template	0.42 kPa^{-1}	0–14 kPa	1 Pa	<70	[128]
	Laser marking Cu template	8053.1 kPa^{-1}	0–34 kPa	0.05 Pa	5.6/5.6	[125]
Porous active layer	Sacrificial PS template	0.63 kPa^{-1}	0–14 kPa	2.42 Pa	≈40/—	[136]
	DMESA	0.86 kPa^{-1}	0–100 kPa	10 Pa	5/—	[137]
	Combined templates	44.5 kPa^{-1}	0–35 kPa	0.14 Pa	50/100	[93]
Porous active layer with filler	Template and CVD method	0.854 kPa^{-1}	0–2.1 kPa	0.58 Pa	—/—	[110]
	Dip-coating	0.062 kPa^{-1}	0–4.5 kPa	∼3 Pa	∼45/—	[138]
	MSPS and hydrothermal	10.5 kPa^{-1}	0–5 kPa	0.1 Pa	5.6/5.6	[126]
Piezoresistive						
Pair of plane electrodes	ISG technology	1875.53 kPa^{-1}	0–40 kPa	1.8 Pa	0.5/0.8	[4]
	Si template and conformal coating	23 kPa^{-1}	0–3 kPa	—	10/10	[89]
	Infiltration method	291699.6 kPa^{-1}	0–20 kPa	2 Pa	40/40	[99]
	Lithography and CVD	8.5 kPa^{-1}	0–12 kPa	1 Pa	40/—	[141]
	Lithography and Ppy deposition	17 kPa^{-1}	0–100 kPa	2 Pa	—/—	[142]
	SU-8 mold	2.0 kPa^{-1}	0–9 kPa	15 Pa	50/—	[143]
Top-bottom electrodes	Si template	14.5 kPa^{-1}	0–4 kPa	15 Pa	15/18	[20]
	Bionic template	70 kPa^{-1}	0–2 kPa	0.88 Pa	30/40	[90]
	Si template and spray coating	−3.26 kPa^{-1}	0–3 kPa	—	200/100	[144]
	Self-assembly PS sacrificial template	−15 kPa^{-1}	<5 kPa	4 Pa	<100/<100	[145]
	Wet chemical etching method	−4.48 kPa^{-1}	0–20 kPa	≈1 Pa	52/40	[146]
	Abrasive paper template and rGO	25.1 kPa^{-1}	0–40 kPa	16 Pa	120/80	[147]
	Freeze drying	424.8 kPa^{-1}	0–1.5 kPa	—	100/—	[66]

Abbreviation: LOD, limit of detection.

the tactile e-skins. Polymer materials with flexible, stretchable, or even other excellent properties tend to be designed with microstructures as the supporting layer or combined with other conductive materials like CNTs and graphene as the functional layer of the piezoresistive e-skin.[4,89,99,141–147,151] Chung et al. proposed a piezoresistive tactile sensor by incorporating a hierarchical structured PDMS with the deposition of monolayer graphene, which achieves a high sensitivity of 8.5 kPa^{-1} and a good linear response over a wide pressure range of 0–12 kPa.[141] Figure 5A illustrates the preparation process of such a piezoresistive tactile sensor. First, by performing photolithography and selective wet etching procedure, a copper sheet was successfully patterned with a reverse-dome shape. The patterned copper sheet was oxidized in a furnace with ambient air and an operating temperature of 850°C, forming nanostructured CuO/Cu_2O on the surface of the copper sheet. Next, the growth of hierarchically structured graphene was realized by placing the nanostructured copper film with

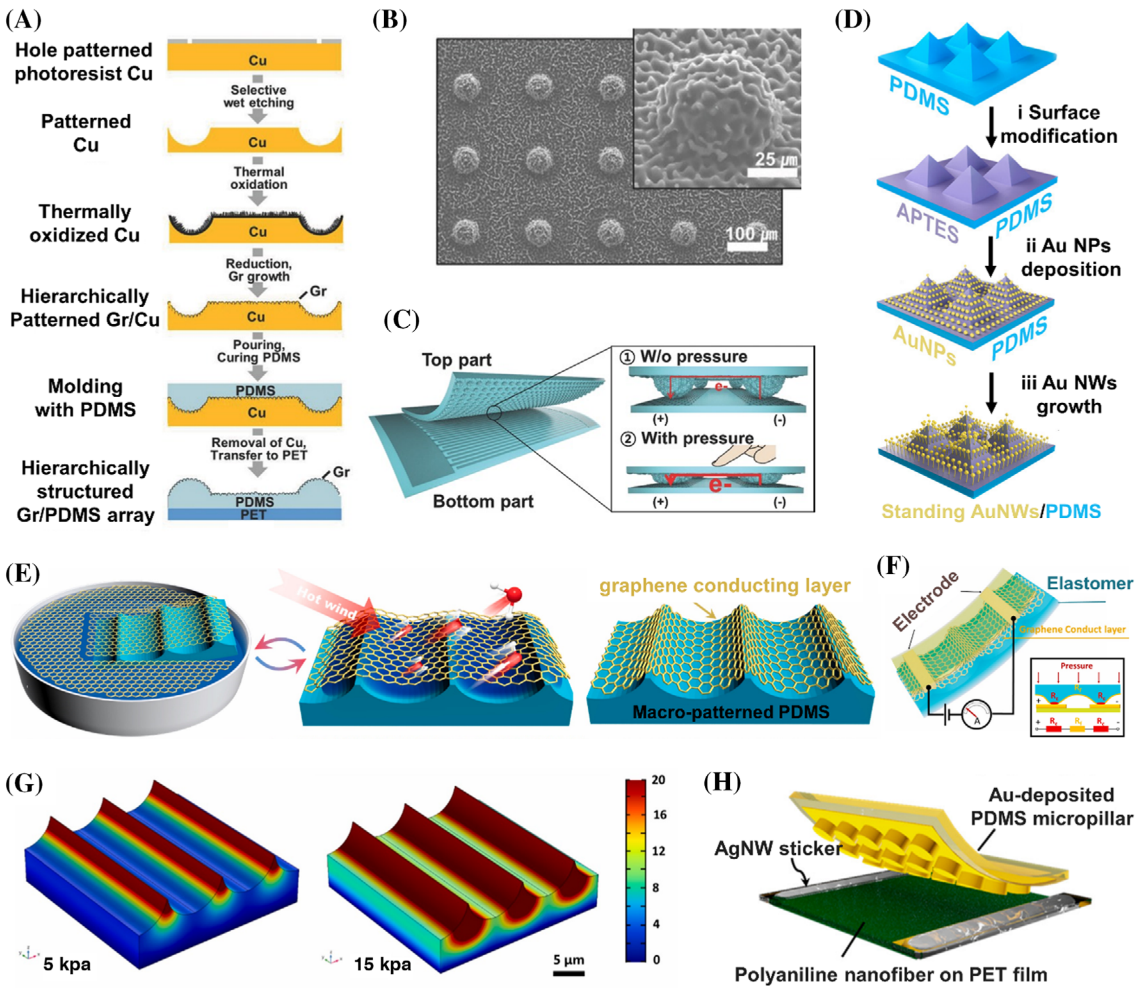

FIGURE 5 (A) Preparation of hierarchical structured monolayer graphene (Gr)/PDMS. (B) SEM image of the hierarchical structured graphene/PDMS. (C) Schematic diagram of the sensing mechanism of the sensor using the hierarchical structured graphene/PDMS. Reproduced with permission.[141] Copyright 2016, Wiley-VCH. (D) Schematic of the growth process of v-Au NWs on the micro-pyramid structured PDMS film. Reproduced with permission.[89] Copyright 2019, American Chemical Society. (E) Fabrication of a sensing layer consisting of ISG and microstructured PDMS. (F) Piezoresistive sensor based on this sensing layer and its pressure sensing principle. (G) Simulation on contact area changes of the piezoresistive sensor under pressures. Reproduced with permission.[4] Copyright 2019, Elsevier Ltd. (H) Schematic diagram of a piezoresistive sensor incorporating a top sensing layer of Au-deposited PDMS micropillar array and a bottom sensing layer of conductive PANI nanofibers. Reproduced with permission.[143] Copyright 2015, American Chemical Society.

CuO/Cu_2O in a chemical vapor deposition (CVD) furnace and annealing it with hydrogen gas at an operating temperature up to 850°C–1000°C. According to the authors, the roughness of the graphene deposited on the surface of the nanostructured CuO/Cu_2O was quite large compared with the sample prepared on the copper film that was not conducted to an oxidation process. And then, PDMS mixture was poured onto the pre-fabricated hierarchically structured graphene and cured for a period. After etching the copper sheet, the author obtained a hierarchically structured PDMS array deposited with a conformal graphene film (i.e., graphene/PDMS array), and Figure 5B shows the scanning electron microscope (SEM) image of the hierarchically structured graphene/PDMS array. Finally, the piezoresistive pressure sensor was constructed by placing the fabricated hierarchical graphene/PDMS array on the two separated interdigital graphene electrodes upside down (Figure 5C). Here, the hierarchical graphene/PDMS array serves as the conductive path between the separated planar electrodes. The contact area between the graphene/PDMS array and the planar electrodes increases due to the deformation of the graphene/PDMS array when external pressure is applied, which gives rise to a decrease of the resistance of the piezoresistive pressure sensor. In addition, Cheng et al. deposited vertically aligned gold nanowires (v-Au NWs) on the PDMS film with micro-pyramids via a modified seed-mediated growth method at room temperature.[89] As shown in Figure 5D, the PDMS film with pyramid patterns replicated from a silicon mold that was fabricated through photolithography and wet etching process was first pre-treated with air plasma and then immersed in a 3-aminopropyltriethoxysilane solution to achieve modification. Thereafter, by immersing the modified PDMS microstructures film into a gold nanoparticle (Au NPs) suspension, an Au seeds layer was formed on the surface of the PDMS microstructures film. When the PDMS microstructures film, coated with Au seeds, was immersed in the growth solution composed of gold precursors, the v-Au NWs spontaneously formed on the surface of the PDMS micro-pyramids to obtain micro-pyramidal v-Au NWs/PDMS film. Finally, a high-performance tactile sensor was developed by laminating the micro-pyramidal v-Au NWs/PDMS film on the interdigitated electrodes that were made of silver nanoparticles (Ag NPs), showing a high sensitivity of 23 kPa^{-1} over a pressure range of 0–600 Pa. Pan et al. presented a facile method to build a high-performance piezoresistive tactile e-skin device that adopted a sensing layer consisting of highly conductive interfacially self-assembled graphene (ISG) and microstructured PDMS elastomer.[4] As depicted in Figure 5E, a homogenous graphene nanoplatelets dispersion was first sprayed onto the water surface to form uniform Langmuir monolayers at the interface of water and air, and then the ultra-large conductive ISG layer was successfully assembled under the assistance of the capillary force effect. Next, the fabricated conductive ISG layer was transferred onto a PDMS elastomer with microstructures and deposited on that elaborate 3D microstructure after an annealing process. By integrating the microstructured PDMS layer deposited with conductive ISG onto interdigitated Ni/Au electrodes (Figure 5F), the tactile sensor simultaneously realized high sensitivity of 1875.53 kPa^{-1} and a wide linear detection range of 0–40 kPa due to the effective contact area change under pressure loading (Figure 5G). Guo et al. fabricated a sensitive layer of spinosum structured PU coated with MXene conductive layer by using a universal spray approach and proposed a high-performance flexible pressure sensor by assembling such a sensitive layer and MXene-based interdigital electrodes, providing an accurate tactile feedback capability for the manipulator.[61] It is worthwhile to mention that the sensor was also endowed with a self-healing function because of the hydrogen bond of PU.

Different from the above pressure sensors that only involved a top sensing layer composed of polymer microstructures and conductive materials, many researchers also developed another strategy to design pressure sensors by combining two parts of the sensing components including the top and bottom sensing layers.[99,142,143] For instance, Ha et al. demonstrated a tactile sensor incorporating a top sensing layer of Au-deposited PDMS micropillar array and a bottom sensing layer of polyaniline (PANI) nanofibers (Figure 5H).[143] Here, a pair of Ag nanowire stickers were fabricated as electrodes, and the sensing behavior of such a tactile sensor was analyzed. The contact resistance between the surface of the top sensing layer of the Au-deposited PDMS micropillar and the bottom sensing layer of the PANI nanofibers decreases since the vertical applied pressure, which results in a decrease in the total resistance of the sensor. With further increase in the applied pressure, the above-mentioned contact resistance becomes quite lower, and the current tends to flow through the deposited Au film on the surface of the PDMS micropillar, resulting in a sensor with a resistance that is several orders of magnitude lower and with highly improved sensitivity. In addition, Li et al. fabricated a high-performance tactile e-skin by using a top sensing layer of eggshell membranes (CNTs-EM) decorated with CNTs, a bottom resistor layer of PEDOT:PSS thin-film, and a couple of Cu electrodes with micro-fence structures. Benefiting from that, the top sensing layer of CNTs-EM hardly makes contact with the Cu electrode when there is no externally applied pressure.[99] Thus, the bottom PEDOT:PSS layer aims to provide a steady and relatively high initial resistance for the reported e-skin. When loading pressures, the contact area between the top CNTs-EM sensing layer and the microstructured Cu electrode increases, which contributes to a decreased contact resistance and the total resistance value of the tactile e-skin device. Furthermore, the fibers of the CNTs-EM layer are also further compressed under pressures, and the conductive paths between CNTs-EM fibers increase with the increasing contact areas. As a result, the e-skin shows a decreased total resistance value after loading pressures and realizes a super-high sensitivity of 291 699.6 kPa^{-1}. Interestingly, the authors pointed out that the sensitivity of the reported e-skin could be easily adjusted by altering the resistance value of the bottom resistor layer of the PEDOT:PSS thin-film, illustrating that this e-skin is endowed with the adjustable sensitivity indicating its potential use in different applications.

3.2.2 | Tactile e-skins based on piezoresistive sensors with top-bottom electrodes

For the piezoresistive sensors that adopt the top-bottom electrode configuration, surface microstructures are also intentionally introduced on both top and bottom electrode layers to achieve the construction of e-skins with outstanding tactile sensing behaviors.[20,76,144–147,151–154]

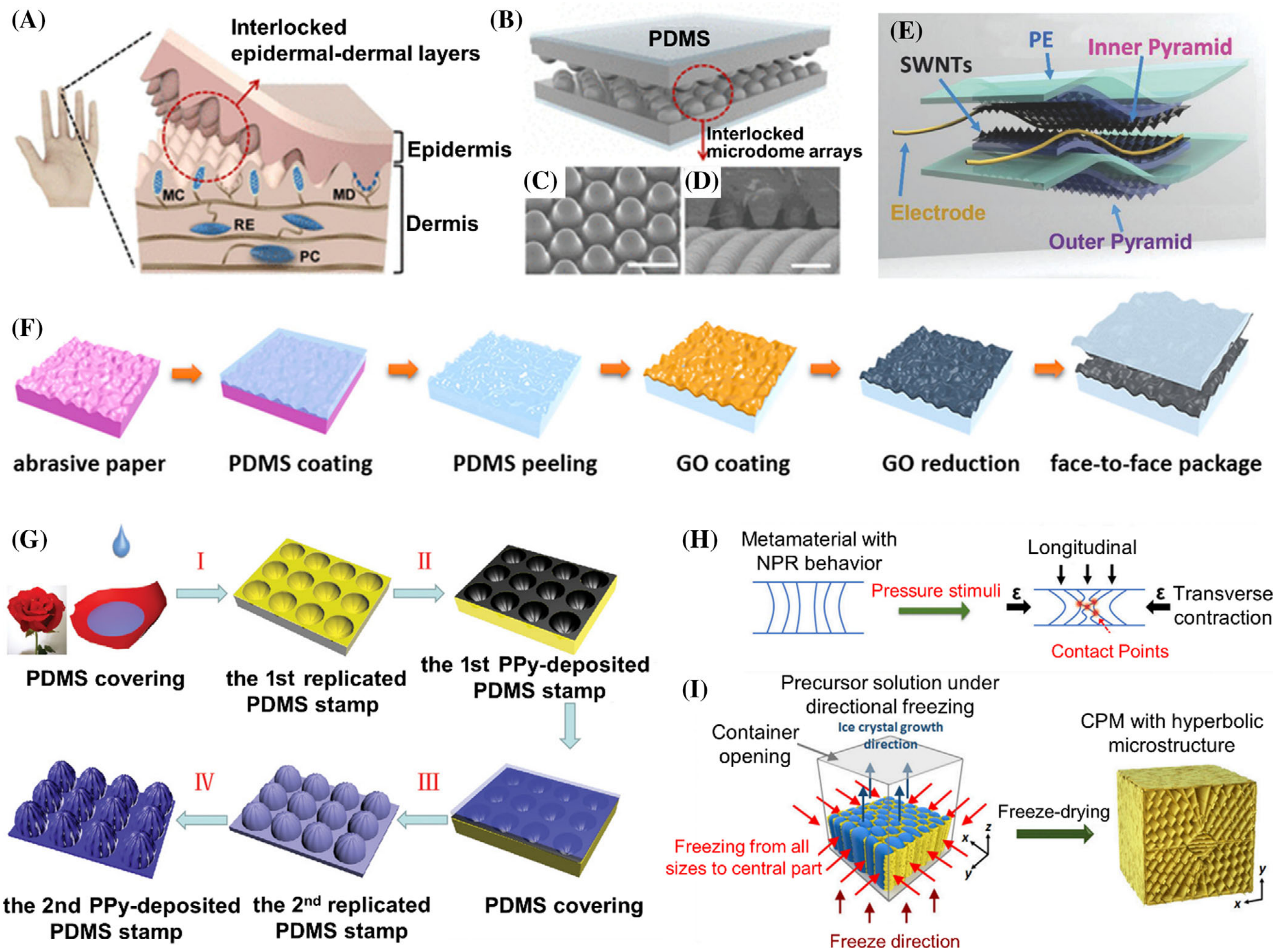

FIGURE 6 (A) Schematic of the epidermal-dermal layers of human skin. (B) Schematic illustration and (C,D) SEM images of the interlocking epidermal-dermal layers of the tactile e-skin. Reproduced with permission.[151] Copyright 2014, American Chemical Society. (E) A flexible tactile sensor consisting of two interlocked sensing layers of CNTs-coated PDMS micro-pyramid arrays, PE substrates, and the outer micro-pyramid PDMS layer. Reproduced with permission.[144] Copyright 2018, Wiley-VCH. (F) Preparation and face-to-face packaging of a flexible pressure sensor using two rGO deposited PMDS films with spinosum-like morphology. Reproduced with permission.[147] Copyright 2018, American Chemical Society. (G) Fabrication of the sensing layer with a multiscale hierarchical structure. Reproduced with permission.[90] Copyright 2020, Wiley-VCH. (H) Illustration of the NPR effect of the materials under pressure. (I) Schematic illustration of the auxetic cellular structured piezoresistive sensor with an NPR effect. Reproduced with permission.[66] Copyright 2022, Elsevier Ltd.

For instance, Suh et al. proposed a simple architecture of two interlocked arrays of high-aspect-ratio Pt-coated ultraviolet-curable polyurethane acrylate (PUA) nanofibers for building a flexible and highly sensitive tactile sensor.[76] It is the key to obtaining excellent tactile perception that numerous tiny contacts are ensured between the conductive Pt layers on both the top and bottom PUA nanofibers. Ko et al. interlocked the top and bottom conductive layers of the CNTs/PDMS composite with a micro-dome array simulating the epidermal-dermal layers in the human skin and presented an excellent tactile e-skin capable of detecting mechanical stimuli including pressure, shear, strain (Figure 6A–D).[151] Inspired by the interlocking epidermis-dermis structure and the outer microstructures of the human fingerprint, a novel flexible tactile sensor (Figure 6E) was designed by Zhang et al. to improve tactile perception, which consisted of two interlocked sensing layers of CNTs-coated PDMS micro-pyramid arrays, polyethylene (PE) substrates, and the outer micro-pyramid PDMS layer.[144] Benefiting from the above unique architecture, such a flexible tactile sensor exhibited highly enhanced sensitivity and proved that it could be applied for the detection of tiny pressure signals such as that of the pulse by attaching it to a finger. However, the above polymer layers with various microstructures like nanofibers, micro-domes, and micro-pyramids were prepared by duplicating the micropatterns of the different silicon templates, and the fabrication of silicon templates involves complicated photolithography and wet etching procedures, which was difficult to realize the large-area, high-quality production of microstructures. Therefore, numerous low-cost and simple approaches to fabricated microstructures on a large scale have been developed and adopted to design advanced tactile sensors. For example, with the assistance of an abrasive paper template, Ren et al. prepared a sensing layer that was composed of a PMDS flexible substrate with a randomly distributed spinosum-like morphology and the deposited conductive reduced graphene oxide (rGO) layer.[147] And then, a flexible tactile sensor was reported by assembling two such identical sensing layers through a face-to-face package (Figure 6F). According to the authors, the sensor achieved a high sensitivity and good linearity due to the random distribution of the spinosum-like microstructures of the sensing layers. In addition, an approach combining the rose petal–templating method and the surface wrinkling process was proposed by Lu et al. to create a sensing layer with a multiscale hierarchical structure of a microstructured PDMS supporting layer and the nanostructured PPy conductive layer.[90] As illustrated in Figure 6G, there are four steps involved in the preparation process of such a multiscale hierarchical structured sensing layer: (1) replicating the 1st PDMS stamp from a rose petal template, (2) depositing and in situ self-wrinkling of the 1st PPy layer on the 1st PDMS stamp (the preparation of the 1st PPy-deposited PDMS stamp), (3) fabricating the 2nd PDMS stamp by replicating the 1st PPy-deposited PDMS stamp, (4) preparing the final multiscale hierarchical structured sensing layer through the deposition and in situ self-wrinkling method of the 2nd PPy layer on the 2nd replicated PDMS stamp. Finally, two multiscale hierarchical structured sensing layers were assembled face-to-face to build a sensor with excellent pressure-sensing performance. The authors pointed out that the sensitivity of such a sensor could be highly boosted under the condition of light illumination owing to photocurrent response and the photothermal effect of the PPy layer. According to the variation of the contact resistance, these sensors have significantly optimized the device sensing performance, which offers opportunities for the construction of high-performance tactile e-skins. To further achieve the rapid changes in contact resistance and a highly sensitive as well as energy-saving piezoresistive pressure sensor, researchers have proposed novel architectures that sandwiched a porous AAO membrane or a thin layer of photoresist (SU-8) with the micro-holes by assembling the two flexible conductive layers face-to-face.[155,156] Here, the porous AAO membrane and the SU-8 layer with micro-holes were used as insulation layers to separate the two conductive layers in the initial state, and the two conductive layers were likely to make contact with each other when loading a tiny pressure, achieving a highly sensitive tactile e-skin device with a zero power consumption when unloading pressures.

Another effective approach for building a highly improved pressure sensor and a high-performance tactile e-skin is to introduce microporous features in the elastic and conductive piezoresistive sensing layers. The same with the situation when we discussed tactile e-skins based on the capacitive mechanism, such porous piezoresistive sensing layers are more easily compressed due to the presence of the microporous features, causing the increase of the changes in the contact area and enhancing the sensitivity of the tactile e-skin.[157–161] For instance, Bao et al. fabricated an elastic microstructured conductive polymer (EMCP) and invented a resistive tactile sensor by sandwiching the EMCP layer between a copper electrode and a PET film deposited with an indium tin oxide (ITO) electrode.[157] Here, a multiphase synthesis technique was used to fabricate the EMCP layer composed of interconnected PPy hollow-sphere structures. First, an oxidative reagent solution was mixed with a mixture of isopropanol, pyrrole monomer, and phytic acid in a petri dish. As a result, an emulsion was obtained because of the phase separation effect between the aqueous and organic bi-component. With the help of the dopant and crosslinker of PPy, PPy polymerization was realized and gelated within $\sim$3 s. Finally, a conductive sensing layer of PPy hollow-sphere structures with 3D porous foam morphology was formed after that the impurities were exchanged with the deionized water and then underwent a drying process. The authors claimed that the hollow-sphere structures formed by such a multiphase reaction endowed the conductive sensing layer of PPy with an effectively decreased elastic modulus and excellent elasticity, and demonstrated that such a sensing layer enabled tactile e-skin could achieve the detection of tiny pressures less than 1 Pa. Guo et al. reported an elastic, high porosity, and robust composite aerogel of PPy and rGO via a sol–gel approach in combination with a hydrothermal reduction process.[161] Benefiting from the strong π–π interactions between PPy and rGO, such a composite aerogel exhibited an enhanced interfacial strength and was able to maintain good film integrity. A number of electrically conductive paths would be created in the composite aerogel due to high porosity and the increased contact area between the conductive components when external pressure was applied, resulting in a highly sensitive wearable piezoresistive device. In addition, considering the advantages of hybrid porous microstructures fabricated from *Epipremnum aureum*

TABLE 3 Typical polymer materials-based tactile e-skins with high performances (including piezoelectric and TENG tactile e-skins).

	Fabrication method	Device size	Sensitivity	Power density	Refs.
Piezoelectric					
Piezoelectric polymers	Si template	—	1.62 V kPa^{-1}	—	[20]
	Spin-coating and copolymer	0.09 cm^2	7 V (V_{oc})	3.92 μW cm^{-2}	[169]
	Polymerization	25 × 15 mm^2	228.2 mV N^{-1}	1.68 μW cm^{-2}	[170]
	AAO template	—	5 V (V_{oc})	151.6 nW m^{-2}	[68]
Polymer substrate with inorganic piezoelectric material	Hydrothermal	1 × 1 cm^2	403 mV MPa^{-1}	—	[171]
	Si template and hydrothermal	1 × 1.5 cm^2	—	5.9 mW m^{-2}	[172]
	Electrospinning	—	3.12 mV kPa^{-1}	—	[173]
Piezoelectric composite materials	Nanoimprinting	1 cm^2	257.9 mV N^{-1}	12.7 μW cm^{-2}	[174]
	Electrospinning	1 × 1 cm^2	9.5 mV/10^5 Pa^{-1}	—	[175]
	Electrospinning	1.8 × 2 cm^2	3.95 V N^{-1}	—	[176]
TENG					
Vertical contact-separation mode	PS sacrificial template	1 × 1 cm^2	—	2.45 μW cm^{-2}	[24]
	Si template	5.4 cm^2	18 V (V_{oc})	2.34 μW cm^{-2}	[177]
	Self-assembly	2 × 3 $in.^2$	1200 V (V_{oc})	313 W m^{-2}	[178]
	Si template	3 × 2.8 cm^2	230 V (V_{oc})	3.56 mW cm^{-2}	[179]
Contact-sliding mode	ICP reactive ion etching	71 × 50 mm^2	1300 V (V_{oc})	5.3 W m^{-2}	[180]
	ICP reactive ion etching	40.54 cm^2	230 V (V_{oc})	1 W m^{-2}	[181]
Single electrode mode	Infiltration and coating	5 × 5 cm^2	5.2 mV Pa^{-1}	21.5 μW m^{-1}	[10]
	Electrospinning	1 × 1 cm^2	0.18 V k Pa^{-1}	85.4 mW m^{-2}	[61]
	Pre-stretching and coating	6 × 3 cm^2	0.08 kPa^{-1}	4.06 mW m^{-2}	[79]
	Laser cutting	16 cm^2	0.06 kPa^{-1}	—	[182]
	Si template	1 × 1 cm^2	0.29 V kPa^{-1}	500 mW m^{-2}	[183]

Abbreviations: hydrothermal, special low-temperature hydrothermal process; ICP, inductively coupled plasma; V_{oc}, open circuit voltage.

leaf and sugar templates, Zhang et al. proposed a highly sensitive tactile e-skin by using such hybrid porous microstructures sensing layer.[158] Compared with the above complex fabrication processes, conductive porous sponge structures combining polymer elastomer with good mechanical ability and conductive materials are commonly used to fabricate the microporous piezoresistive sensing layers for developing high-performance tactile e-skin due to the facile and low-cost preparation process.[66,162–168] For example, by repeatedly dip-coating a PU sponge in a mixture solution of conductive cellulose nanofibril (CNF)/Ag NWs, Guo et al. prepared a conductive CNF/Ag NWs-coated PU (CA@PU) sponge and designed a CA@PU e-skin to demonstrate promising application prospect in detecting human body motion.[162] Through the same dip-coating method, Zhu et al. modified the polyimide scaffolds with conductive graphene layers and prepared a graphene sponge with a 3D microstructure to assemble a tactile e-skin device with excellent flexibility and high sensitivity.[163] Recently, different from the above porous piezoresistive sensing layers that presented a positive Poisson's ratio (PPR) phenomenon, Liang et al. proposed an auxetic cellular structured piezoresistive sensing layer with a negative Poisson's ratio (NPR) and significantly improved the sensing behaviors of the piezoresistive tactile sensor (Figure 6H,I).[66] According to the authors, the NPR effect of the auxetic cellular structure enhanced the mechanical elasticity and durability compared with the PPR phenomenon of the conventional structures, giving rise to a sensor showing outstanding stability and reliability even though performing more than 5000 cycles of repeated compressive deformation.

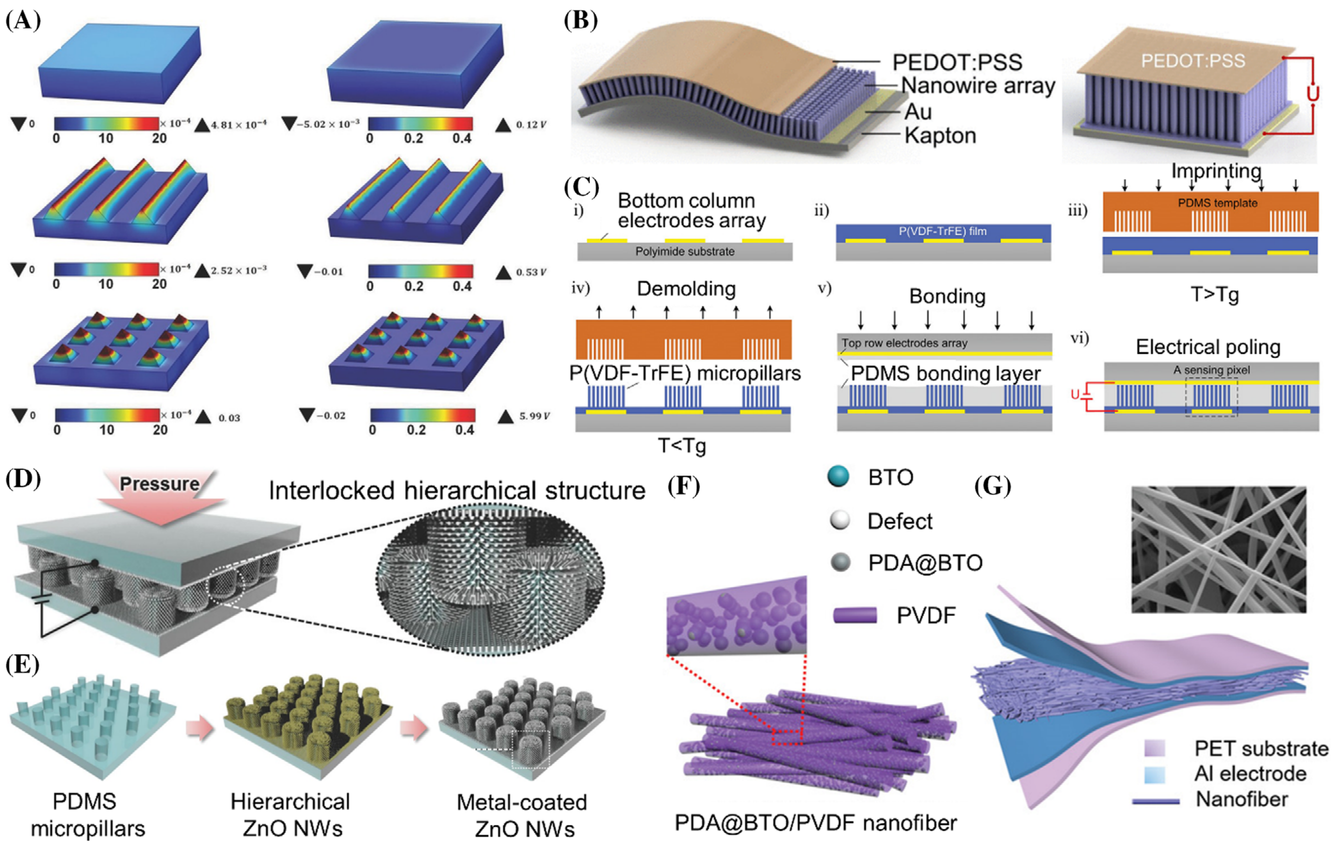

FIGURE 7 (A) COMSOL simulation of strain distribution and output voltage results of the flat, trigonal line-shaped, and pyramid-shaped P(VDF-TrFE)-based pressure sensors under the pressure. Reproduced with permission.[185] Copyright 2015, Wiley-VCH. (B) Schematic of the tactile e-skin exploiting the P(VDF-TrFE) piezoelectric layer with nanowire structures. Reproduced with permission.[68] Copyright 2014, IEEE. (C) Detailed preparation process of a nanoimprinting method for fabricating the P(VDF-TrFE) nanowire-based piezoelectric pressure sensor. Reproduced with permission.[186] Copyright 2020, Wiley-VCH. (D) Schematic illustration of the tactile e-skin based on the interlocking piezoelectric layers of the metal-coated ZnO NWs on PDMS micropillars. (E) Fabrication of the piezoelectric layer of the metal-coated ZnO NWs on PDMS micropillars. Reproduced with permission.[172] Copyright 2015, Wiley-VCH. (F) Schematic and SEM image of the PDA-modified BTO/PVDF electrospinning nanofibers. (G) Human muscle–fiber-inspired piezoelectric wearable device developed by the PDA-modified BTO/PVDF electrospinning nanofibers. Reproduced with permission.[176] Copyright 2020, Wiley-VCH.

3.3 | Tactile e-skins based on piezoelectric sensors

Benefiting from the piezoelectric effect of the piezoelectric materials, the piezoelectric sensor does not need an external power supply to respond to the pressure information and has been widely used to build high-performance self-powered tactile e-skins (Table 3). Common piezoelectric polymer materials such as PVDF and P(VDF-TrFE) present fascinating piezoelectric properties and high flexibility, which have been paid increasing attention in the field of fabricating flexible piezoelectric tactile e-skins.[20,68,169,170,184–186] Kim et al. demonstrated a flexible piezoelectric tactile e-skin with a high power-generating performance by adopting micropatterned P(VDF-TrFE) film as the piezoelectric material layer.[185] The voltage outputs of the P(VDF-TrFE) piezoelectric tactile e-skins with the trigonal line-shaped and pyramid-shaped micropatterns were measured and compared with that of the nonpatterned P(VDF-TrFE) e-skin, observing that the introduction of microstructures in P(VDF-TrFE) piezoelectric film contributed to an obvious enhancement in the output voltage and current. Meanwhile, a COMSOL simulation was further conducted to prove that the pyramid microstructured P(VDF-TrFE) film exhibited a higher strain variation than the other two P(VDF-TrFE) films, resulting in a stronger output voltage and current signal (Figure 7A). In addition, P(VDF-TrFE) piezoelectric layers with nanowire and micropillar structures were fabricated by the nanoimprinting method and were developed to construct tactile sensors for satisfying the requirements of e-skins (Figure 7B).[68,186] Figure 7C presents the steps of such a nanoimprinting method for the preparation of a flexible piezoelectric tactile sensor assembled by the P(VDF-TrFE) nanowire structures. First, a spin-coating process was performed to deposit a thickness of 4–5 μm P(VDF-TrFE) film on the surface of the Au-coated Kapton substrate and then pressed with an AAO porous template under a temperature of 170°C. After that, free-standing P(VDF-TrFE) nanowire structures were fabricated by successively immersing the AAO template in $CuCl_2$ and HCl mixed solution and NaOH solution to remove it. Lastly, a polymethyl methacrylate (PMMA) layer for avoiding short circuit and a top flexible PEDOT:PSS conducting electrode were sequentially deposited on top of the P(VDF-TrFE) nanowires by using spin-coating processes, and the P(VDF-TrFE) nanowires-based piezoelectric tactile sensor was successfully obtained.

In fact, compared with the piezoelectric polymer materials, inorganic piezoelectric materials involving lead zirconate titanate (PZT), ZnO, and BTO present a much higher piezoelectric coefficient (d_{33}) which is a physical parameter to evaluate the energy conversion efficiency of piezoelectric materials.[187–189] However, considering their inherently hard and brittle properties, single and bulk inorganic piezoelectric films are unsuitable for building flexible and wearable tactile e-skins. Therefore, considerable researchers have developed nanoscale inorganic piezoelectric materials such as ultrathin membranes, nanorods, nanowires, and nanofibers to be aligned with a flexible polymer matrix.[19,171,190] For instance, Rogers et al. proposed a thin conformable piezoelectric tactile sensor by connecting an ultrathin (400 nm) PZT piezoelectric membrane supported by a flexible PI substrate to the gate electrode of a MOSFET that was composed of silicon nanomembranes (SiNMs).[190] Here, the coupling of the SiNMs-based MOSFET and the PZT piezoelectric membrane could effectively amplify the voltage response of this pressure sensor, enabling low hysteresis and highly sensitive measurements for human arterial pulse signals. Further, Yang et al. demonstrated a self-powered e-skin device that was composed of the piezoelectric tactile sensor array of the ordered ZnO nanorods (NRs) on a flexible Kapton substrate, which offered accurate and reliable tactile sensory feedback for hand prostheses.[171] The preparation process of such a self-powered tactile sensor array was systematically described. First, a 300-nm thick copper film was deposited as the bottom electrode layer on the surface of the flexible Kapton substrate by using an evaporation technique. Next, an RF-magnetron sputtering process was performed to form a seed layer of ZnO with a thickness of ∼100 nm on the bottom electrode layer. By immersing the substrate deposited with the bottom electrode and ZnO seed layer into a mixture solution of $Zn(NO_3)_2 \cdot 6H_2O$ and hexamethylenetetramine, the ordered ZnO NRs were synthesized on the ZnO seed layer after a low-temperature hydrothermal process. After that, a thin and flexible PMMA layer was spin-coated on the top surface of the synthesized ZnO NRs structures, followed by the deposition of the top copper electrodes that presented the same shape and size ($1 \times 1\ cm^2$). To offer flexible mechanical support, the moisture and dust resistance capability, the author packaged all the above components with PDMS, and the final tactile sensor array was successfully assembled. In addition to selecting the plat polymer film as the flexible supporting layer, researchers have introduced nanoscale inorganic piezoelectric materials into polymer substrates designed with microstructures to effectively enhance the deformation ability of the functional layer and achieve high-performance piezoelectric tactile sensors. For example, Ko et al. decorated PDMS micropillars with ZnO NWs arrays to fabricate a hierarchical micro- and nano-structured piezoelectric layer and then adopted such a piezoelectric layer to develop a tactile e-skin, as illustrated in Figure 7D,E.[172] Benefiting from the design of interlocked and hierarchical structures, the developed tactile e-skin exhibited a strong piezoelectric voltage response toward extremely small dynamic stimuli involving minute vibration and sound stimuli. Yang et al. presented a highly sensitive piezoelectric tactile e-skin based on the 3D PVDF/ZnO core-shell nanofibers fabricated by an epitaxial growing process of ZnO NRs on PVDF nanofibers.[173] It is worth noting that the high flexibility and air permeability enabled by such a special structure endows this piezoelectric sensor with high wearable comfort when used it for physiological monitoring.

Alternatively, the strategy of the piezoelectric composite materials that combine the advantages of both inorganic piezoelectric materials and polymer materials has been adopted by researchers to enable piezoelectric sensors with enlarged output performance, high sensitivity, and excellent flexibility.[174–176,191] For instance, Shao et al. fabricated a piezoelectrically enhanced nanocomposite layer by embedding inorganic BTO nanoparticles in a highly flexible P(VDF-TrFE) micropillar array polymer and demonstrated a high-performance piezoelectric pressure sensor for the energy harvesting and self-powered sensing.[174] In general, to obtain such a composite material, P(VDF-TrFE) powder and BTO nanoparticles were dispersed in N, N-dimethylformamide (DMF) solution accompanied by ultrasonic stirring and formed a uniform P(VDF-TrFE)/BTO mixture. Then, the P(VDF-TrFE)/BTO mixture was coated on the Au bottom electrode supported by a flexible Kapton substrate and hot pressed by a PDMS mold at 160°C for 1 h to fabricate P(VDF-TrFE)/BTO composite micropillar array. After an annealing process and PDMS mold removal, the crystallinity of P(VDF-TrFE) was improved, and a piezoelectrically enhanced

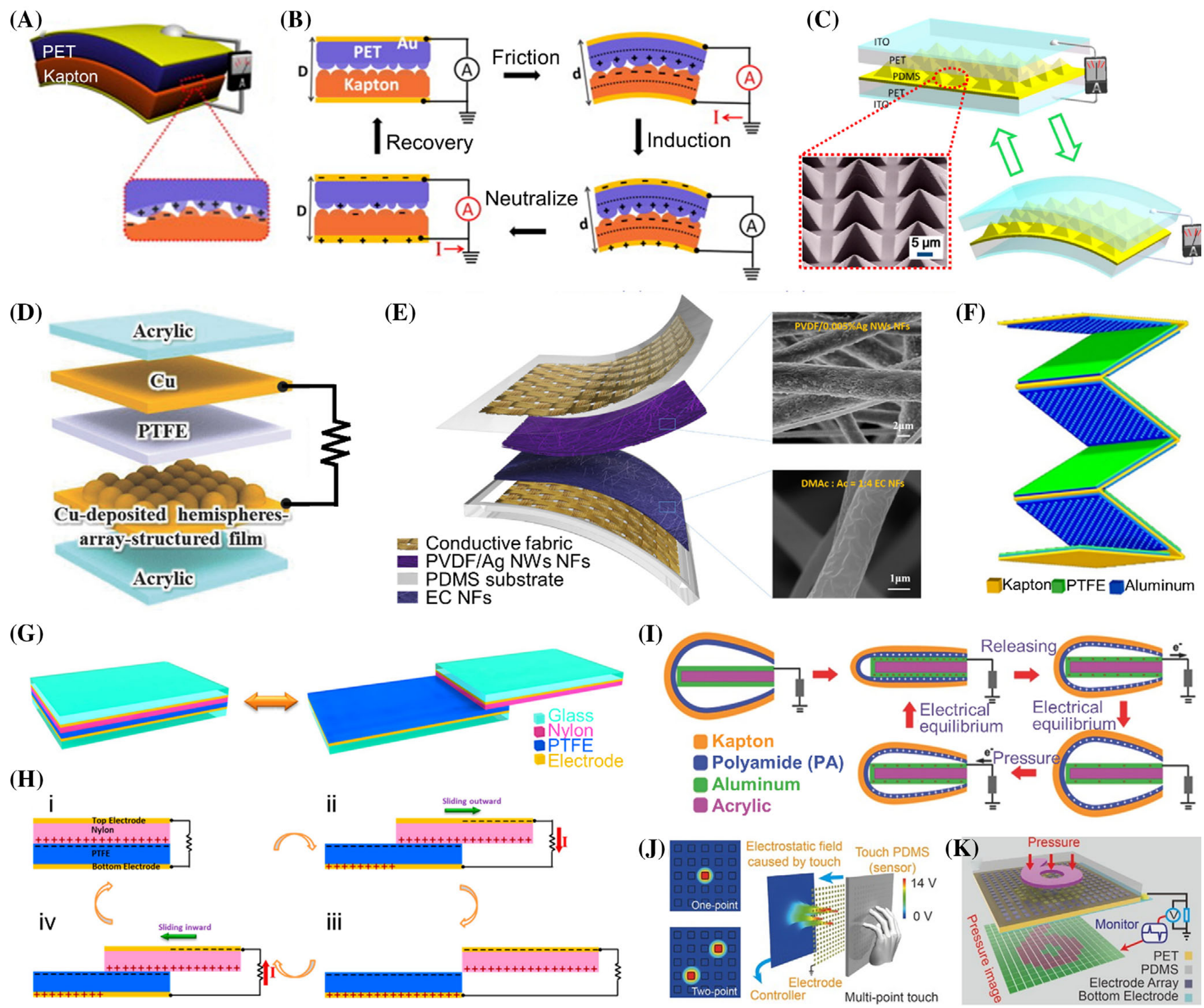

FIGURE 8 (A) Schematic and (B) working principle of a TENG sensor in vertical contact-separation mode Reproduced with permission.[194] Copyright 2012, Elsevier Ltd. (C) Illustration of a TENG sensor using a pyramid-structured PDMS functional layer and SEM image of the pyramid-structured PDMS. Reproduced with permission.[69] Copyright 2012, American Chemical Society. (D) Schematic illustration of a hemispheres-array-structured TENG sensor. Reproduced with permission.[24] Copyright 2016, Wiley-VCH. (E) A self-powered pressure sensor including two friction layers of PVDF/Ag NW NFM and EC NFM. Reproduced with permission.[197] Copyright 2019, American Chemical Society. (F) A TENG that stacks five layers of triboelectrification units. Reproduced with permission.[196] Copyright 2013, American Chemical Society. (G) A typical example and (H) working mechanism of a TENG sensor based on the contact-sliding mode. Reproduced with permission.[180] Copyright 2013, American Chemical Society. (I) Working behavior of a single-electrode TENG sensor. Reproduced with permission.[23] Copyright 2013, Wiley-VCH. (J) Schematic illustration of the mapping process of the tactile information pressure-sensitive sensor matrix. (K) Mapping of the tactile information pressure-sensitive sensor matrix under a module in the shape of a "6". Reproduced with permission.[182] Copyright 2016, Wiley-VCH.

microstructured composite layer based on the P(VDF-TrFE)/BTO micropillar array was obtained. Finally, for guaranteeing electric stability and mechanical durability of the piezoelectric pressure sensor, a PDMS insulation layer was coated on top of the P(VDF-TrFE)/BTO micropillar array before coating the multiwalled carbon nanotube (MWCNT) as the top electrode layer. Inspired by the human muscle–fiber structure, Su et al. achieved a piezoelectric composite layer with outstanding sensitivity by dispersing polydopamine (PDA) into electrospinning BTO/PVDF composite nanofibers (Figure 7F,G), and demonstrated the promising application in personalized healthcare such as monitoring pulse.[176] According to the authors, the introduced PDA could contribute to the physical contact and stress transfer efficiency between the inorganic BTO piezoelectric fillers and the flexible

PVDF matrix in such composite nanofibers, which boosted the mechanical strength and electromechanical coupling efficiency of such piezoelectric composite layers.

3.4 | Tactile e-skins based on triboelectric sensors

Since Wang et al. first reported a seminal work on TENG in 2012,[192] TENG utilizing the coupling effects between triboelectrification and electrostatic induction has attracted considerable attention in the construction of self-powered tactile sensors and wearable e-skins.[177,187,193,194] Polymer materials such as Kapton,[69,177] PET,[178] PDMS,[179] Ecoflex,[195,196] PVDF,[197,198] and others have been widely adopted to work as triboelectrification materials or the flexible substrate layer to support the device. According to the different operation modes, vertical contact-separation mode, contact-sliding mode, and single-electrode mode three different TENGs are invented.[69] And, we have summarized the fabrication methods and performance comparison on these three different TENGs devices, as shown in Table 3.

3.4.1 | Vertical contact-separation mode

Figure 8A presents a typical example of an all-polymer-based TENG sensor in vertical contact-separation mode,[194] in which two films (PET and Kapton) with different triboelectric properties were stacked and then metal electrodes on the top and bottom of these two polymer films are deposited. Figure 8B schematically illustrates the working mechanism of this TENG device. When loading pressure to the TENG sensor, the PET and Kapton films are contacted and rubbed with each other, resulting in the distribution of opposite electrical charges on the surfaces of these two films because of their different abilities to capture electrons. After releasing the pressure, the PET and Kapton films are separated, and the compensating charges are induced on the two electrodes, which gives rise to a potential difference between the top and bottom electrodes. Based on the working principle of the above TENG sensor, Wang et al. studied the effect of the surface structure and morphology of the functional layer on nanogenerator efficiency by fabricating three kinds of TENG sensors using differently patterned PDMS films (line, cube, and pyramid).[69] The pyramid microstructured PDMS film-enabled TENG tactile sensor exhibited the largest power generation and far surpassed the sensors made of non-microstructured PDMS films, which can be interpreted that the triboelectric effect and the generated surface charges during the friction progress are significantly improved for the pyramid microstructured PDMS film. A flexible, transparent, and high-performance TENG tactile sensor with an output voltage (up to 18 V) and current (~0.7 μA) was thus developed by using such a pyramid microstructured PDMS as the electrification layer (Figure 8C), showing its promising applications in future personalized electronics applications such as self-powered touchscreens and electronic displays. Kim et al. presented a packaged TENG tactile sensor based on a hemispheres-array-structure (Figure 8D) and demonstrated its excellent mechanical durability, good robustness.[24] By optimizing the structure and nanoscale surface modification, Wang et al. realized a TENG tactile e-skin device with an ultrahigh electric output (1200 V).[178] Here, two PMMA layers were performed as the top and bottom substrates owing to their excellent mechanical strength, lightweight, and easy processing. On the surface of the upper PMMA substrate, a thin Au film and a PDMS film were successively prepared as the top electrode layer and negative friction layer, respectively. A contact electrode layer consisting of the thin Au film and Au nanoparticles was fabricated on the bottom PMMA substrate, which performed dual roles of the bottom electrode and positive friction layer. Lastly, two PMMA substrates were connected by installing four springs, and a spacing between the PDMS film and the contact electrode layer was created, enabling a fixed separation distance between them in the contact-separation process. In addition, Wang et al. developed a reasonable arch-shaped TENG sensor by respectively designing pyramid patterns on the PDMS negative friction layer and cubic patterns on the Al positive friction layer.[179] The output electrical energy of this sensor could be used to continuously drive light-emitting diodes (LEDs) and charge lithium-ion batteries to power a commercial cell phone or even a wireless sensor system.

Apart from introducing various designed surface microstructures in friction layers of TENG,[178,179,195,196] TENG tactile sensors of the nanofibers-based friction layers that are fabricated through a facile electrospinning method have been widely explored in recent years.[197,198] Ding et al. reported an all-fiber-structured self-powered pressure sensor,[197] two friction layers of which are the nanofibrous membrane of PVDF/Ag NW (PVDF/Ag NW NFM) and an ethyl cellulose nanofibrous membrane (EC NFM), respectively, as shown in Figure 8E. Two types of homogeneous precursors of the mixed solutions containing PVDF/Ag NW and EC were first prepared, and then an electrospinning technology was performed for the fabrication of the PVDF/Ag NW NFM and EC NFM. After that, the electrospun PVDF/Ag NW NFM and EC NFM were thus obtained. And two conductive fabric layers were pasted onto the back side of these two electrospun films to work as electrode layers. Finally, by respectively placing the PVDF/Ag NW NFM and EC NFM pasted with electrodes onto the surface of the PU and PDMS substrates, the self-powered TENG pressure sensor assembly was completed. According to the authors, the introduction of Ag NWs in the PDVF NFM and the extremely rough surface morphology of the EC NFM were beneficial for improving the surface charge potential and induced triboelectric charges, which contributed to the enhancement in performance and sensing capability of the self-powered TENG tactile e-skin. Brugger et al. developed a wearable hybrid piezoelectric-enhanced TENG tactile sensor by exploiting the friction layers of electrospun silk fibroin nanofibers and PVDF nanofibers, realizing the harvesting of mechanical energy and the self-powered detection of human body motion.[198] In light of the large specific surface area offered by the nanofiber structures and the remarkable capability to donate electrons of the silk fibroin during the triboelectrification process, such a hybrid piezoelectric-enhanced TENG tactile sensor exhibited excellent output performance, enabling a high power density of 310 μW/cm^2. Since the conducting fabrics were selected as the top and bottom electrodes, the novel all-fiber configuration of such a hybrid piezoelectric-enhanced TENG sensor not only shows a flexible appearance but is also accompanied by a good air permeability, which is essential for designing and building wearable and comfortable tactile e-skin devices. The literature discussed thus far involved only a single layer of triboelectrification unit, which presented a big challenge for substantially scaling up the output power density of the TENG tactile sensor. To address this issue, Wang et al. presented an innovative design of a TENG tactile sensor where multiple triboelectrification units were stacked on the same substrate, achieving a multifold higher output power density of the TENG tactile sensor.[196] As shown in Figure 8F, five layers of triboelectrification units were used in such a TENG sensor. For each layer of the triboelectrification unit, an Al electrode on the polytetrafluoroethylene (PTFE) thin film serves as the negative friction layer, while a nanopore microstructured Al foil works as the other electrode and the positive friction layer. In this way, such a TENG sensor achieved an instantaneous current reaching 0.66 mA and an output voltage of 215 V at an instantaneous maximum power density of 9.8 mW/cm^2.

3.4.2 | Contact-sliding mode

Figure 8G shows the configuration schematic of a TENG sensor based on the contact-sliding mode.[180] Here, Nylon and PTFE are respectively utilized as the positive and negative friction layers. As depicted in Figure 8H-i, the contact triboelectrification process of such a TENG sensor is similar to that in the vertical contact-separation mode. Once the Nylon and the PTFE relatively slide to each other (Figure 8H-ii), the contact surface area between the Nylon and PTFE decreases. Then, the opposite charges are electrostatically induced on the surfaces of the top and bottom electrodes, generating a potential difference between electrodes and driving a current flow from the top electrode to the bottom electrode. And, the generated potential difference constantly increases until the Nylon layer slides out of the PTFE layer (Figure 8H-iii). When the Nylon and PTFE layers are in contact again, positive charges on the Nylon surface and negative charges on the PTFE surface cancel each other (Figure 8H-iv), and the redundant induced charges on the electrodes flow away through the external load to keep the electrostatic equilibrium. In fact, due to the necessary condition of the relative sliding between two different friction material layers, only a few research works on the construction of tactile e-skins adopted such a TENG sensor based on the contact-sliding mode.[180,181,199]

3.4.3 | Single-electrode mode

Different from the above two situations, the TENG sensor based on a single-electrode mode is straightforward, where only one functional layer and electrode layer connected to the ground are needed.[10,200,201] Figure 8I shows the working principle of a typical single-electrode TENG sensor.[23] Here, the Al film deposited on a flexible acrylic substrate layer is simultaneously used as the electrification layer and electrode layer. A counter friction layer, polyamide (PA) film, was utilized to contact the Al foil for analyzing the contact sensing behaviors and electrical output performance of such a single-electrode TENG sensor. When applying pressures, the PA film contacts the Al layer, and charge transfer between these two layers is triggered because of the different triboelectric properties. As a result, the negative charges are injected from PA film into the Al layer, leaving positive charges on the PA film. Once the pressure is released, with the help of the elasticity of the Kapton supporting layer, the PA film immediately separates from the Al layer. Negative charges would flow from the Al layer to the ground through an external load, and an electrical current and an output voltage could be observed on the load. Subsequently, when the sensor is pressed and the PA film contacts the Al layer again, negative charges tend to flow from the ground to the surface of the Al layer to balance the positive charges on the PA film, which induces an

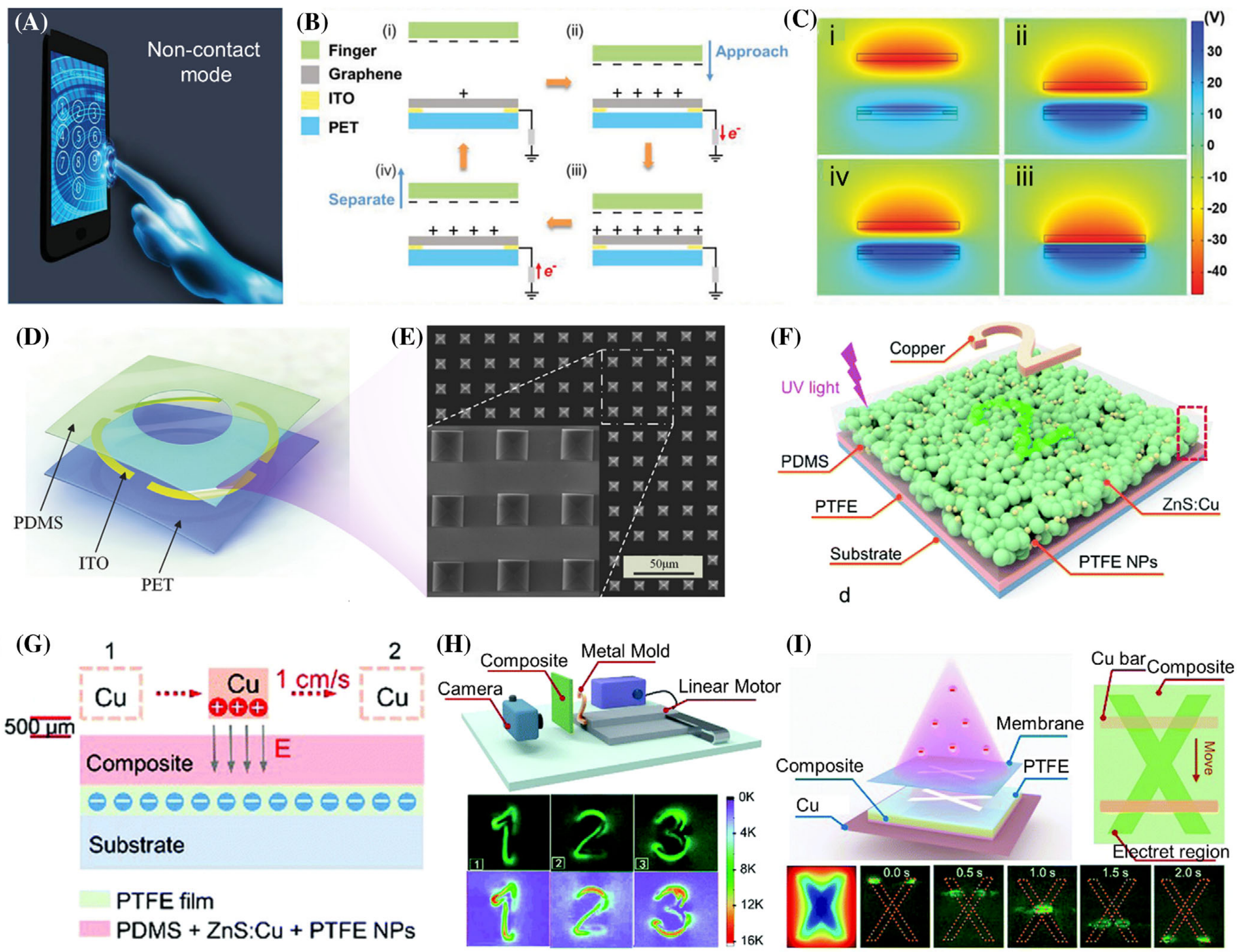

FIGURE 9 (A) Image showing that the TSS works in the non-contact mode for the application of smartphone unlocking interface. (B) Working mechanism of the TSS device in the non-contact operating mode. (C) COMSOL simulation on the electrical potential distributions of the TTS device. Reproduced with permission.[204] Copyright 2019, Wiley-VCH. (D) Schematic illustration of a self-powered e-skin with non-contact sensing capability. (E) SEM image of the self-powered e-skin. Reproduced with permission.[70] Copyright 2017, Wiley-VCH. (F) Schematic illustration of the device structure of the NCIVS. (G) Working principle of the NCIVS. (H–I) Demonstrations of the NCIVS in non-contact sensing application. Reproduced with permission.[27] Copyright 2020, Royal Society of Chemistry.

electrical current and output voltage in the opposite direction. In light of the simple device layout and fabrication process, increasingly works based on such single-electrode TENG tactile sensors have been explored to build the advanced, self-powered, high-performance tactile e-skins in the past years.[23,61,79,182,183,202,203] Pan et al. proposed a self-powered, sensitive tactile e-skin based on the single-electrode TENG arrays that are composed of the PDMS electrification layer and Al electrode layer, achieving the accurate detection and real-time mapping of the tactile information (Figure 8J,K).[183] The same with the former vertical contact-separation mode, various microstructures such as wrinkled PEDOT:PSS, pyramid PDMS, and PVDF nanofibers have been adopted to optimize the electrical output performance of such single-electrode TENG tactile e-skins. And, the obtained TENG tactile e-skin was demonstrated to realize the high-performance active tactile perception, and the array of these e-skins was also widely used in the fields of smart robots, artificial prosthetics, and human-machine interface applications.

4 | POLYMER MATERIALS ENABLED NON-CONTACT E-SKINS

As we previously discussed, to effectively avoid the direct abrading of functional materials and the contact infection of various hazardous viruses, it is highly desired and meaningful to apply the non-contact e-skins to the human–machine interfaces. Currently, many non-contact working principles and mechanisms have been embraced to design and construct e-skins that could achieve non-contact information perception, which attracted tremendous interest in the past few years. For example, the coupling effects of triboelectric and electrostatic induction were proved to be capable of detecting the motion of the charged object over its surface as a non-contact working principle.[70,82,204–206] Human body is easily charged with negative charges by the triboelectric effect between the shoes and the ground, and these charges usually gather at the fingertips because of the tip effect. Accordingly, Tang et al. reported a touch-free screen sensor (TSS) that enabled the recognition of diverse gestures in a non-contact operating mode (Figure 9A).[204] In specific, when the charged human fingertip approaches the TSS, the different polarity charges would be electrostatically induced on the surface of the TSS, and thus the output voltage and current signals of the TSS were observed (Figure 9B,C). As a demonstration, an array involving 10 TSS sensor units was fabricated to correspond to the 10 numbers from 0 to 9 on the smartphone unlocking interface. As a result, the smartphone interface was successfully unlocked by the human finger motion in a non-contact operating mode, which shows the considerable potential of such a TSS in establishing future non-contact human-machine interfaces. Also, Zhang et al. presented a self-powered e-skin with a fascinating non-contact sensing behavior and illustrated its capability to detect the movement of the electrified object across the plane that is parallel to the device.[70] Figure 9D illustrates the structure schematic diagram of the e-skin, which consists of a transparent substrate layer of PET film, four ITO electrodes where each electrode is in the shape of a quartered annulus, and the microstructured PDMS film (Figure 9E). Before working in the non-contact mode, the object that was attached with the above micro-structured PDMS film was performed to contact and separate with a PET film for several times, giving rise to accumulate triboelectric negative charges on the surfaces of the micro-structured PDMS. After that, the electrified object is capable to complete the several cycles of non-contact sensing, which was based on the electrodes potential variations when changing the distance between the electrified object and the electrodes.

However, a triboelectric process based on contact and separation is required for the above non-contact e-skins to obtain an electrified object,[70,204–206] which is undesirable for developing advanced technologies and constructing high-performance non-contact e-skins. Therefore, considering that the electret retains the charge for a long time and the surface charge distribution being uniform, Zhang et al. realized self-powered non-contact sensing based on the electrostatic induction of an electret.[207] First, the patterned PDMS-Ag NWs thin films were fabricated by using the spray coating method and stacked to comprise the e-skin in the overlapped electrode-substrate configuration, where five Ag NWs electrodes in the same layer are parallel to each other and perpendicular to the five Ag NWs electrodes in different layers. Next, the charge injection process of the PTFE electret was performed by high voltage corona-charging, which was attached to the surface of the moving object. Once the object moves, the injected charges in the PTFE electret result in the electric field distribution and the electric potential is generated on the electrode of the e-skin. The authors pointed out that the center of the electronic skin could be regarded as the origin of a two-dimensional rectangular coordinate system, and the generated electric potential of each electrode becomes the function of the position of the moving object. Lastly, according to the variation of the electric potential of each electrode, the proposed e-skin successfully achieved the detection of the planar linear displacements in non-contact mode. Zhu et al. developed a novel interactive visualized sensor (NCIVS) in non-contact sensing mode by incorporating a PET substrate layer, a negatively charged electret layer of PTFE film, as well as a luminescent layer of PDMS matrix, PTFE NPs, and ZnS:Cu particles (ZCPs) (Figure 9F).[27] Due to the existence of the negatively charged electret layer, when a floating conductive object (Cu) moves over the NCIVS, positive charges would be induced on the bottom surface of the Cu, which gives rise to an alternating current (AC) electric field between the floating conductive object and electret layer (Figure 9G). Such an AC electric field induced by the movement of a floating Cu could be utilized to modulate the photon-excited emission of the luminescent layer, successfully realizing the demonstration of the visualization of the contour of the floating conductive object (Figure 9H,I).

Alternatively, the outstanding humidity sensing characteristic of some materials is also considered as a promising way to offer opportunities to develop state-of-the-art technology for building the non-contact e-skins.[30,32,64,208–210] For instance, Yang et al. decorated the electrospinning nanofibers of polyamide 66 (PA66) with the two-dimensional (2D) multilayer graphene (MG) and reported a non-contact e-skin device with a high-performance humidity sensing behavior, demonstrating its application potential in the remote detection of human health information and noncontact control systems (Figure 10A).[32] As the authors analyzed, the synergistic effect of the large specific surface area offered by the PA66 nanofiber and the copious water-absorbing functional groups contributes to a dramatic variation in

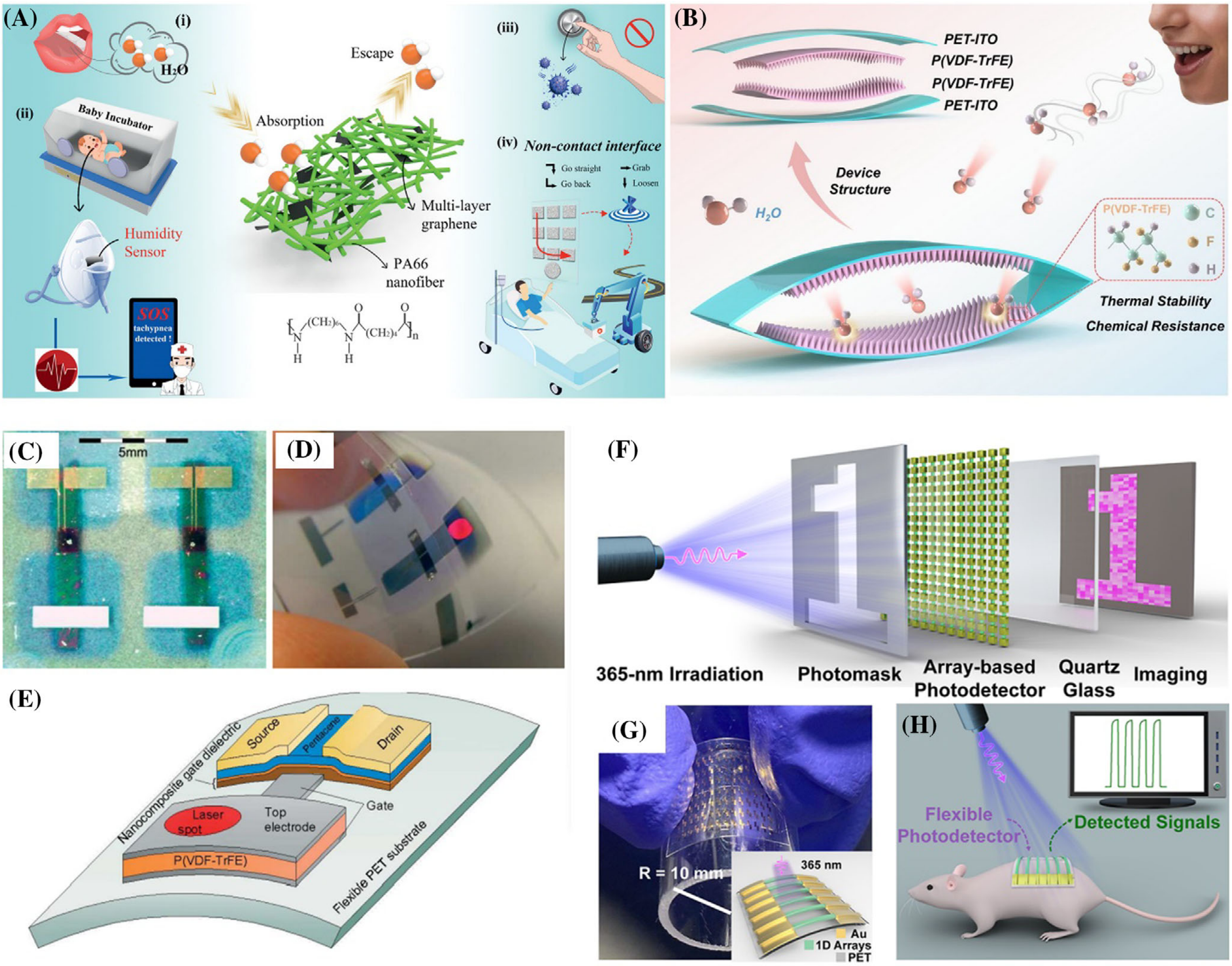

FIGURE 10 (A) Demonstration of the potential application of a flexible humidity sensor and arrays in the remote detection of human health information and non-contact control systems. Reproduced with permission.[32] Copyright 2021, Wiley-VCH. (B) Schematic illustration of a flexible capacitive humidity sensor based on a novel arc-shaped hollow structure. Reproduced with permission.[71] Copyright 2021, Elsevier Ltd. (C) Microscope image and (D) photo of the optothermal sensor as a light-activated switch. (E) Schematic illustration of the integrated optothermal sensor composed of a transistor device and pyroelectric polymer sensor. Reproduced with permission.[211] Copyright 2021, Wiley-VCH. (F) An array composed of 14 × 18 polymer array-based photodetectors for application in image sensing. (G) Photograph and schematic illustration of the array with excellent mechanical flexibility. (H) Schematic of the demonstration of the flexible array as a wearable electronics in monitoring UV photodetection signals. Reproduced with permission.[212] Copyright 2022, American Chemical Society.

the contiguous MG conductive networks and results in a highly sensitive humidity sensing performance. Benefiting from that, such a humidity sensor was mounted on the inside of the mask of a volunteer, and the measured variations in the conductive properties of the sensor could be utilized to monitor the respiratory-related information because the exhaled air from the volunteer carried water vapor molecules. In fact, there also exists a humidity field near the surface of the human skin, and the humidity value increases as the distance from the skin surface decreases. Thus, the authors adopted such a humidity sensor to propose a 3 × 3 flexible sensor array and proved the capability for dynamic sliding gesture monitoring in non-contact mode, which exhibits the tremendous potential applications of such a sensor in the next-generation intelligent non-contact human–machine interaction systems. In addition, based on the humidity sensing property of the sulfonated poly(ether ether ketone) (SPEEK), Zhao et al. fabricated two humidity sensors that adopted the SPEEK thin film obtained by a drip casting way and the SPEEK nanofiber via electrospinning method, respectively.[63] It was observed that the nanofiber-structured SPEEK layer significantly improved the hysteresis phenomenon and response/recovery (Res./Rec.) time of the humidity sensor by measuring and comparing the sensing properties of the above two humidity sensors. Furthermore, the authors introduced polyvinyl butyral (PVB) into the SPEEK nanofiber and investigated the effect of the incorporation of the PVB on the sensing performance of the SPEEK/PVB composite nanofiber. On the one hand, the surface morphology of the SPEEK/PVB composite nanofiber with the introduction of a proper proportion of PVB shows a porous structure. It creates a large contact area between the water molecules and the water-absorbing groups, which could facilitate the transmission and diffusion of water molecules. On the other hand, for the SPEEK/PVB composite nanofiber, the hydrogen bonds formed between the sulfonic groups of SPEEK and the hydroxyl group of PVB may guarantee outstanding long-term stability for humidity sensing. In this way, the obtained SPEEK/PVB composite nanofiber presents conspicuous merits including high sensitivity over a wide relative humidity range, rapid Res./Rec. time (<1/5 s), small hysteresis (2.86%), excellent humidity sensing repeatability, and enables its successful application in human breath monitoring in non-contact sensing mode. Considering the excellent linear response and simple structure of the capacitive humidity sensor, Li et al. developed a flexible capacitive humidity sensing device with a novel arc-shaped hollow structure.[71] As depicted in Figure 10B, such an arc-shaped capacitive humidity sensor was composed of two face-to-face fixed arc-shaped PET-ITO free-standing electrode layers that were attached with the functional dielectric layer of P(VDF-TrFE) nanocone arrays. The authors pointed out that the particular arc-shaped hollow structure of such a humidity sensing device and the large specific surface area of the P(VDF-TrFE) nanocones sensing layer are beneficial for the absorption and desorption of water molecules, contributing to the good linear relationships at both the lower and upper RH ranges, as well as an ultrafast Res./Rec. time (3.693/3.430 s). More importantly, the relationship between the humidity response of the proposed capacitive sensor and the environment temperatures was investigated here. It was observed that such a sensor shows a considerably stable capacitance response toward humidity variation in a temperature range of 20°C–50°C, which proves the superiority of such a sensor in monitoring physiological signals like breathing in the non-contact sensing mode.

As another non-contact and non-destructive measurement strategy, flexible optical sensors based on extensive polymer materials have also obtained great advances and progress in terms of structure design, the working mechanism, and state-of-the-art approaches, exhibiting their potential application prospects in electronic skin, wearable devices, and soft robotics.[213–218] As early as 2007, Zirkl reported a flexible optothermal sensor that integrates a transistor device and pyroelectric polymer sensor (Figure 10C,D), which can serve as a laser pointer-activated switch and a sensitive infrared sensor.[211] As shown in Figure 10E, the bottom electrode of the pyroelectric polymer sensor serves as the gate electrode of the transistor device, and then two components are integrated. Due to the pyroelectric effect of the P(VDF-TrFE) copolymer film, the transistor device could be switched on by a 40 on–off ratio when an infrared laser with a modulation frequency of 0.01 Hz is applied on the top electrode of the pyroelectric sensor. Zhang et al. assembled the polymer microwire arrays via an efficient solution-processing method combined with the strictly regulated dewetting of liquid, and then proposed a high-performance ultraviolet (UV) photodetector with a high on/off ratio of 137 and responsivity of 19.1 mA W^{-1}.[212] To demonstrate the application in image sensing, an array composed of 14 × 18 polymer array-based photodetectors was fabricated. Figure 10F presents the image-sensing system that involves a 365-nm UV irradiation, a shadow photomask with the pattern of Arabic numerals, a photodetectors array, and a quartz substrate. As a result, with UV irradiation, the photocurrent response mappings of the photodetectors array consistent with the Arabic numerals on the shadow photomask were obtained. More importantly, such a photodetector array with good flexibility (Figure 10G) shows an outstanding fatigue characteristic even after 4000 cycles of bending processes and demonstrates its promising potential in wearable electronics by attaching it to the mouse skin (Figure 10H). In addition to the pure polymer materials,8,9 the heterojunction structures of polymer materials and other materials are widely used to design and create the high-performance photodetector.[219–221] For example, a phototransistor based on the heterostructure of In_2O_3/poly{5,5′-bis[3,5-bis(thienyl)phenyl]-2,2′bithiophene-3-ethylesterthiophene} (PTPBT-ET) was reported by Li et al., which combines the merits of the fast electron transport of In_2O_3 and the high photoresponse of PTPBT-ET, achieving a large current on/off ratio (>10^7).[221] Considering the superiorities of the inorganic perovskite materials, Liu et al. presented a photodetector enabled by lead-free perovskite ($FASnI_3$)/polymer material (PEDOT:PSS) vertical heterostructure, proving its excellent photoresponse over a broad range from UV to near-infrared (NIR).[220] According to the authors, the sensitivity and the photoresponse speed of the $FASnI_3$/PEDOT:PSS photodetector can be adjusted by altering the thickness of the PEDOT:PSS polymer layer. Also, many research works have focused on the investigation of polymer composites and adopted them to develop more outstanding photodetectors than that based on pure polymer materials.[222–224] For instance, Zhao et al. fabricated a new composite (RE–SCP) consisting of a semiconducting polymer (SCP) and rare earth-doped nanoparticles (RENPs) and assembled a flexible short-wave infrared (SWIR) photodetector. Due to the introduction of RENPs with distinctive SWIR-responsive characteristics, the photon-to-electron conversion of such a photodetector was efficiently improved, which enhanced the SCP's detection performance at multiple wavelengths including 808, 975, and 1532 nm.[223] Most recently, by dispersing 2D materials of graphene and black phosphorus (BP) in a polymer matrix with good self-healing capability, An et al. explored a self-healing photodetector that does not present electrical and optoelectrical behavior degradation even after cutting-and-healing for 30 cycles.[224] With the help of graphene and BP, such a self-healing photodetector shows enhanced broad light spectrum absorption and empowers prominent photocurrent under visible and NIR light illumination, demonstrating its feasibility for wearable electronics in various application circumstances.

To further build e-skins that are comparable to the sensation system of human skin, researchers have also achieved the detection of approaching objects in non-contact mode by capitalizing on the fringe fields of capacitive sensors.[12,225–228] In general, when an object approaches such a capacitive sensor, the fringe electric field lines of the sensor were disturbed, and there is a corresponding change in its capacitance. Based on this technology, Bao et al. adopted entire biodegradable materials to design a fringe field capacitive sensor and successfully achieved arterial blood flow monitoring in both contact and non-contact sensing modes by implanting it in the arterial during surgery.[226] Benefiting from the superiorities of entirely using biodegradable material and sensing modes of contact as well as non-contact, the authors addressed the issue that requires careful fixation for accurate detection and post-use removal when using the clinically available wired implantable monitoring technology. Simulation data predicted that the fringe field of the planar capacitive sensor with the interdigitated electrodes was more sensitive to approaching objects when compared with the conventional “sandwich” configuration capacitive sensor. Therefore, the authors performed the experiment and found the sensor with the interdigitated electrodes presented an approximately seven times non-contact capacitance response greater than that with a “sandwich” configuration, which was consistent with the simulation data results.[227] According to the authors, such a planar capacitive sensor with interdigitated design not only enabled to non-contact sensing through the fringe effect but also can be utilized to distinguish the conductive and insulating materials. Guo et al. presented a “sandwich” configuration capacitive sensor with non-contact sensing capability and demonstrated its interesting application in material recognition in the non-contact mode.[12] For approaching finger, paper, plastics, glass, wood, ceramics, silicon, aluminum, and copper, the sensor exhibited distinct capacitance responses. It was obvious that the capacitance response increased with decreasing distance between the external objects and the sensor. In all, with the assistance of the fringe field, these capacitive sensors are a promising way to achieve the design of non-contact e-skins and the recognition of different materials.

Apart from that, non-contact e-skins based on other sensing mechanisms have been explored to further improve user-interacting experiences, convenience, and degree of freedom in the interaction. For example, Wang et al. deposited the Co/Cu multilayers on highly stretchable and conformable polymer substrates, and a giant magnetoresistive (GMR)-sensing e-skin was obtained to achieve the detection of the static or dynamic magnetic field. Relying on the GMR effect, such a magnetoreceptive e-skin was capable of detecting the distance between the e-skin device and the magnetic field, which will likely attract increasing attention for the application in magnetic field proximity detection, navigation, and noncontact control.[121] Besides, flexible gas sensing devices can also provide a novel and non-contact way for environmental pollution gas monitoring and human disease diagnosis.[228–231] For example, He et al. fabricated a multi-hierarchical and porous PANI/sponge composite through a facile in situ polymerization and developed a flexible NH_3 gas-sensing device with adjustable sensitivity.[231] The considerable interconnected pores in the sponge structure provide a sufficient surface and give rise to the formation of the PANI nanostructures, contributing to abundant NH_3 adsorption sites and a fast response toward NH_3. Tam et al. developed an e-skin with flexibility, anti-damage, and non-contact sensing capabilities by implanting an MWCNT into the surface of a PVA flexible matrix, enabling the detection of approaching finger in the range of 0–20 mm via a spatially weak field.[29,232] In specific, due to the existence of a human electric field, a coupling capacitor between the surface of the sensor and the finger is formed when the finger approaches the sensor. Also, as mentioned before, the induced charge tends to be generated and accumulated on the surface of the finger once the human body is close to a charged object. Then, a potential difference (U) between the finger and the sensor circuit board could be calculated according to the equation $U = Q/C$ (Q: the accumulated charges; C: the coupling capacitor). Finally, the increasing U caused by the coupling capacitor between the finger and the sensor circuit board would increase the resistance (R) of the sensor circuit based on the formula $R = U/I$ (I: the current of the sensor circuit).

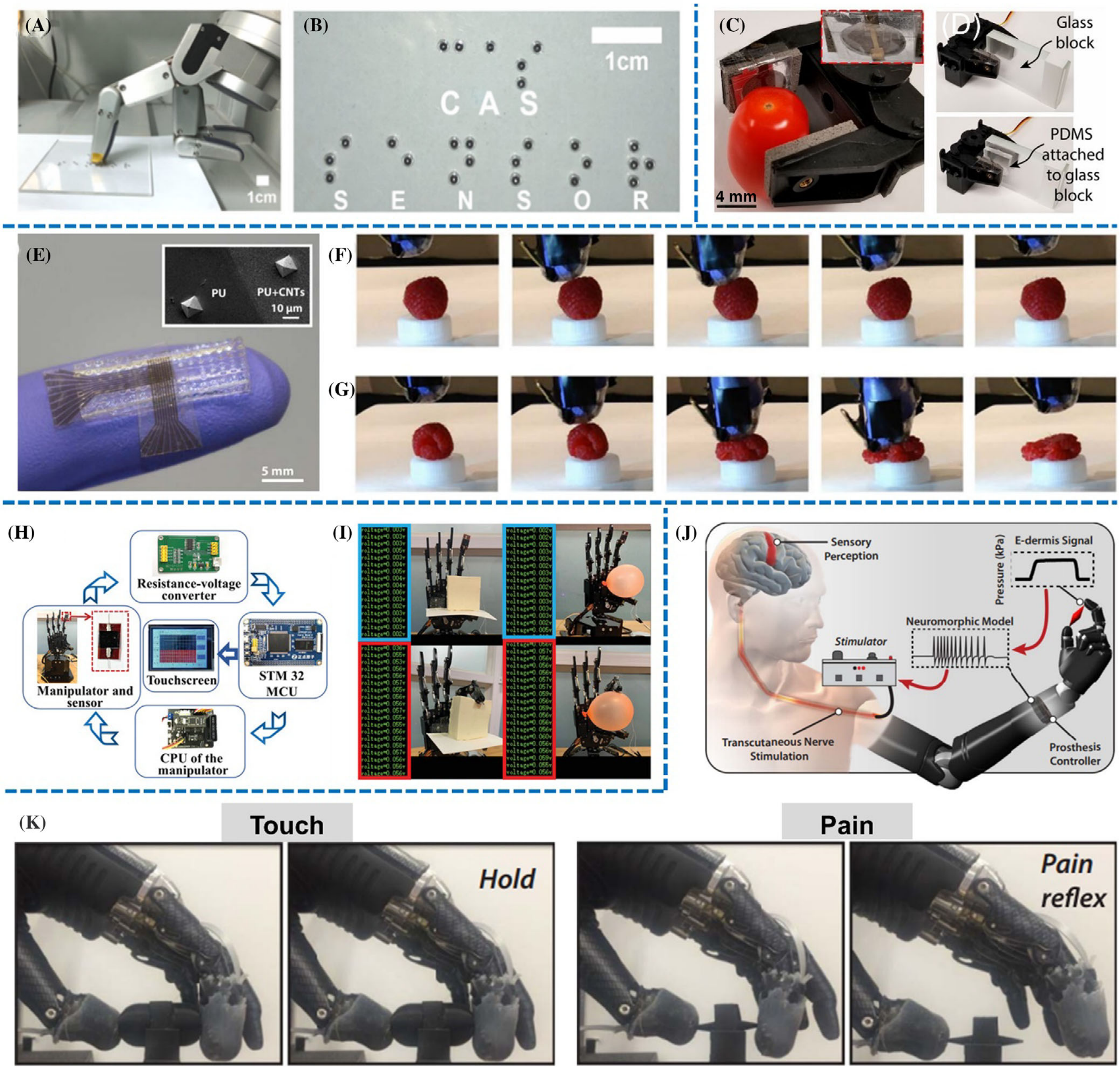

FIGURE 11 A robotic hand wearing a flexible tactile sensor (A) touching a braille board, (B) discerning the braille of “CAS” and “SENSOR” on the braille board. Reproduced with permission.[234] Copyright 2020, Elsevier Ltd. (C) Compliance sensor integrated into a robotic finger for grasping a fresh tomato. (D) A robotic finger touching and distinguishing the glass and PDMS materials. Reproduced under the terms of the CC BY-NC-ND License.[65] Copyright 2020, The authors. (E) Optical image and SEM image of the e-skin sensor array. Interaction between a fragile raspberry and a robotic artificial hand equipped (F) with and without (G) tactile feedback of the e-skin sensor array. Reproduced with permission.[130] Copyright 2018, The authors. (H) A general schematic diagram of a tactile sensing and feedback system for the manipulator. (I) Manipulator catching fragile tofu and deformable balloon. Reproduced with permission.[60] Copyright 2022, The authors. (J) Schematic diagram of the prosthesis system. (K) A tactile sensor fixed on the prosthesis system enabling the perceptions of touch and pain in the amputee. Reproduced with permission.[235] Copyright 2018, The authors.

5 | INTEGRATED E-SKINS FOR APPLICATIONS IN HUMAN-MACHINE INTERACTION

From the above-reviewed research works, great progress has been obtained in the aspects of polymer materials fabrication, the construction of both tactile and non-contact e-skins enabled by polymer materials, which promotes the practical applications of both tactile and non-contact e-skins. In this section, we focused on the applications of tactile and non-contact e-skins in human-machine interactions such as robots and prostheses, smart gloves, and VR/AR.

5.1 | Applications in robots and prostheses

With the development and progress of artificial e-skins technologies, many research groups have designed various tactile sensors to offer the necessary tactile information required in robotic and prosthetic applications.[43,60,65,130,233–235] For example, by assembling a capacitive tactile sensor on a robotic finger, Yang et al. demonstrated a robotic hand with remarkable accuracy in discerning braille (Figure 11A).[234] The capacitive tactile sensor was designed by integrating a graphene nanowalls (GNWs) electrode layer with pyramid microstructure and a conformally microstructured hybrid dielectric layer composed of PDMS and ZnO. Benefiting from the microstructured electrode-dielectric layer and polarized electric field induced by the piezoelectric property of ZnO, such a capacitive tactile sensor exhibited a significantly improved sensitivity and a very short response time (25 ms). Finally, with the assistance of the proposed tactile sensor, the robotic finger successfully completed the identification of the braille patterns of “CAS” and “SENSOR” (Figure 11B). In addition, a thin compliance sensor consisting of a strain sensor and a pressure sensor was developed by Bao et al.,[65] which was placed on one side of a robot finger (Figure 11C) and enabled the robot finger with a humanlike compliance sensation. As depicted in Figure 11D, a glass block and PDMS blocks with varying compliance were placed between the robot fingers to analyze the capability to discriminate the touched materials. It was observed that the compliance sensor presented different resistance readings when the robot finger grasped the different materials, which indicated the promising potential of the compliance sensor in providing the human-like compliance sensation for robot fingers. In fact, the perception system of the skin, in conjunction with tactile feedback, endows humans with the ability to perceive external stimuli and perform complex daily tasks by relying on the manipulation of our hands, which provides a learning paradigm for advanced robots and prosthetic devices to manipulate objects rationally.[75,236–242] Bao et al. reported a biomimetic soft e-skin and adopted such an e-skin to provide tactile feedback to a robotic arm to perform various tasks such as the dexterous manipulation of objects.[130] Here, the biomimetic soft e-skin was an array of capacitive tactile sensors that could be utilized to quantify and discriminate both normal and tangential forces in real-time. The 3D structure mimicking the interlocked human dermis–epidermis interface and the nature-inspired pyramid microstructures contributed to an e-skin with enhanced sensitivity, excellent fatigue characteristics, and fast response speed. An e-skin sensor array was mounted on a gripper of a robotic artificial hand (Figure 11E). An LCR meter was connected to measure the capacitance changes of the e-skin sensor array, and the recorded data was collected by a server to be utilized in a closed-loop feedback procedure to regular the movement of the artificial robotic hand. As shown in Figure 11F, when the artificial robotic hand, equipped with tactile feedback of the e-skin sensor array interacted with the fragile object, such as a raspberry, the raspberry would not be flattened. Without the tactile feedback system, the raspberry would be irreversibly crushed by the robotic hand (Figure 11G). Liu et al. developed a high-performance flexible tactile sensor by selecting a structure of PU/MXene and the sprayed MXene on a flexible substrate as the functional layer and interdigital electrodes.[60] The authors accurately realized a tactile feedback function by integrating such a sensor into the tactile sensing and feedback system of the manipulator. As illustrated in Figure 11H, there are five important parts in such tactile sensing and feedback system, including a manipulator and a sensor that captures the pressure change when the manipulator touches an object, a resistance–voltage converter for collecting the electric signal of the sensor, an STM 32 microcontroller unit (MCU) for analyzing and processing data, a central processing unit controlling the manipulator, and a touchscreen displaying the electrical signal curves. Figure 11I shows that the manipulator in a tactile sensing and feedback system successfully grabbing fragile tofu and a deformable balloon without changing their shape. It is no doubt that effective perception and meaningful tactile feedback are of great importance for solving the issue of lack of sensory capabilities in current prostheses, which offers opportunities for advanced prostheses to help an amputee's ability to regain their lost function. Thakor et al. invented a multilayered e-skin to provide neuromorphic perceptions of touch and pain to the amputee wearing prostheses.[235] Figure 11J presents the schematic diagram of the prosthesis system. When the prosthesis wearing such multilayered e-skin grasps or touches an object, tactile signal could be obtained from the e-skin fixed on the finger of the prosthesis. And then, the prosthesis controller was used to transform the tactile signal into a neuromorphic signal that would be further conducted to guide the transcutaneous stimulation of the peripheral nerves of an amputee and enable the perceptions of touch and pain in the amputee (Figure 11K). With the development of non-contact electronic skin, the non-contact human–machine interaction system has presented a conspicuous superiority in controlling robots for daily operations. For instance, Lu et al. proposed a 3×3 sensor array and demonstrated that it could enable multipoint detection and sliding gesture monitoring in a non-contact mode.[32] In this way, a robot car could perform different commands like forward and clamp opening when a volunteer gave sliding gestures of “reversed L” and “I”, proving tremendous potential applications of such a sensor array in non-contact human–machine interaction.

5.2 | Applications in smart gloves

As an interaction method, gestures have offered a convenient, and intuitive approach to promoting communication between humans and machines. Tactile e-skins are of great significance in gesture detection and recognition, which have been widely applied in the fields of artificial intelligence and human–machine interaction.[20,74,243–249] Recently, Yu et al. reported an ultrathin, and stretchable human–machine interactive sensor, and then the sensor was worn by a volunteer on hand to collect multiple physical data on muscle movement, which allows the volunteer to guide a robot to mimic the human hand shape.[243] Besides, Wu et al. presented a novel flexible dual-mode tactile e-skin consisting of piezoelectric and piezoresistive two sections, which yielded a high sensitivity and linear response over a broad pressure range of 0.015–9 kPa.[20] Most importantly, the e-skin that combined the piezoelectric section detected the pressure dynamic loading rate and direction with the piezoresistive sectioned recorded pressure magnitude and duration provided the possibility to monitor the complex grasping and the dynamic pressure loading process. Such a dual-mode sensor was mounted on the human wrist, and its ability to control a manipulator for gestures with varying bending directions, rates, and angles was demonstrated. Benefiting from that, the smart gloves integrated with high-performance tactile sensors have been widely explored and showed promising potential in the applications of the human–machine interfaces.[72,250–258] Wei et al. developed a multistage sensing pressure sensor and assembled it into the knuckle regions of a textile glove to establish a smart glove system for the human–machine interface (Figure 12A).[251] To realize multistage sensing, the functional layer of such a sensor adopts a micro- and nanohybrid structure of multidimensional carbon materials on the microscale and the arched micro-patterns that mimic the surface structure of human fingerprint on the macroscale. Then, it was demonstrated that the smart glove system integrated with the multistage sensing pressure sensor could detect the bending signals from the volunteer joints and help to successfully operate the manipulator for gesture imitation (Figure 12B) and grabbing objects (Figure 12C). In another work,[43] a smart glove-based human–robot interaction system was proposed by Zhang et al., where such a smart glove was armed with a tactile sensor array that was composed of a CNT network, a combined polymer layer of polypyrrole-polydopamine-perfluorodecyltrlethoxysilane (PPy-PDA-PFDS), and a textile substrate. As shown in Figure 12D, the robot fingers in such a system synchronously and continuously expressed three different gestures of “I”, “Love”, and “You” under the control of the volunteer's fingers. Also, this sensor array exhibited desirable superlyophobicity to a series of agents because of the introduction of multifunctional polymers of PPy-PDA-PFDS, and thus the volunteer wearing the smart glove could still control the robot to gesture “I love you” even with sweat and/or water exposure (Figure 12E). In addition to a robot hand and the smart glove with a tactile sensor array, there is a voltage divider circuit connected to a data acquisition (DAQ) in such a human–robot interaction system (Figure 12F). Such a voltage divider circuit was used to convert the resistance signals of the sensors on the smart glove to voltage signals. The recorded voltage signals were further processed in the microcontroller and communicated with the robot hand using a Bluetooth module. As the authors claimed, with the help of the intelligent glove, the robot hand in such a system could not only synchronously repeat the gestures of the volunteer but also it could respond to the action of the human hand and accurately capture a flying ball (Figure 12G). Zhang et al. proposed a wearable self-powered sensor and integrated it into a glove for a homemade automatic recognition system, allowing the volunteer gestures to interact with a vehicle.[256] Figure 12H shows the command definitions of four different gestures relating to the motion direction of a vehicle, and Figure 12I illustrates the confusion map related to the gestures and vehicle motion test results indicating that the overall accuracy of the test was over 96.8%. The authors showed a car can successfully travel out of the maze with the homemade automatic recognition system (Figure 12J). Overall, mart glove systems armed with high-performance tactile sensors enable the detection of human gestures and guide the robot in the interaction with humans and gripping objects, indicating its potential for providing dexterity to the robot and achieving better human–machine interface.

5.3 | Applications in VR/AR

Apart from effectively boosting the communication between the user and the robots, human–machine interface exploiting the high-performance e-skins also provides a window for the user to establish an intuitive connection with the virtual world,[46,73,150,253,259–261] such as the applications of virtual reality (VR) and augmented

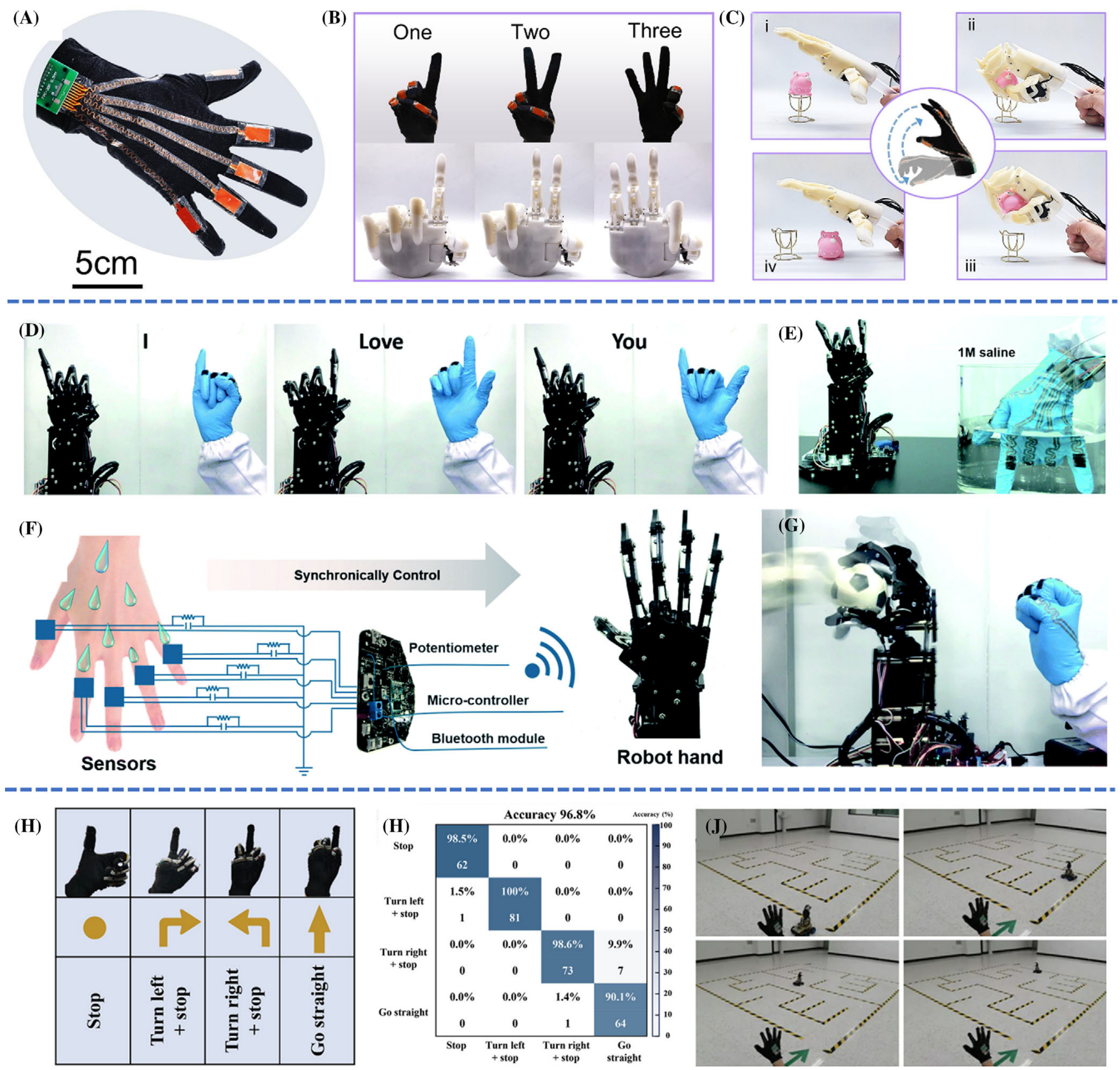

FIGURE 12 (A) Image of a smart glove system for the human–machine interface. Images showing a manipulator imitating the (B) hand gestures and (C) grabbing objects with the assistance of the smart glove system. Reproduced with permission.[251] Copyright 2021, Elsevier Ltd. (D) Demonstration of a robot hand controlled by human hand gestures. (E) A robot hand responding the human hand gestures even under water exposure. (F) Schematic illustration of a human–robot interaction system. (G) Robot hand in such a system could respond to the human hand action and accurately capture a flying ball. Reproduced with permission.[43] Copyright 2019, Royal Society of Chemistry. (H) Four hand gestures related to different motor commands guiding the movement of the vehicle. (I) Classification test confusion matrix on the gestures and vehicle motion test results. (J) Photographs showing a car successfully passing through the maze. Reproduced with permission.[256] Copyright 2022, Wiley-VCH.

reality (AR). Conventional VR and AR technologies mostly enhance human experiences in the human–machine interaction systems via visual and auditory stimuli. In fact, in addition to the eyes and the ears, the human skin is another sensory interface that is underexplored in VR and AR technologies, which may greatly enhance human experiences in fields of future communications, entertainment, and medicine. Wen et al. developed a high-performance triboelectric textile with superhydrophobicity via a facile coating approach and integrated it into a smart glove to achieve complex gesture recognition by training finger motion signals with

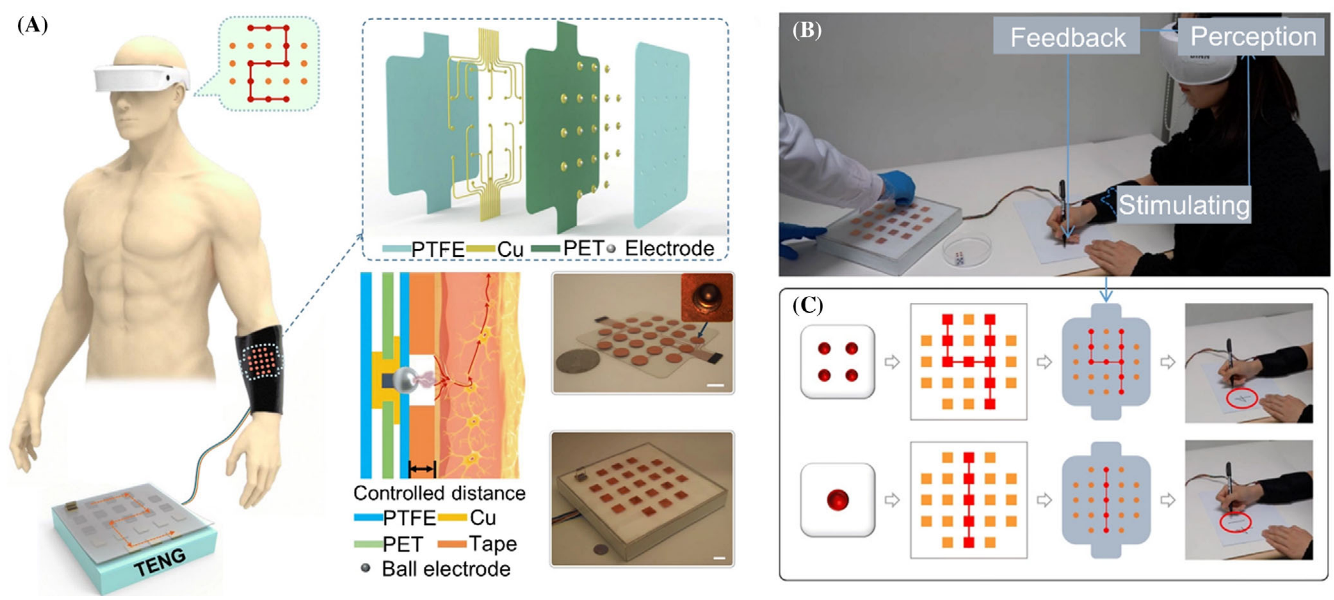

FIGURE 13 (A) A highly sensitive ET system composed of a TENG and ET interface for achieving enhanced virtual tactile experiences. (B,C) A demonstration of this ET interface applied to enhancing the tactile VR experience of percepting virtual spatial patterns (random numbers). Reproduced under the terms of the CC BY-NC license.[73] Copyright 2021, The authors.

machine learning. With help of the machine learning technology, these gestures were also successfully realized to highly accurate VR/AR complex controls such as gun shooting, baseball pitching, and even flower arrangement. Recently, Rogers et al. introduced a haptic interface that incorporates vibratory actuator arrays in millimeter-scale and conformal electronic sheets that were laminated onto human skin in a repeatable and non-invasive method.[253] Through such a haptic interface-based VR device, the grandmother in the video could experience haptic sensation in the form of continuous vibrational excitation waves, and the experienced touch was fully consistent with the image of her granddaughter's fingertip on the touchscreen. Then, such a haptic interface was also applied to offer tactile feedback for a robotic prosthetic device. As a result, a haptic interface-based VR device placed on a man who has lost his lower arm could help build virtual haptic information about the object's shape when grasping the object. Zhu et al. printed a smart glove involving triboelectric tactile sensors based on elastomer and piezoelectric haptic mechanical stimulators based on PZT and presented its potential in achieving multidimensional and multipurpose manipulations in VR/AR.[207] Here, triboelectric tactile sensors endow the smart glove with the capability to detect the motions of each finger knuckle with high precision and multiple degrees of freedom. And, in conjunction with advanced manipulation, such a smart glove could respond to a real-time impact event and enhance our sensation against the interaction through piezoelectric haptic stimulation. Considering that tactile sensation can play an important role in VR and AR applications, Shi et al. developed a highly sensitive electro-tactile (ET) system by combining a TENG with an ET interface formed with a ball-shaped electrode array and achieved an enhanced virtual tactile experience (Figure 13A).[73] Figure 13B,C demonstrate the possible application of such an ET system in virtual interactions. It was obvious that the volunteer, although whose eyes were covered, was able to give the right feedback when a random number was written on the surface of TENG. In a short, building high-performance e-skins and integrating them with VR/AR technologies or applications are still far-reaching for exploring a full, immersive human–machine interactive experience involving interactive images, sounds, and even sensations of touch in the future.

6 | CONCLUSION AND OUTLOOK

6.1 | Summary

The sensory system of the human skin where tactile and non-contact sensing complement each other provides humans with a full range and sensitive information perception capabilities. To build high-performance e-skins that are comparable to the sensory system of human skin, great improvement has been obtained in terms of the preparation technologies of polymer materials, the mechanism exploration providing underlying knowledge for e-skins, and the approaches for assembling and constructing various e-skins. Therefore, this review first introduced the unique superiorities and fabrication methods of polymer materials in flexible electronics. Then, we mainly focus on the approaches and strategies for constructing high-performance e-skins with tactile and non-contact sensing capabilities by using polymer materials. After that, the applications of these polymer-based tactile and non-contact e-skins in human–machine interactions including robots and prostheses, smart gloves, and VR/AR are summarized. In summary, the appreciable achievements in the construction of both tactile and non-contact e-skins based on the polymer material have been promoting their practical applications in human-machine interactions. However, the currently developed e-skins enabled by the polymer material and the human–machine interaction systems have not yet extensively succeeded in commercial applications. The complexities of the application environment have imposed quite strict requirements on the design of high-performance e-skins, and there are still individual challenges that need to be addressed to further develop this field. Here, according to the above-reviewed works, we respectively summarize the challenges for achieving the breakthrough in human–machine interaction applications of the polymer-based tactile and non-contact e-skins from three aspects: materials, additive fabrication approaches, and rational design of integration protocols. Correspondingly, the possible solutions to addressing these challenges are also proposed in this review.

6.2 | Challenges and perspectives

6.2.1 | Materials

The selection of the polymer material is crucial for the construction of tactile and non-contact e-skins with excellent sensing properties and achieving their application in human–machine interactions. The use of toxic and harmful solvents in the manufacturing process of certain polymer materials poses a significant threat to the safety of experimental personnel and the environment. Furthermore, the possible left residual solvents on the e-skin device may cause the damage to the user's skin and result in serious skin problems. Therefore, we strongly recommend the use of polymer materials that do not involve toxic and harmful solvents in the fabrication process. To provide a safe and comfortable user experience in human–machine interactions, polymer materials with good breathability biocompatibility and environmental friendliness are expected to become the first choice for building future e-skin devices in human-machine interactions. Besides, regarding the challenges of additional power supply of the e-skin device or even system and the environmental issues caused by the high volume of e-skin waste, self-powered and biodegradable e-skin devices enabled by polymer materials can provide opportunities to make e-skin devices more practical, sustainable, and reduce the environmental impact in various applications. More importantly, to realize an e-skin device that is comparable to the human skin, it is essential to select polymer materials with good self-healing property device for developing e-skin devices with the improved durability and extending service life. Typically, the configuration of the e-skin device consists of multi-layer structures (more than two layers), which results in the problem of weak adhesion and mechanical mismatch in the multiple layers of the e-skin device. As a result, polymer materials with similar mechanical properties are highly desired for overcoming the challenge of the adhesion and mechanical mismatch between interlayers during the construction of a multiple-layered e-skin device.

6.2.2 | Additive fabrication approaches

Currently, the packaging is usually ignored, or just simple encapsulation is considered in the design process of the e-skin device. The e-skin device may often encounter environmental humidity changes, sweat, grease, or other pollutants because of the complex application environment, raising some concerns about the performance and service life of the unpackaged or inappropriate packaged e-skin devices. Advanced additive fabrication approaches and packaging technologies offer versatile and scalable methods for assembling e-skin devices with tailored properties and functionalities, which contributes to environmental stability and robustness in practical applications, avoiding the contamination and performance degradation of the e-skin device caused by exposure to the complex environment. Further, the influence of the packaging layers on the sensing performance and the physical/chemical properties of the e-skin device should be negligible in the advanced packaging technology. Finally, the advanced packaging technology of the e-skin device without any influence on signal transmission and data processing is highly needed because the e-skin device is integrated as the most important component of the data acquisition in the human–machine interaction system.

6.2.3 | Rational design of integration protocols

As above discussed, both tactile and non-contact e-skin devices based on polymer materials have been widely used to integrate with other peripheral devices/circuits and obtained some achievements in human–machine interaction applications such asrobots and prostheses, smart gloves, and VR/AR. However, the currently established human–machine interactive system is not highly integrated a good compatibility, which has poor mechanical and environmental stability, and gives rise to an uncomfortable wearing experience for the user. Therefore, rational design of integration protocols should be encouraged to achieve the reliable and scalable integration of distinct components in the human–machine interactive system based on the tactile and non-contact e-skins. Firstly, the use of compatible materials and components as well as the proper electrical connectivity between each component is essential when considering the reasonable and highly integration strategies for the e-skins and human–machine interactive system, which ensures the effectively electrical signals transmission of each component of the system. Then, it is highly desired for the integration methods to realize good mechanical and environmental stability, enabling the reliable and robust operation under various environmental conditions. Lastly, it is necessary to consider the flexibility and reliability of the other peripheral devices/circuits in the human–machine interactive system, which could guarantee the wearer good comfort and realize a true e-skin system.

Overall, continuous efforts focused on the above individual aspects would be further considered to improve the overall properties of both tactile and non-contact e-skins using the polymer material to the level of superiority to that of the human skin, and realizing wide commercial applications in human–machine interactions. We believe that the joint improvements in polymer-based e-skins, human–machine interactive hardware system, signal processing, computer technology, and VR/AR technology will bring new opportunities and make the commercial applications of human–machine interaction into a reality.

ACKNOWLEDGMENTS

This work was supported in part by the Basic Science Research Program through the National Research Foundation of Korea (NRF) funded by the Ministry of Education under Grant 2018R1A6A1A03025242 and Grant 2018R1D1A1A09083353, the Korea Ministry of Environment (MOE) Graduate School specialized in Integrated Pollution Prevention and Control Project and a Research Grant of Kwangwoon University in 2022.

CONFLICT OF INTEREST STATEMENT

The authors declare no conflict of interest.

ORCID

Feifei Yin https://orcid.org/0000-0002-3312-0389
Hongsen Niu https://orcid.org/0000-0002-1925-7274

REFERENCES

1. Chortos A, Bao Z. Skin-inspired electronic devices. *Mater Today*. 2014;17(7):321-331.
2. Sun JY, Keplinger C, Whitesides GM, Suo Z. Ionic skin. *Adv Mater*. 2014;26(45):7608-7614.
3. Lin Q, Huang J, Yang J, et al. Highly sensitive flexible iontronic pressure sensor for fingertip pulse monitoring. *Adv Healthc Mater*. 2020;9(17):2001023.
4. He J, Xiao P, Lu W, et al. A universal high accuracy wearable pulse monitoring system via high sensitivity and large linearity graphene pressure sensor. *Nano Energy*. 2019;59:422-433.
5. Chang H, Kim S, Jin S, et al. Ultrasensitive and highly stable resistive pressure sensors with biomaterial-incorporated interfacial layers for wearable health-monitoring and human–machine interfaces. *ACS Appl Mater Interfaces*. 2018;10(1):1067-1076.
6. Duan S, Yang H, Hong J, et al. A skin-beyond tactile sensor as interfaces between the prosthetics and biological systems. *Nano Energy*. 2022;102:107665.
7. Wang N, Dou W, Hao S, et al. Tactile sensor from self-chargeable piezoelectric supercapacitor. *Nano Energy*. 2019;56:868-874.
8. Xu J, Li X, Chang H, et al. Electrooculography and tactile perception collaborative Interface for 3D human–machine interaction. *ACS Nano*. 2022;16(4):6687-6699.
9. Heng W, Solomon S, Gao W. Flexible electronics and devices as human–machine interfaces for medical robotics. *Adv Mater*. 2022;34(16):2107902.
10. Ning C, Dong K, Cheng R, et al. Flexible and stretchable fiber–shaped triboelectric nanogenerators for biomechanical monitoring and human–interactive sensing. *Adv Funct Mater*. 2021;31(4):2006679.
11. Mannsfeld SC, Tee BC, Stoltenberg RM, et al. Highly sensitive flexible pressure sensors with microstructured rubber dielectric layers. *Nat Mater*. 2010;9(10):859-864.
12. Guo Y, Gao S, Yue W, Zhang C, Li Y. Anodized aluminum oxide-assisted low-cost flexible capacitive pressure sensors based on double-sided nanopillars by a facile fabrication method. *ACS Appl Mater Interfaces*. 2019;11(51):48594-48603.
13. Niu H, Gao S, Yue W, Li Y, Zhou W, Liu H. Highly morphology–controllable and highly sensitive capacitive tactile sensor based on epidermis–dermis–inspired interlocked asymmetric–nanocone arrays for detection of tiny pressure. *Small*. 2020;16(4):1904774.
14. Yin F, Guo Y, Li H, et al. A waterproof and breathable cotton/rGO/CNT composite for constructing a layer-by-layer structured multifunctional flexible sensor. *Nano Res*. 2022;15(10):9341-9351.
15. Choong CL, Shim MB, Lee BS, et al. Highly stretchable resistive pressure sensors using a conductive elastomeric composite on a micropyramid array. *Adv Mater*. 2014;26(21):3451-3458.
16. Duan S, Lin Y, Wang Z, et al. Conductive porous MXene for bionic, wearable, and precise gesture motion sensors. *Research*. 2021;2021:1-11. doi:10.34133/2021/9861467

17. Guo Y, Zhong M, Fang Z, Wan P, Yu G. A wearable transient pressure sensor made with MXene nanosheets for sensitive broad-range human–machine interfacing. *Nano Lett*. 2019;19(2):1143-1150.
18. Lei M, Feng K, Ding S, et al. Breathable and waterproof electronic skin with three-dimensional architecture for pressure and strain sensing in nonoverlapping mode. *ACS Nano*. 2022;16(8):12620-12634.
19. Wang ZL, Song J. Piezoelectric nanogenerators based on zinc oxide nanowire arrays. *Science*. 2006;312(5771):242-246.
20. Qiu Y, Tian Y, Sun S, et al. Bioinspired, multifunctional dual-mode pressure sensors as electronic skin for decoding complex loading processes and human motions. *Nano Energy*. 2020;78:105337.
21. Park KI, Son JH, Hwang GT, et al. Highly–efficient, flexible piezoelectric PZT thin film nanogenerator on plastic substrates. *Adv Mater*. 2014;26(16):2514-2520.
22. Deng W, Yang T, Jin L, et al. Cowpea–structured PVDF/ZnO nanofibers based flexible self–powered piezoelectric bending motion sensor towards remote control of gestures. *Nano Energy*. 2019;55:516-525.
23. Yang Y, Zhou YS, Zhang H, Liu Y, Lee S, Wang ZL. A single–electrode based triboelectric nanogenerator as self–powered tracking system. *Adv Mater*. 2013;25(45):6594-6601.
24. Lee KY, Yoon HJ, Jiang T, et al. Fully packaged self–powered triboelectric pressure sensor using hemispheres–array. *Adv Energy Mater*. 2016;6(11):1502566.
25. Seol ML, Woo JH, Lee DI, Im H, Hur J, Choi YK. Nature–replicated nano–in–micro structures for triboelectric energy harvesting. *Small*. 2014;10(19):3887-3894.
26. Li Y, Xiao S, Zhang X, et al. Silk inspired in-situ interlocked superelastic microfibers for permeable stretchable triboelectric nanogenerator. *Nano Energy*. 2022;98:107347.
27. Wang HL, Su L, Li HY, Wang ZL, Zhu G. Electret-induced electric field assisted luminescence modulation for interactive visualized sensing in a non-contact mode. *Mater Horiz*. 2020;7(4):1144-1149.
28. Liu R, Lai Y, Li S, et al. Ultrathin, transparent, and robust self-healing electronic skins for tactile and non-contact sensing. *Nano Energy*. 2022;95:107056.
29. Wang DC, Yu HY, Jiang L, et al. Flexible, anti-damage, and non-contact sensing electronic skin implanted with MWCNT to block public pathogens contact infection. *Nano Res*. 2022;15(3):2616-2625.
30. Lu Y, Yang G, Shen Y, Yang H, Xu K. Multifunctional flexible humidity sensor systems towards noncontact wearable electronics. *Nano Micro Lett*. 2022;14(1):1-34.
31. Miao P, Wang J, Zhang C, Sun M, Cheng S, Liu H. Graphene nanostructure-based tactile sensors for electronic skin applications. *Nano Micro Lett*. 2019;11(1):1-37.
32. Lu L, Jiang C, Hu G, Liu J, Yang B. Flexible noncontact sensing for human–machine interaction. *Adv Mater*. 2021;33(16):2100218.
33. Guo Y, Wei X, Gao S, Yue W, Li Y, Shen G. Recent advances in carbon material–based multifunctional sensors and their applications in electronic skin systems. *Adv Funct Mater*. 2021;31(40):2104288.
34. Liu MY, Hang CZ, Zhao XF, et al. Advance on flexible pressure sensors based on metal and carbonaceous nanomaterial. *Nano Energy*. 2021;87:106181.
35. Joo Y, Byun J, Seong N, et al. Silver nanowire-embedded PDMS with a multiscale structure for a highly sensitive and robust flexible pressure sensor. *Nanoscale*. 2015;7(14):6208-6215.
36. Yi L, Jiao W, Wu K, et al. Nanoparticle monolayer-based flexible strain gauge with ultrafast dynamic response for acoustic vibration detection. *Nano Res*. 2015;8(9):2978-2987.
37. Yi P, Zou H, Yu Y, et al. MXene-reinforced liquid metal/polymer fibers via Interface engineering for wearable multifunctional textiles. *ACS Nano*. 2022;16(9):14490-14502.
38. Liu W, Duo Y, Liu J, et al. Touchless interactive teaching of soft robots through flexible bimodal sensory interfaces. *Nat Commun*. 2022;13(1):1-14.
39. Xu Y, Sun B, Ling Y, et al. Multiscale porous elastomer substrates for multifunctional on-skin electronics with passive-cooling capabilities. *Proc Natl Acad Sci U S A*. 2020;117(1):205-213.
40. Song WZ, Wang XX, Qiu HJ, et al. Sliding non-contact inductive nanogenerator. *Nano Energy*. 2019;63:103878.
41. Xu L, Liu C, Ma X, et al. Two-birds-one-stone: flexible PANI film with bionic microstructures for multifunctional sensing of physical and chemical stimuli. *Chem Eng J*. 2023;451:138820.
42. Fan X, Nie W, Tsai H, et al. PEDOT:PSS for flexible and stretchable electronics: modifications, strategies, and applications. *Adv Sci*. 2019;6(19):1900813.
43. Zhang L, He J, Liao Y, et al. A self-protective, reproducible textile sensor with high performance towards human–machine interactions. *J Mater Chem A*. 2019;7(46):26631-26640.
44. Zhu J, Zhang N, Yin Y, Xu B, Zhang W, Wang C. High–sensitivity and low–hysteresis GO–NH_2/mesoporous SiO_2 Nanosphere–fabric–based humidity sensor for respiratory monitoring and noncontact sensing. *Adv Mater Interfaces*. 2022;9(1):2101498.
45. Yang Q, Liu N, Yin J, Tian H, Yang Y, Ren TL. Understanding the origin of tensile response in a graphene textile strain sensor with negative differential resistance. *ACS Nano*. 2022;16(9):14230-14238.
46. Wen F, Sun Z, He T, et al. Machine learning glove using self–powered conductive superhydrophobic triboelectric textile for gesture recognition in VR/AR applications. *Adv Sci*. 2020;7(14):2000261.
47. Xiong Y, Han J, Wang Y, Wang ZL, Sun Q. Emerging Iontronic sensing: materials, mechanisms, and applications. *Research*. 2022;2022:9867378.
48. Zhang H, Chen H, Lee JH, et al. Bioinspired Chromotropic ionic skin with In–plane strain/temperature/pressure multimodal sensing and ultrahigh stimuli discriminability. *Adv Funct Mater*. 2022;32(47):2208362.
49. Wang P, Liu J, Yu W, Li G, Meng C, Guo S. Flexible, stretchable, breathable and sweatproof all–nanofiber iontronic tactile sensor for continuous and comfortable knee joint motion monitoring. *Nano Energy*. 2022;103:107768.

50. Liu Q, Liu Z, Li C, et al. Highly transparent and flexible iontronic pressure sensors based on an opaque to transparent transition. *Adv Sci*. 2020;7(10):2000348.
51. Qi D, Zhang K, Tian G, Jiang B, Huang Y. Stretchable electronics based on PDMS substrates. *Adv Mater*. 2021;33(6):2003155.
52. Chen X, Liu H, Zheng Y, et al. Highly compressible and robust polyimide/carbon nanotube composite aerogel for high–performance wearable pressure sensor. *ACS Appl Mater Interfaces*. 2019;11(45):42594-42606.
53. Stadlober B, Zirkl M, Irimia-Vladu M. Route towards sustainable smart sensors: ferroelectric polyvinylidene fluoride–based materials and their integration in flexible electronics. *Chem Soc Rev*. 2019;48(6):1787-1825.
54. Wang K, Yap LW, Gong S, Wang R, Wang SJ, Cheng W. Nanowire–based soft wearable human–machine interfaces for future virtual and augmented reality applications. *Adv Funct Mater*. 2021;31(39):2008347.
55. Wen N, Zhang L, Jiang D, et al. Emerging flexible sensors based on nanomaterials: recent status and applications. *J Mater Chem A*. 2020;8(48):25499-25527.
56. Surmenev RA, Orlova T, Chernozem RV, et al. Hybrid lead–free polymer-based nanocomposites with improved piezoelectric response for biomedical energy–harvesting applications: a review. *Nano Energy*. 2019;62:475-506.
57. Chen J, Zhu Y, Huang J, et al. Advances in responsively conductive polymer composites and sensing applications. *Polym Rev*. 2021;61(1):157-193.
58. Qin J, Yin LJ, Hao YN, et al. Flexible and stretchable capacitive sensors with different microstructures. *Adv Mater*. 2021;33(34):2008267.
59. Gong M, Zhang L, Wan P. Polymer nanocomposite meshes for flexible electronic devices. *Prog Polym Sci*. 2020;107:101279.
60. Yang M, Cheng Y, Yue Y, et al. High–performance flexible pressure sensor with a self–healing function for tactile feedback. *Adv Sci*. 2022;9(20):2200507.
61. Li Z, Zhu M, Shen J, Qiu Q, Yu J, Ding B. All–fiber structured electronic skin with high elasticity and breathability. *Adv Funct Mater*. 2020;30(6):1908411.
62. Zhou K, Xu W, Yu Y, et al. Tunable and nacre–mimetic multifunctional electronic skins for highly stretchable contact–noncontact sensing. *Small*. 2021;17(31):2100542.
63. Li X, Zhuang Z, Qi D, Zhao C. High sensitive and fast response humidity sensor based on polymer composite nanofibers for breath monitoring and non–contact sensing. *Sens Actuators B*. 2021;330:129239.
64. Zhou L, Wang M, Liu Z, Guan J, Li T, Zhang D. High–performance humidity sensor based on graphitic carbon nitride/polyethylene oxide and construction of sensor array for non–contact humidity detection. *Sens Actuators B*. 2021;344:130219.
65. Beker L, Matsuhisa N, You I, et al. A bioinspired stretchable membrane–based compliance sensor. *Proc Natl Acad Sci U S A*. 2020;117(21):11314-11320.
66. Shi X, Zhu Y, Fan X, et al. An auxetic cellular structure as a universal design for enhanced piezoresistive sensitivity. *Matter*. 2022;5(5):1547-1562.
67. Wan Y, Qiu Z, Hong Y, et al. A highly sensitive flexible capacitive tactile sensor with sparse and high–aspect–ratio microstructures. *Adv. Electron. Mater.* 2018;4(4):1700586.
68. Chen X, Shao J, Li X, Tian H. A flexible piezoelectric–pyroelectric hybrid nanogenerator based on P (VDF–TrFE) nanowire array. *IEEE Trans Nanotechnol*. 2016;15(2):295-302.
69. Fan FR, Lin L, Zhu G, Wu W, Zhang R, Wang ZL. Transparent triboelectric nanogenerators and self-powered pressure sensors based on micropatterned plastic films. *Nano Lett*. 2012;12(6):3109-3114.
70. Wu H, Su Z, Shi M, et al. Self–powered noncontact electronic skin for motion sensing. *Adv Funct Mater*. 2018;28(6):1704641.
71. Niu H, Yue W, Li Y, et al. Ultrafast-response/recovery capacitive humidity sensor based on arc-shaped hollow structure with nanocone arrays for human physiological signals monitoring. *Sens Actuators B*. 2021;334:129637.
72. Dong B, Yang Y, Shi Q, et al. Wearable triboelectric–human–machine interface (THMI) using robust nanophotonic readout. *ACS Nano*. 2020;14(7):8915-8930.
73. Shi Y, Wang F, Tian J, et al. Self-powered electro-tactile system for virtual tactile experiences. *Sci Adv*. 2021;7(6):abe2943.
74. Wen F, Zhang Z, He T, Lee C. AI enabled sign language recognition and VR space bidirectional communication using triboelectric smart glove. *Nat Commun*. 2021;12(1):5378.
75. Qu X, Liu Z, Tan P, et al. Artificial tactile perception smart finger for material identification based on triboelectric sensing. *Sci Adv*. 2022;8(31):abq2521.
76. Pang C, Lee GY, Kim TI, et al. A flexible and highly sensitive strain–gauge sensor using reversible interlocking of nanofibres. *Nat Mater*. 2012;11(9):795-801.
77. Li T, Luo H, Qin L, et al. Flexible capacitive tactile sensor based on micropatterned dielectric layer. *Small*. 2016;12(36):5042-5048.
78. Cheng W, Wang J, Ma Z, et al. Flexible pressure sensor with high sensitivity and low hysteresis based on a hierarchically microstructured electrode. *IEEE Electron Dev Lett*. 2017;39(2):288-291.
79. Wen Z, Yang Y, Sun N, et al. A wrinkled PEDOT:PSS film based stretchable and transparent triboelectric nanogenerator for wearable energy harvesters and active motion sensors. *Adv Funct Mater*. 2018;28(37):1803684.
80. Li F, Wang R, Song C, et al. A skin–inspired artificial mechanoreceptor for tactile enhancement and integration. *ACS Nano*. 2021;15(10):16422-16431.
81. Zhang J, Wan L, Gao Y, et al. Highly stretchable and self–healable MXene/polyvinyl alcohol hydrogel electrode for wearable capacitive electronic skin. *Adv. Electron. Mater.* 2019;5(7):1900285.
82. Rana SS, Zahed MA, Rahman MT, et al. Cobalt-nanoporous carbon functionalized nanocomposite-based triboelectric nanogenerator for contactless and sustainable self-powered sensor systems. *Adv Funct Mater*. 2021;31(52):2105110.
83. Tian K, Sui G, Yang P, Deng H, Fu Q. Ultrasensitive thin-film pressure sensors with a broad dynamic response range and excellent versatility toward pressure, vibration, bending, and temperature. *ACS Appl Mater Interfaces*. 2020;12(18):20998-21008.
84. Chhetry A, Sharma S, Yoon H, Ko S, Park JY. Enhanced sensitivity of capacitive pressure and strain sensor based on

$CaCu_3Ti_4O_{12}$ wrapped hybrid sponge for wearable applications. *Adv Funct Mater*. 2020;30(31):1910020.
85. Wang Y, Zhu M, Wei X, Yu J, Li Z, Ding B. A dual-mode electronic skin textile for pressure and temperature sensing. *Chem Eng J*. 2021;425:130599.
86. Shi J, Wang L, Dai Z, et al. Multiscale hierarchical design of a flexible piezoresistive pressure sensor with high sensitivity and wide linearity range. *Small*. 2018;14(27):1800819.
87. Bae GY, Han JT, Lee G, et al. Pressure/temperature sensing bimodal electronic skin with stimulus discriminability and linear sensitivity. *Adv Mater*. 2018;30(43):1803388.
88. Wang Z, Zhang L, Liu J, Jiang H, Li C. Flexible hemispheric microarrays of highly pressure–sensitive sensors based on breath figure method. *Nanoscale*. 2018;10(20):10691-10698.
89. Zhu B, Ling Y, Yap LW, et al. Hierarchically structured vertical gold nanowire array–based wearable pressure sensors for wireless health monitoring. *ACS Appl Mater Interfaces*. 2019; 11(32):29014-29021.
90. Yu S, Li L, Wang J, et al. Light–boosting highly sensitive pressure sensors based on bioinspired multiscale surface structures. *Adv Funct Mater*. 2020;30(16):1907091.
91. Ha M, Lim S, Cho S, et al. Skin–inspired hierarchical polymer architectures with gradient stiffness for spacer-free, ultrathin, and highly sensitive triboelectric sensors. *ACS Nano*. 2018; 12(4):3964-3974.
92. Meng K, Wu Y, He Q, et al. Ultrasensitive fingertip–contacted pressure sensors to enable continuous measurement of epidermal pulse waves on ubiquitous object surfaces. *ACS Appl Mater Interfaces*. 2019;11(50):46399-46407.
93. Yang JC, Kim JO, Oh J, et al. Microstructured porous pyramid–based ultrahigh sensitive pressure sensor insensitive to strain and temperature. *ACS Appl Mater Interfaces*. 2019; 11(21):19472-19480.
94. Xiong Y, Shen Y, Tian L, et al. A flexible, ultra–highly sensitive and stable capacitive pressure sensor with convex microarrays for motion and health monitoring. *Nano Energy*. 2020;70:104436.
95. Yu Z, Cai G, Tong P, Tang D. Saw-toothed microstructure–based flexible pressure sensor as the signal readout for point-of-care immunoassay. *ACS Sens*. 2019;4(9):2272-2276.
96. Asghar W, Li F, Zhou Y, et al. Piezocapacitive flexible E–skin pressure sensors having magnetically grown microstructures. *Adv. Mater. Technol.* 2020;5(2):1900934.
97. Cho SH, Lee SW, Yu S, et al. Micropatterned pyramidal ionic gels for sensing broad-range pressures with high sensitivity. *ACS Appl Mater Interfaces*. 2017;9(11):10128-10135.
98. Wei Y, Chen S, Lin Y, Yang Z, Liu L. Cu–Ag core–shell nanowires for electronic skin with a petal molded microstructure. *J. Mater. Chem. C*. 2015;3(37):9594-9602.
99. Wei X, Li H, Yue W, et al. A high-accuracy, real–time, intelligent material perception system with a machine-learning-motivated pressure–sensitive electronic skin. *Matter*. 2022; 5(5):1481-1501.
100. Nie P, Wang R, Xu X, et al. High–performance piezoresistive electronic skin with bionic hierarchical microstructure and microcracks. *ACS Appl Mater Interfaces*. 2017;9(17):14911-14919.
101. Su B, Gong S, Ma Z, Yap LW, Cheng W. Mimosa–inspired design of a flexible pressure sensor with touch sensitivity. *Small*. 2015;11(16):1886-1891.
102. Hansen TS, West K, Hassager O, Larsen NB. Highly stretchable and conductive polymer material made from poly (3, 4-ethylenedioxythiophene) and polyurethane elastomers. *Adv Funct Mater*. 2007;17(16):3069-3073.
103. Teng C, Lu X, Zhu Y, Wan M, Jiang L. Polymer in situ embedding for highly flexible, stretchable and water stable PEDOT:PSS composite conductors. *RSC Adv*. 2013;3(20):7219-7223.
104. Oh JY, Kim S, Baik HK, Jeong U. Conducting polymer dough for deformable electronics. *Adv Mater*. 2016;28(22):4455-4461.
105. Kee S, Kim N, Kim BS, et al. Controlling molecular ordering in aqueous conducting polymers using ionic liquids. *Adv Mater*. 2016;28(39):8625-8631.
106. Zhu G, Wang F, Chen L, et al. Highly flexible TPU/SWCNTs composite–based temperature sensors with linear negative temperature coefficient effect and photo-thermal effect. *Compos. Sci. Technol.* 2022;217(5):109133.
107. Park J, Kim M, Lee Y, Lee HS, Ko H. Fingertip skin–inspired microstructured ferroelectric skins discriminate static/dynamic pressure and temperature stimuli. *Sci Adv*. 2015;1(9):1500661.
108. Lee Y, Park J, Cho S, et al. Flexible ferroelectric sensors with ultrahigh pressure sensitivity and linear response over exceptionally broad pressure range. *ACS Nano*. 2018;12(4):4045-4054.
109. Park J, Lee Y, Hong J, et al. Giant tunneling piezoresistance of composite elastomers with interlocked microdome arrays for ultrasensitive and multimodal electronic skins. *ACS Nano*. 2014;8(5):4689-4697.
110. Tay RY, Li H, Lin J, et al. Lightweight, superelastic boron nitride/polydimethylsiloxane foam as air dielectric substitute for multifunctional capacitive sensor applications. *Adv Funct Mater*. 2020;30(10):1909604.
111. Zheng Y, Li Y, Dai K, et al. A highly stretchable and stable strain sensor based on hybrid carbon nanofillers/polydimethylsiloxane conductive composites for large human motions monitoring. *Compos Sci Technol*. 2018; 156:276-286.
112. Zhang D, Xu S, Zhao X, Qian W, Bowen CR, Yang Y. Wireless monitoring of small strains in intelligent robots via a joule heating effect in stretchable graphene–polymer nanocomposites. *Adv Funct Mater*. 2020;30(13):1910809.
113. Ke K, Wang Y, Li Y, Yang J, Pötschke P, Voit B. Nuomici-inspired universal strategy for boosting piezoresistive sensitivity and elasticity of polymer nanocomposite-based strain sensors. *ACS Appl Mater Interfaces*. 2019;11(38):35362-35370.
114. Yang J, Tang D, Ao J, et al. Ultrasoft liquid metal elastomer foams with positive and negative piezopermittivity for tactile sensing. *Adv Funct Mater*. 2020;30(36):2002611.
115. Liu X, Liu Y, Cheng T, Gao Y, Yang Z. A high performing piezoelectric and triboelectric nanogenerator based on a large deformation of the novel lantern-shaped structure. *Nano Energy*. 2022;92:106699.
116. Mu J, Xian S, Yu J, et al. Flexible and wearable $BaTiO_3$/polyacrylonitrile-based piezoelectric sensor for human posture monitoring. *Sci China Technol Sci*. 2022;65(4):858-869.
117. Sun Y, Liu Y, Zheng Y, et al. Enhanced energy harvesting ability of ZnO/PAN hybrid piezoelectric nanogenerators. *ACS Appl Mater Interfaces*. 2020;12(49):54936-54945.

118. Graham SA, Dudem B, Mule AR, Patnam H, Yu JS. Engineering squandered cotton into eco-benign microarchitectured triboelectric films for sustainable and highly efficient mechanical energy harvesting. *Nano Energy*. 2019;61:505-516.
119. Ruth SR, Feig VR, Kim MG, et al. Flexible fringe effect capacitive sensors with simultaneous high-performance contact and non-contact sensing capabilities. *Small Structures*. 2021;2(2):2000079.
120. Lipomi DJ, Vosgueritchian M, Tee BC, et al. Skin-like pressure and strain sensors based on transparent elastic films of carbon nanotubes. *Nat Nanotechnol*. 2011;6(12):788-792.
121. Hua Q, Sun J, Liu H, et al. Skin-inspired highly stretchable and conformable matrix networks for multifunctional sensing. *Nat Commun*. 2018;9(1):1-11.
122. Niu H, Li H, Gao S, et al. Perception-to-cognition tactile sensing based on artificial-intelligence-motivated human full-skin bionic electronic skin. *Adv Mater*. 2022;34(31):2202622.
123. Niu H, Chen Y, Kim ES, Zhou W, Li Y, Kim NY. Ultrasensitive capacitive tactile sensor with heterostructured active layers for tiny signal perception. *Chem Eng J*. 2022;450:138258.
124. Yao S, Zhu Y. Wearable multifunctional sensors using printed stretchable conductors made of silver nanowires. *Nanoscale*. 2014;6(4):2345-2352.
125. Shuai X, Zhu P, Zeng W, et al. Highly sensitive flexible pressure sensor based on silver nanowires-embedded polydimethylsiloxane electrode with microarray structure. *ACS Appl Mater Interfaces*. 2017;9(31):26314-26324.
126. Pyo S, Choi J, Kim J. Flexible, transparent, sensitive, and crosstalk–free capacitive tactile sensor array based on graphene electrodes and air dielectric. *Adv. Electron. Mater.* 2018;4(1):1700427.
127. Schwartz G, Tee BCK, Mei J, et al. Flexible polymer transistors with high pressure sensitivity for application in electronic skin and health monitoring. *Nat Commun*. 2013;4(1):1-8.
128. Luo Y, Shao J, Chen S, et al. Flexible capacitive pressure sensor enhanced by tilted micropillar arrays. *ACS Appl Mater Interfaces*. 2019;11(19):17796-17803.
129. Yang J, Luo S, Zhou X, et al. Flexible, tunable, and ultrasensitive capacitive pressure sensor with microconformal graphene electrodes. *ACS Appl Mater Interfaces*. 2019;11(16):14997-15006.
130. Boutry CM, Negre M, Jorda M, et al. A hierarchically patterned, bioinspired e-skin able to detect the direction of applied pressure for robotics. *Sci. Robot.* 2018;3(24):aau6914.
131. Miller S, Bao Z. Fabrication of flexible pressure sensors with microstructured polydimethylsiloxane dielectrics using the breath figures method. *J Mater Res*. 2015;30(23):3584-3594.
132. Xu F, Zhu Y. Highly conductive and stretchable silver nanowire conductors. *Adv Mater*. 2012;24(37):5117-5122.
133. Luo S, Yang J, Song X, et al. Tunable–sensitivity flexible pressure sensor based on graphene transparent electrode. *Solid State Electron*. 2018;145:29-33.
134. Deng W, Huang X, Chu W, et al. Microstructure–based interfacial tuning mechanism of capacitive pressure sensors for electronic skin. *J Sens*. 2016;2016:2428305.
135. Zhang Y, Yang J, Hou X, et al. Highly stable flexible pressure sensors with a quasi–homogeneous composition and interlinked interfaces. *Nat Commun*. 2022;13(1):1-12.
136. Kang S, Lee J, Lee S, et al. Highly sensitive pressure sensor based on bioinspired porous structure for real–time tactile sensing. *Adv Electron Mater*. 2016;2(12):1600356.
137. Kim JO, Kwon SY, Kim Y, et al. Highly ordered 3D microstructure-based electronic skin capable of differentiating pressure, temperature, and proximity. *ACS Appl Mater Interfaces*. 2018;11(1):1503-1511.
138. Qiu J, Guo X, Chu RW, et al. Rapid-response, low detection limit, and high-sensitivity capacitive flexible tactile sensor based on three-dimensional porous dielectric layer for wearable electronic skin. *ACS Appl Mater Interfaces*. 2019;11(43):40716-40725.
139. Wang P, Li G, Liu J, et al. Tailorable capacitive tactile sensor based on stretchable and dissolvable porous silver nanowire/polyvinyl alcohol nanocomposite hydrogel for wearable human motion detection. *Adv Mater Interfaces*. 2021;8(20):2100998.
140. Mu C, Li J, Song Y, et al. Enhanced piezocapacitive effect in $CaCu_3Ti_4O_{12}$–polydimethylsiloxane composited sponge for ultrasensitive flexible capacitive sensor. *ACS Appl Nano Mater*. 2017;1(1):274-283.
141. Bae GY, Pak SW, Kim D, et al. Linearly and highly pressure–sensitive electronic skin based on a bioinspired hierarchical structural array. *Adv Mater*. 2016;28(26):5300-5306.
142. Shao Q, Niu Z, Hirtz M, et al. High–performance and tailorable pressure sensor based on ultrathin conductive polymer film. *Small*. 2014;10(8):1466-1472.
143. Park H, Jeong YR, Yun J, et al. Stretchable array of highly sensitive pressure sensors consisting of polyaniline nanofibers and Au–coated polydimethylsiloxane micropillars. *ACS Nano*. 2015;9(10):9974-9985.
144. Cao Y, Li T, Gu Y, Luo H, Wang S, Zhang T. Fingerprint–inspired flexible tactile sensor for accurately discerning surface texture. *Small*. 2018;14(16):1703902.
145. Zhang Y, Hu Y, Zhu P, et al. Flexible and highly sensitive pressure sensor based on microdome–patterned PDMS forming with assistance of colloid self–assembly and replica technique for wearable electronics. *ACS Appl Mater Interfaces*. 2017;9(41):35968-35976.
146. Zhang X, Hu Y, Gu H, et al. A highly sensitive and cost–effective flexible pressure sensor with micropillar arrays fabricated by novel metal–assisted chemical etching for wearable electronics. *Adv. Mater. Technol.* 2019;4(9):1900367.
147. Pang Y, Zhang K, Yang Z, et al. Epidermis microstructure inspired graphene pressure sensor with random distributed spinosum for high sensitivity and large linearity. *ACS Nano*. 2018;12(3):2346-2354.
148. Nguyen T, Dinh T, Phan HP, Pham TA, Nguyen NT, Dao DV. Advances in ultrasensitive piezoresistive sensors: from conventional to flexible and stretchable applications. *Mater. Horiz.* 2021;2021(8):2123-2150.
149. Chen W, Yan X. Progress in achieving high-performance piezoresistive and capacitive flexible pressure sensors: a review. *J Mater Sci Technol*. 2020;43:175-188.
150. Pyo S, Lee J, Bae K, Sim S, Kim J. Recent progress in flexible tactile sensors for human-interactive systems: from sensors to advanced applications. *Adv Mater*. 2021;33(47):2005902.
151. Park J, Lee Y, Hong J, et al. Tactile-direction-sensitive and stretchable electronic skins based on human–skin–inspired

interlocked microstructures. *ACS Nano*. 2014;8(12):12020-12029.
152. Jian M, Xia K, Wang Q, et al. Flexible and highly sensitive pressure sensors based on bionic hierarchical structures. *Adv Funct Mater*. 2017;27(9):1606066.
153. Xia K, Wang C, Jian M, Wang Q, Zhang Y. CVD growth of fingerprint-like patterned 3D graphene film for an ultrasensitive pressure sensor. *Nano Res*. 2018;11(2):1124-1134.
154. Jia J, Huang G, Deng J, Pan K. Skin-inspired flexible and high-sensitivity pressure sensors based on rGO films with continuous-gradient wrinkles. *Nanoscale*. 2019;11(10):4258-4266.
155. Chen W, Gui X, Liang B, et al. Structural engineering for high sensitivity, ultrathin pressure sensors based on wrinkled graphene and anodic aluminum oxide membrane. *ACS Appl Mater Interfaces*. 2017;9(28):24111-24117.
156. Liang B, Chen W, He Z, et al. Highly sensitive, flexible MEMS based pressure sensor with photoresist insulation layer. *Small*. 2017;13(44):1702422.
157. Pan L, Chortos A, Yu G, et al. An ultra-sensitive resistive pressure sensor based on hollow-sphere microstructure induced elasticity in conducting polymer film. *Nat Commun*. 2014;5(1):1-8.
158. Zhao T, Li T, Chen L, Yuan L, Li X, Zhang J. Highly sensitive flexible piezoresistive pressure sensor developed using biomimetically textured porous materials. *ACS Appl Mater Interfaces*. 2019;11(32):29466-29473.
159. Yao HB, Ge J, Wang CF, et al. A flexible and highly pressure–sensitive graphene–polyurethane sponge based on fractured microstructure design. *Adv Mater*. 2013;25(46):6692-6698.
160. Jung S, Kim JH, Kim J, et al. Reverse–micelle–induced porous pressure–sensitive rubber for wearable human–machine interfaces. *Adv Mater*. 2014;26(28):4825-4830.
161. Wei H, Li A, Kong D, et al. Polypyrrole/reduced graphene aerogel film for wearable piezoresisitic sensors with high sensing performances. *Adv Compos Hybrid Mater*. 2021;4(1):86-95.
162. Zhang S, Liu H, Yang S, et al. Ultrasensitive and highly compressible piezoresistive sensor based on polyurethane sponge coated with a cracked cellulose nanofibril/silver nanowire layer. *ACS Appl Mater Interfaces*. 2019;11(11):10922-10932.
163. Zhu L, Wang Y, Mei D, Wu X. Highly sensitive and flexible tactile sensor based on porous graphene sponges for distributed tactile sensing in monitoring human motions. *J Microelectromech Syst*. 2018;28(1):154-163.
164. Pang Y, Tian H, Tao L, et al. Flexible, highly sensitive, and wearable pressure and strain sensors with graphene porous network structure. *ACS Appl Mater Interfaces*. 2016;8(40):26458-26462.
165. Samad YA, Li Y, Alhassan SM, Liao K. Novel graphene foam composite with adjustable sensitivity for sensor applications. *ACS Appl Mater Interfaces*. 2015;7(17):9195-9202.
166. Sun X, Sun J, Li T, et al. Flexible tactile electronic skin sensor with 3D force detection based on porous CNTs/PDMS nanocomposites. *Nano Micro Lett*. 2019;11(1):1-14.
167. Yue Y, Liu N, Liu W, et al. 3D hybrid porous Mxene-sponge network and its application in piezoresistive sensor. *Nano Energy*. 2018;50:79-87.
168. Li W, Jin X, Han X, et al. Synergy of porous structure and microstructure in piezoresistive material for high-performance and flexible pressure sensors. *ACS Appl Mater Interfaces*. 2021;13(16):19211-19220.
169. Pi Z, Zhang J, Wen C, Zhang ZB, Wu D. Flexible piezoelectric nanogenerator made of poly (vinylidenefluoride-co-trifluoroethylene)(PVDF-TrFE) thin film. *Nano Energy*. 2014;7:33-41.
170. Ko EJ, Jeon SJ, Han YW, et al. Synthesis and characterization of nanofiber–type hydrophobic organic materials as electrodes for improved performance of PVDF–based piezoelectric nanogenerators. *Nano Energy*. 2019;58:11-22.
171. Deng W, Jin L, Zhang B, et al. A flexible field-limited ordered ZnO nanorod-based self-powered tactile sensor array for electronic skin. *Nanoscale*. 2016;8(36):16302-16306.
172. Ha M, Lim S, Park J, Um DS, Lee Y, Ko H. Bioinspired interlocked and hierarchical design of ZnO nanowire arrays for static and dynamic pressure–sensitive electronic skins. *Adv Funct Mater*. 2015;25(19):2841-2849.
173. Yang T, Pan H, Tian G, et al. Hierarchically structured PVDF/ZnO core-shell nanofibers for self-powered physiological monitoring electronics. *Nano Energy*. 2020;72:104706.
174. Chen X, Li X, Shao J, et al. High–performance piezoelectric nanogenerators with imprinted P(VDF–TrFE)/$BaTiO_3$ nanocomposite micropillars for self–powered flexible sensors. *Small*. 2017;13(23):1604245.
175. He J, Guo X, Yu J, et al. A high-resolution flexible sensor array based on PZT nanofibers. *Nanotechnology*. 2020;31(15):155503.
176. Su Y, Chen C, Pan H, et al. Muscle fibers inspired high–performance piezoelectric textiles for wearable physiological monitoring. *Adv Funct Mater*. 2021;31(19):2010962.
177. Wang ZL. Triboelectric nanogenerators as new energy technology for self-powered systems and as active mechanical and chemical sensors. *ACS Nano*. 2013;7(11):9533-9557.
178. Zhu G, Lin ZH, Jing Q, et al. Toward large-scale energy harvesting by a nanoparticle-enhanced triboelectric nanogenerator. *Nano Lett*. 2013;13(2):847-853.
179. Wang S, Lin L, Wang ZL. Nanoscale triboelectric-effect-enabled energy conversion for sustainably powering portable electronics. *Nano Lett*. 2012;12(12):6339-6346.
180. Wang S, Lin L, Xie Y, Jing Q, Niu S, Wang ZL. Sliding-triboelectric nanogenerators based on in-plane charge-separation mechanism. *Nano Lett*. 2013;13(5):2226-2233.
181. Lin L, Wang S, Xie Y, et al. Segmentally structured disk triboelectric nanogenerator for harvesting rotational mechanical energy. *Nano Lett*. 2013;13(6):2916-2923.
182. Wang X, Zhang H, Dong L, et al. Self–powered high–resolution and pressure–sensitive triboelectric sensor matrix for real–time tactile mapping. *Adv Mater*. 2016;28(15):2896-2903.
183. Yang Y, Zhang H, Lin ZH, et al. Human skin based triboelectric nanogenerators for harvesting biomechanical energy and as self-powered active tactile sensor system. *ACS Nano*. 2013;7(10):9213-9222.
184. Sharma T, Je SS, Gill B, Zhang JX. Patterning piezoelectric thin film PVDF–TrFE based pressure sensor for catheter application. *Sens Actuators A*. 2012;177:87-92.
185. Lee JH, Yoon HJ, Kim TY, et al. Micropatterned P (VDF–TrFE) film–based piezoelectric nanogenerators for highly sensitive self–powered pressure sensors. *Adv Funct Mater*. 2015;25(21):3203-3209.

186. Chen X, Shao J, Tian H, et al. Scalable imprinting of flexible multiplexed sensor arrays with distributed piezoelectricity–enhanced micropillars for dynamic tactile sensing. *Adv Mater Technol*. 2020;5(7):2000046.
187. Zhang JW, Zhang Y, Li YY, Wang P. Textile-based flexible pressure sensors: a review. *Polym. Rev.* 2022;62(1):65-94.
188. Xu S, Qin Y, Xu C, Wei Y, Yang R, Wang ZL. Self-powered nanowire devices. *Nat Nanotechnol*. 2010;5(5):366-373.
189. Xu CN, Akiyama M, Nonaka K, Watanabe T. Electrical power generation characteristics of PZT piezoelectric ceramics. *IEEE Trans Ultrason Ferroelectr Freq Control*. 1998;45(4):1065-1070.
190. Dagdeviren C, Su Y, Joe P, et al. Conformable amplified lead zirconate titanate sensors with enhanced piezoelectric response for cutaneous pressure monitoring. *Nat Commun*. 2014;5(1):1-10.
191. Wan Y, Wang Y, Guo CF. Recent progresses on flexible tactile sensors. *Mater Today Phys*. 2017;1:61-73.
192. Wang ZL. Triboelectric nanogenerators as new energy technology and self-powered sensors–principles, problems and perspectives. *Faraday Discuss*. 2014;176:447-458.
193. Ha M, Park J, Lee Y, Ko H. Triboelectric generators and sensors for self-powered wearable electronics. *ACS Nano*. 2015;9(4):3421-3427.
194. Fan FR, Tian ZQ, Wang ZL. Flexible triboelectric generator. *Nano Energy*. 2012;1(2):328-334.
195. Zhang Q, Jin T, Cai J, et al. Wearable triboelectric sensors enabled gait analysis and waist motion capture for IoT–based smart healthcare applications. *Adv Sci*. 2022;9(4):2103694.
196. Bai P, Zhu G, Lin ZH, et al. Integrated multilayered triboelectric nanogenerator for harvesting biomechanical energy from human motions. *ACS Nano*. 2013;7(4):3713-3719.
197. Lou M, Abdalla I, Zhu M, Yu J, Li Z, Ding B. Hierarchically rough structured and self-powered pressure sensor textile for motion sensing and pulse monitoring. *ACS Appl Mater Interfaces*. 2019;12(1):1597-1605.
198. Guo Y, Zhang XS, Wang Y, et al. All-fiber hybrid piezoelectric-enhanced triboelectric nanogenerator for wearable gesture monitoring. *Nano Energy*. 2018;48:152-160.
199. Zhu G, Chen J, Liu Y, et al. Linear-grating triboelectric generator based on sliding electrification. *Nano Lett*. 2013;13(5):2282-2289.
200. Wei X, Wang B, Wu Z, Wang ZL. Open-environment tactile sensing system: towards simple and efficient material identification. *Adv Mater*. 2022;34(29):2203073.
201. Chen J, Wen X, Liu X, Cao J, Ding Z, Du Z. Flexible hierarchical helical yarn with broad strain range for self-powered motion signal monitoring and human-machine interactive. *Nano Energy*. 2021;80:105446.
202. Yun J, Jayababu N, Kim D. Self-powered transparent and flexible touchpad based on triboelectricity towards artificial intelligence. *Nano Energy*. 2020;78:105325.
203. Meng B, Tang W, Too ZH, et al. A transparent single-friction-surface triboelectric generator and self-powered touch sensor. *Energ Environ Sci*. 2013;6(11):3235-3240.
204. Tang Y, Zhou H, Sun X, et al. Triboelectric touch–free screen sensor for noncontact gesture recognizing. *Adv Funct Mater*. 2020;30(5):1907893.
205. Guo H, Jia X, Liu L, Cao X, Wang N, Wang ZL. Freestanding triboelectric nanogenerator enables noncontact motion-tracking and positioning. *ACS Nano*. 2018;12(4):3461-3467.
206. Zhang N, Qin C, Feng T, et al. Non–contact cylindrical rotating triboelectric nanogenerator for harvesting kinetic energy from hydraulics. *Nano Res.* 2020;13(7):1903-1907.
207. Guo H, Wu H, Song Y, et al. Self-powered digital-analog hybrid electronic skin for noncontact displacement sensing. *Nano Energy*. 2019;58:121-129.
208. Yang J, Shi R, Lou Z, Chai R, Jiang K, Shen G. Flexible smart noncontact control systems with ultrasensitive humidity sensors. *Small*. 2019;15(38):1902801.
209. Yin F, Guo Y, Qiu Z, et al. Hybrid electronic skin combining triboelectric nanogenerator and humidity sensor for contact and non-contact sensing. *Nano Energy*. 2022;101:107541.
210. An J, Le TSD, Huang Y, et al. All-graphene-based highly flexible noncontact electronic skin. *ACS Appl Mater Interfaces*. 2017;9(51):44593-44601.
211. Zirkl M, Haase A, Fian A, et al. Low-voltage organic thin-film transistors with high-k nanocomposite gate dielectrics for flexible electronics and optothermal sensors. *Adv Mater*. 2007;19(17):2241-2245.
212. Zhang Z, Geng Y, Cao S, et al. Ultraviolet photodetectors based on polymer microwire arrays toward wearable medical devices. *ACS Appl Mater Interfaces*. 2022;14(36):41257-41263.
213. Peng W, Wu H. Flexible and stretchable photonic sensors based on modulation of light transmission. *Adv Opt Mater*. 2019;7(12):1900329.
214. Xu H, Liu J, Zhang J, Zhou G, Luo N, Zhao N. Flexible organic/inorganic hybrid near-infrared photoplethysmogram sensor for cardiovascular monitoring. *Adv Mater*. 2017;29(31):1700975.
215. Khan Y, Han D, Pierre A, et al. A flexible organic reflectance oximeter array. *Proc Natl Acad Sci U S A*. 2018;115(47):E11015-E11024.
216. Park S, Fukuda K, Wang M, et al. Ultraflexible near-infrared organic photodetectors for conformal photoplethysmogram sensors. *Adv Mater*. 2018;30(34):1802359.
217. Park JB, Ha JW, Yoon SC, Lee C, Jung IH, Hwang DH. Visible-light-responsive high-detectivity organic photodetectors with a 1 μm thick active layer. *ACS Appl Mater Interfaces*. 2018;10(44):38294-38301.
218. Qiu LZ, Wei SY, Xu HS, et al. Ultrathin polymer nanofibrils for solar-blind deep ultraviolet light photodetectors application. *Nano Lett*. 2019;20(1):644-651.
219. Reddy BKS, Veeralingam S, Borse PH, Badhulika S. A flexible, rapid response, hybrid inorganic–organic SnSe 2–PEDOT: PSS bulk heterojunction based high-performance broadband photodetector. *Mater Chem Front*. 2022;6(3):341-351.
220. Liu CK, Tai Q, Wang N, Tang G, Hu Z, Yan F. Lead-free perovskite/organic semiconductor vertical heterojunction for highly sensitive photodetectors. *ACS Appl Mater Interfaces*. 2020;12(16):18769-18776.
221. Li D, Du J, Tang Y, et al. Flexible and air-stable near-infrared sensors based on solution-processed inorganic-organic hybrid phototransistors. *Adv Funct Mater*. 2021;31(47):2105887.
222. Jun S, Choi KW, Kim KS, et al. Stretchable photodetector utilizing the change in capacitance formed in a composite film

containing semiconductor particles. *Compos. Sci. Technol.* 2019;182:107773.
223. Zhao X, Song L, Zhao R, Tan MC. High-performance and flexible shortwave infrared photodetectors using composites of rare earth-doped nanoparticles. *ACS Appl Mater Interfaces*. 2018;11(2):2344-2351.
224. An C, Nie F, Zhang R, et al. Two-dimensional material-enhanced flexible and self-healable photodetector for large-area Photodetection. *Adv Funct Mater*. 2021;31(22):2100136.
225. Zhang B, Xiang Z, Zhu S, et al. Dual functional transparent film for proximity and pressure sensing. *Nano Res.* 2014;7(10):1488-1496.
226. Yuan W, Yang K, Peng H, Li F, Yin F. A flexible VOCs sensor based on a 3D Mxene framework with a high sensing performance. *J Mater Chem A*. 2018;6(37):18116-18124.
227. Ye J, Tan H, Wu S, et al. Direct laser writing of graphene made from chemical vapor deposition for flexible, integratable micro-supercapacitors with ultrahigh power output. *Adv Mater*. 2018;30(27):1801384.
228. Xu H, Xiang JX, Lu YF, et al. Multifunctional wearable sensing devices based on functionalized graphene films for simultaneous monitoring of physiological signals and volatile organic compound biomarkers. *ACS Appl Mater Interfaces*. 2018;11(2):2344-2351.2018; 10(14):11785-11793.
229. He XX, Li JT, Jia XS, et al. Facile fabrication of multi-hierarchical porous polyaniline composite as pressure sensor and gas sensor with adjustable sensitivity. *Nanoscale Res Lett*. 2017;12:476.
230. Boutry CM, Beker L, Kaizawa Y, et al. Biodegradable and flexible arterial-pulse sensor for the wireless monitoring of blood flow. *Nat Biomed Eng*. 2019;3(1):47-57.
231. Ruth SRA, Feig VR, Kim MG, Khan Y, Phong JK, Bao Z. Flexible fringe effect capacitive sensors with simultaneous high–performance contact and non–contact sensing capabilities. *Small Struct*. 2021;2(2):2000079.
232. Kulkarni MR, John RA, Rajput M, et al. Transparent flexible multifunctional nanostructured architectures for non-optical readout, proximity, and pressure sensing. *ACS Appl Mater Interfaces*. 2017;9(17):15015-15021.
233. Kim J, Lee M, Shim HJ, et al. Stretchable silicon nanoribbon electronics for skin prosthesis. *Nat Commun*. 2014;5(1):1-11.
234. Luo S, Zhou X, Tang X, et al. Microconformal electrode-dielectric integration for flexible ultrasensitive robotic tactile sensing. *Nano Energy*. 2021;80:105580.
235. Osborn LE, Dragomir A, Betthauser JL, et al. Prosthesis with neuromorphic multilayered e-dermis perceives touch and pain. *Sci. Robot.* 2018;3(19):aat3818.
236. Byun J, Lee Y, Yoon J, et al. Electronic skins for soft, compact, reversible assembly of wirelessly activated fully soft robots. *Sci. Robot.* 2018;3(18):eaas9020.
237. Fang B, Wang C, Sun F, et al. Simultaneous sEMG recognition of gestures and force levels for interaction with prosthetic hand. *IEEE Trans Neural Syst Rehabil Eng*. 2022;30:2426-2436.
238. Sundaram S, Kellnhofer P, Li Y, Zhu JY, Torralba A, Matusik W. Learning the signatures of the human grasp using a scalable tactile glove. *Nature*. 2019;569(7758):698-702.
239. O'Brien KW, Xu PA, Levine DJ, et al. Elastomeric passive transmission for autonomous force-velocity adaptation applied to 3D-printed prosthetics. *Sci Robot*. 2018;3(23):aau5543.
240. Zhao H, O'Brien K, Li S, Shepherd RF. Optoelectronically innervated soft prosthetic hand via stretchable optical waveguides. *Sci. Robot.* 2016;1(1):aai7529.
241. Gu G, Zhang N, Xu H, et al. A soft neuroprosthetic hand providing simultaneous myoelectric control and tactile feedback. *Nat. Biomed. Eng.* 2021;7(4):1-10.
242. Xu K, Lu Y, Takei K. Flexible hybrid sensor systems with feedback functions. *Adv Funct Mater*. 2021;31(39):2007436.
243. Sim K, Rao Z, Zou Z, et al. Metal oxide semiconductor nanomembrane–based soft unnoticeable multifunctional electronics for wearable human–machine interfaces. *Sci Adv*. 2019;5(8):aav9653.
244. Huang Z, Hao Y, Li Y, et al. Three-dimensional integrated stretchable electronics. *Nat Electron*. 2018;1(8):473-480.
245. Lim S, Son D, Kim J, et al. Transparent and stretchable interactive human machine interface based on patterned graphene heterostructures. *Adv Funct Mater*. 2015;25(3):375-383.
246. Su L, Xiong Q, Wang H, Zi Y. Porous-structure-promoted tribo-induced high-performance self-powered tactile sensor toward remote human-machine interaction. *Adv Sci*. 2022;9(32):2203510.
247. Li J, Bao R, Tao J, Peng Y, Pan C. Recent progress in flexible pressure sensor arrays: from design to applications. *J Mater Chem C*. 2018;6(44):11878-11892.
248. Shi Z, Meng L, Shi X, et al. Morphological engineering of sensing materials for flexible pressure sensors and artificial intelligence applications. *Nano Micro Lett.* 2022;14(1):1-48.
249. Li Y, Liu Y, Bhuiyan SRA, Zhu Y, Yao S. Printed strain sensors for on-skin electronics. *Small Struct.* 2022;3(2):2100131.
250. Zhang H, Han W, Xu K, et al. Metallic sandwiched-aerogel hybrids enabling flexible and stretchable intelligent sensor. *Nano Lett*. 2020;20(5):3449-3458.
251. Zhong M, Zhang L, Liu X, et al. Wide linear range and highly sensitive flexible pressure sensor based on multistage sensing process for health monitoring and human-machine interfaces. *Chem Eng J*. 2021;412:128649.
252. Han S, Liu C, Xu H, et al. Multiscale nanowire-microfluidic hybrid strain sensors with high sensitivity and stretchability. *Npj Flexible Electron*. 2018;2(1):1-10.
253. He Q, Wu Y, Feng Z, et al. An all-textile triboelectric sensor for wearable teleoperated human–machine interaction. *J Mater Chem A*. 2019;7(47):26804-26811.
254. Yu X, Xie Z, Yu Y, et al. Skin-integrated wireless haptic interfaces for virtual and augmented reality. *Nature*. 2019;575(7783):473-479.
255. Pan J, Li Y, Luo Y, et al. Hybrid-flexible bimodal sensing wearable glove system for complex hand gesture recognition. *ACS Sens*. 2021;6(11):4156-4166.
256. Zhang T, Ding Y, Hu C, et al. Self–powered stretchable sensor arrays exhibiting Magnetoelasticity for real–time human–machine interaction. *Adv Mater*. 2022;2203786. doi:10.1002/adma.202203786
257. Chen X, Gong L, Wei L, et al. A wearable hand rehabilitation system with soft gloves. *IEEE Trans Ind Inform*. 2020;17(2):943-952.
258. Guo Y, Guo Z, Zhong M, Wan P, Zhang W, Zhang L. A flexible wearable pressure sensor with bioinspired microcrack and

interlocking for full–range human–machine interfacing. *Small*. 2018;14(44):1803018.
259. Zhu M, Sun Z, Zhang Z, et al. Haptic-feedback smart glove as a creative human-machine interface (HMI) for virtual/augmented reality applications. *Sci Adv*. 2020;6(19): aaz8693.
260. Sun Z, Zhu M, Shan X. Augmented tactile-perception and haptic-feedback rings as human-machine interfaces aiming for immersive interactions. *Lee C c Nat Commun*. 2022;13(1): 5224.
261. Liu Y, Yiu C, Song Z, et al. Electronic skin as wireless human-machine interfaces for robotic VR. *Sci Adv*. 2022;8(2):abl6700.

AUTHOR BIOGRAPHIES

Feifei Yin received her Bachelor's degree and Master's degree in the School of Information Science and Engineering from the University of Jinan, China in 2018 and 2021. She is currently a PhD candidate student in the Department of Electronics Engineering at Kwangwoon University, South Korea. Her current research focuses on gas-sensing devices and flexible electronic devices.

Yang Li has been a professor at the School of Information Science and Engineering at the University of Jinan, China since 2016. He received his PhD degree in the Department of Electronics Engineering at Kwangwoon University, South Korea in 2015. He has published over 50 peer-reviewed journal papers and has been authorized over 30 Chinese and Korean patents. His research interests include advanced semiconductor fabrication, nanostructured flexible materials, gas sensors, and memristors.

Nam-Young Kim received the PhD degree in electronic engineering from the State University of New York (SUNY) at Buffalo, the PhD degree with a DCE in theology from Midwest University, and the MS degree with Clinical Pharmacy, Aju University. He joined the Department of Electronic Engineering, Kwangwoon University, as a professor, in 1994. As the Founder of the RFIC Center, he has also researched as the Director of the Fusion Technology Center of RF and Bio-Related Research. He has published 255 SCI papers, 33 books, and registered 215 patents. His research interests include RF and bio-sensors and application.

How to cite this article: Yin F, Niu H, Kim E-S, Shin YK, Li Y, Kim N-Y. Advanced polymer materials-based electronic skins for tactile and non-contact sensing applications. *InfoMat*. 2023; e12424. doi:10.1002/inf2.12424